

Piezoelectric Vibrational Energy Harvesting

Mechanical reliability of piezoelectric cantilevers

J.A.Brans

 TU Delft

Piezoelectric Vibrational Energy Harvesting

**Mechanical reliability of piezoelectric
cantilevers**

by

J.A. Brans

to obtain the degree of Master of Science
at the Delft University of Technology,
to be defended publicly on Tuesday March 12, 2019 at 12:00 PM.

Student number: 4239725
Project duration: February 14, 2019 – March 12, 2020
Thesis committee: Prof. Dr J. Dankelman TU Delft, committee chair
Asst. Prof. Dr. Eng. N. Tolou, TU Delft, supervisor
Ir. T. Blad, TU Delft, daily supervisor

An electronic version of this thesis is available at <http://repository.tudelft.nl/>.

Preface

Fascination for technique, in specific mechanical engineering, started when I was young playing with Lego. This versatile durable toy is an example for a lot of products. This has been an inspiration for me during this research. Including with my motivation to contribute to a more sustainable world, I came upon the possibilities of energy harvesting. The high potential for micro scale vibration energy harvesting made me aware of the impact this research could have.

The first time vibrating the piezoelectric cantilever at the resonant frequency showed the magic of generating electricity from ambient vibrations with piezo electricity. At the same time, the brittle properties of the material became noticeable; the power output dropped at the large amplitudes. Nevertheless, I am convinced that piezoelectric vibration energy harvesting will become a versatile and reliable energy source for low power electronics. Just like the first Lego bricks future will show.

I am grateful for the endless possibilities, socially and academically, offered in Delft that shaped me as an Engineer. I am delighted to share my work with my family, friends and academic world. For now, I hope you enjoy reading my thesis. Please don't hesitate to contact me if it sparked your interests or you want to discuss it.

*J.A. Brans
Delft, March 2020*

Summary

Piezoelectric vibration energy harvesting can provide a sustainable source of energy for low-power sensors. The vibrational energy is converted to electrical energy by piezoceramic cantilevers. Replacing batteries by vibrational energy harvesters, reduces the footprint of the device and no continuous replacement of batteries is required cutting down the maintenance costs. However, the greatest issue preventing these system from being widely used is their poor reliability. The main failure mechanisms identified are ageing, temperature degradation, humidity degradation and most of all mechanical degradation. In the aim to maximise the power output, the piezoceramic cantilevers are resonating at the eigenfrequency close to the point of the fracture strength. It is found that too large tensional deformations result in fractures in the active piezoceramic material. Experiments show that fractures significantly drops the power output and reduces the eigenfrequency. Literature suggest that tapered piezoceramic cantilevers are a reliable replacement for the conventional rectangular piezoceramic cantilevers. Experiments confirm the severity of fractures in the piezoceramic cantilevers reduction of power output as low as 75% have been measured. Tapered cantilevers show to have a higher electrical power output per unit area compared to rectangular cantilevers. Therefore less deformation is needed to achieve the same electrical output. It can be concluded that tapered cantilevers increase the reliability of the vibrational energy harvester.

Contents

Preface	iii
Summary	v
1 Project introduction	1
1.1 Relevance and applications	2
1.2 How do piezoceramic materials generate charge?	2
1.3 Problem statement	3
1.4 Thesis structure.	4
2 Failure Mechanisms of Piezoelectric cantilevers	5
2.1 Reliability, failure and degradation	6
2.2 Ageing.	6
2.3 Temperature	6
2.4 Humidity.	8
2.5 Mechanical strain	8
2.6 Other practical considerations	9
3 Geometric Design Principles for Reliable Cantilever Piezoelectric Energy Harvesters	11
3.1 Introduction	12
3.2 Classification of literature	12
3.3 Strain distribution	12
3.4 Strain limitation	14
3.5 Compressive strain.	16
3.6 Discussion	16
3.7 Conclusion	17
4 Experimental study to tapered cantilever energy harvesters	19
4.1 Introduction	20
4.2 Method	21
4.3 Results	22
4.4 Discussion	24
4.5 Conclusion	25
5 Discussion	27
5.1 Relevance	28
5.2 Generalisation & Limitations	28
5.3 Reflection	28
6 Conclusions	31
6.1 Conclusions.	32
6.2 Recommendations	32
6.3 Future research recommendations	33
Acknowledgements	35
A Literature paper	37
B Conference	47
C Clamping design	49
D Electrical circuit	53
E Test samples	55

F Test protocols experiments	59
G Partial differential equations	65
H Mechanical analytical background	69
Bibliography	75

1

Project introduction

This first chapter shows the challenges that lays ahead for future powering small electronic devices, and how piezoelectric energy harvesting can contribute to this. The reader is introduced with the direct piezoelectric effect for energy harvesting applications. It is stated in the problem statement why piezoceramic energy harvester are not yet widely used. The resulting research objective and research questions are stated. Finally, the thesis outline is given.

1.1. Relevance and applications

Nowadays, history has proven that we should look into renewable energy sources. Wind, solar and hydro power are the sustainable energy sources that are common to all people. But less known is that ambient vibrations around us are also a potential energy source for providing electrical power. Vibration energy harvesters could replace the batteries as an infinite energy source to power low power devices. An invention by the brothers Curie, 7 years after the prediction of Professor Augustine Mouchot, showed that deformation of certain crystals could produce electric potential[9]. It is only in the last decades that this piezoelectric effect is used for energy harvesting applications. Piezoelectric vibration energy harvesting uses the piezoelectric effect to convert vibrations to electrical power.

Piezoelectric vibration energy harvesters(PVEH) have the greatest potential in small remote sensor applications, which consume low power. Replacing the batteries by PVEH's takes away the disadvantages such as, large footprint on the device and finite energy supply. Hence, no periodic replacement of batteries is needed. Especially for hard to reach applications the infinite energy supply of PVEH is promising. For example, monitoring the tire pressure of vehicles can be a good application where the vibration energy of the tire is used to power the pressure sensor by PVEH [48, 59]. Another application where interesting research is done, is the piezoelectric powering of artificial cardiac pacemakers [20]. Pacemakers have to be replaced every 7 to 10 years. The PVEH's can function as an infinite energy source to power the pacemakers. Along with the rapid development of low-power integrated circuits the energy harvesting generators are expected to give rise to an era of self-powered autonomous devices [64].

1.2. How do piezoceramic materials generate charge?

Piezoceramic materials have the ability to generate an electric charge in response to applied mechanical stress. This is called the **direct piezoelectric effect**. The unique characteristics of the piezoelectric effect is that it is reversible, meaning that when a electric field is applied to the piezoelectric material stress is generated. For the energy harvesting applications the direct piezoelectric effect is utilised. Figure 1.1, depicts the working principle of the piezoelectric effect used in vibrational energy harvesting. A base vibration resonates a piezoelectric structure, resulting in mechanical strain that generates charge in the piezoceramic material. The charge can be used to provide electrical power to electronic circuits.

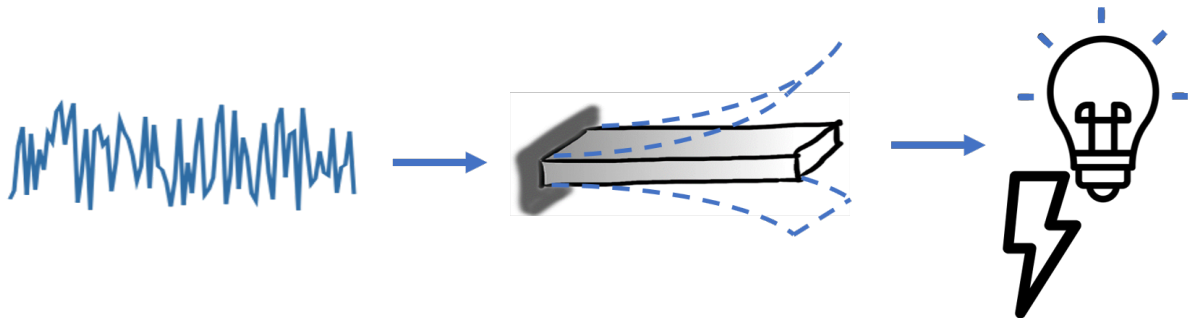


Figure 1.1: **Schematic overview of the direct piezoelectric effect used in vibration energy harvesting. Vibrations resonate a piezoceramic structure, resulting in mechanical strain that generates charge.**

Figure 1.2, shows a typical piezoelectric cantilever cross section fixed with a clamping at $x=0$. In specific this is a bimorph piezoelectric cantilever, since it consists of two active piezoceramic layers. Separated by a composite substrate layer ensuring pure bending modes. Each piezoceramic layer has electrodes at the top and bottom conducting the generated charge.

The piezoceramic materials have a crystal structure, in specific a perovskite structure. Imagine an idealised cubic unit cell. At rest the molecular dipole moment of the unit cell is balanced and the charge cancels out. When deformed the dipole moment changes and netto negative charge occurs where on the other side positive charge occurs. A group of unit cells form a domain, naturally the domains are randomly oriented in the crystal(non-polarised). When an external electrical field is applied the domains

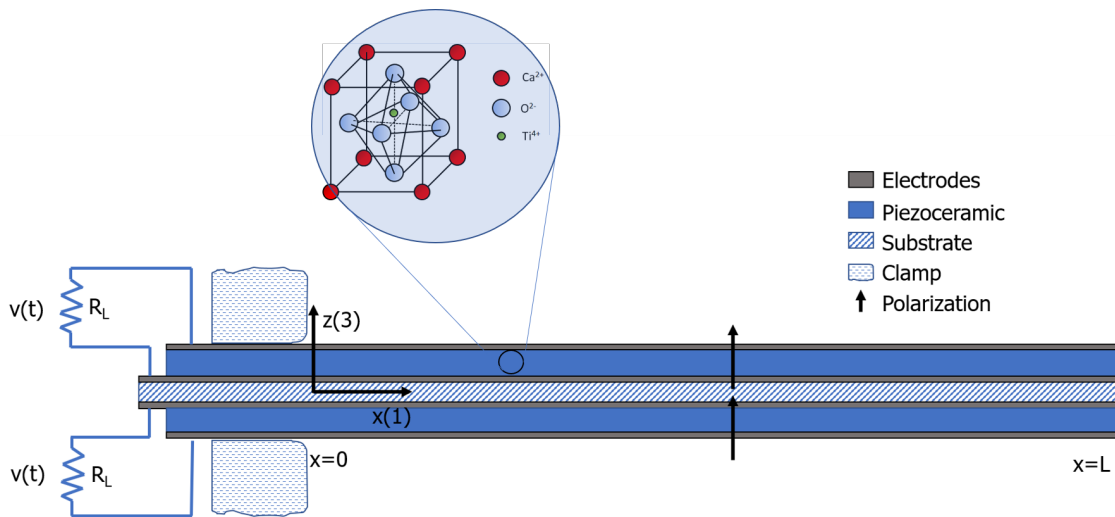


Figure 1.2: Side view cross section of bimorph piezoelectric cantilever parallel connected configuration.

align with the potential field giving the ceramic material the ability to generate charge when deformed. Figure 1.2 depicts a typical piezoceramic unit cell with a asymmetric center (green atom).

There are many different geometries for Piezoelectric Vibrational Energy Harvesters. The focus of this research is set to single Degree of Freedom(DoF) PZT cantilever beam structures. This choice has been made since cantilevers are the most used structures for vibration energy harvesters [5]. Commonly, a force is applied in, 31-mode, perpendicular to the poling direction of the ceramic [3, 57], since the lateral stresses are easily coupled with piezoelectric material on the cantilever beam. Moreover, cantilevers are often the basis of more complex energy harvesting designs [5]. Increasing the reliability of single DoF PVEH's will also be profitable for the more sophisticated architectures.

1.3. Problem statement

The greatest issue preventing current piezoceramic energy harvesters to be widely used is the poor reliability of the energy harvesters. There is a trade-off between energy output and lifetime of the energy harvesters. Current rectangular PVEH's are operated at the limit of the material strength to maximize the electrical power output. This results in degradation of the piezoceramic energy harvester. Therefore, the goal of this research is to improve the reliability of PVEH's without being at the cost of electrical power output.

Research objective

Explore the influence of tapering for PZT cantilevers on the reliability and power output for piezoelectric energy harvesting

To reach this objective the following research question is formulated:

Research question

How is the reliability and power output of tapered piezoceramic cantilevers affected relative to the conventional rectangular piezoceramic cantilevers?

Before answering the above mentioned research question, it is necessary to answer the following two subquestions:

- What are the main failure causes of piezoceramic degradation?
- What design principles are used in literature to increase the reliability of PVEH's?

1.4. Thesis structure

The structure of the thesis is summarised in Figure 1.3. The arrows indicate how chapters interconnect. The first two chapters are a general introduction to the background, problem and piezoceramic failure mechanisms. Chapter 3 gives an overview of design principles for improved mechanical reliability of cantilever piezoelectric energy harvesting. Chapter 4 presents the experimental research that is done towards reliability of piezoelectric cantilever energy harvesting, keeping in mind the design principles for improved reliability. This chapter is written in order to be individually understandable by experienced readers in the field of piezoelectric energy harvesting. Chapter 5 discusses the results of the previous chapters and links them together, concluding with the future potential and what this research contributes to the field of piezoelectric energy harvesting. The main findings and future recommendations are concluded in Chapter 6.

Work that not directly contributes to the main conclusions of the research, but support the considerations taken and validation processes, can be found in the appendices. Appendix A presents the literature review as how it is published at the ICCMA 2019 conference in Delft. Appendix B includes the conference poster summarising the literature review, used for the conference poster presentations. The following three appendices support the experimental research. In Appendix C includes the technical drawing of the clamping holding the piezoceramic cantilevers and validation of the dynamics. Appendix D shows the electrical circuit of the test setup with some considerations. Appendix E gives the technical information of the piezoceramic cantilevers from the supplier and validates the influence of the shaping process on the material. In appendix F the test protocols used for experiments and sample production are included for reproducibility. Appendix G demonstrates an attempt to numerically model piezoelectric cantilever behaviour by partial differential equations in Matlab. Finally, Appendix H shows an attempt to calculate the eigenfrequency by material properties of tapered cantilevers.

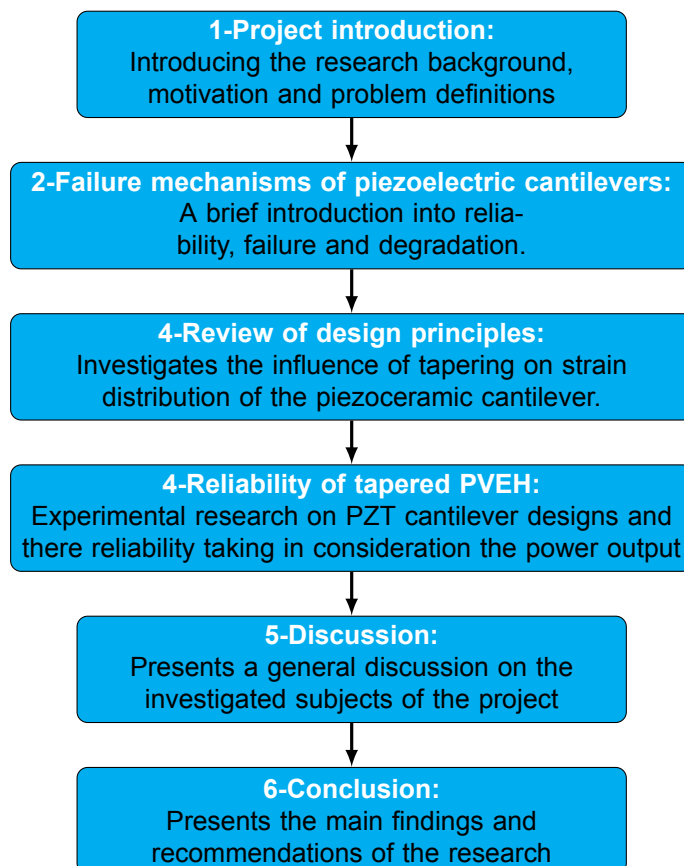


Figure 1.3: The structure of this study by chapter and there relations indicated by arrows

2

Failure Mechanisms of Piezoelectric cantilevers

In this chapter, the difference between failure and degradation of piezoceramic cantilevers for energy harvesting is given. Then, four failure mechanisms are discussed that contribute to the degradation of piezoceramic cantilevers. Finally, some practical considerations are given that contributes to the safety and reliability of piezoelectric energy harvesters.

2.1. Reliability, failure and degradation

Reliability, failure and degradation are three terms that are used often when talking about lifetime of products, each having their own definition. **Reliability** is defined as the ability of the device to perform its designed function in terms of years/cycles of operational lifetime[1]. This can be inversely related to the probability of **failure**: " $P(\text{Reliability}) = 1 - P(\text{Failure})$ ". Understanding the failure modes creates, therefore, an understanding of the reliability of the device. In the field of energy harvesting, there are different definitions of failure found in literature [11, 12, 30, 56]. M.Gall et al. regarded a specimen as failed if the sensor voltage dropped below 90% of the initial state value [12][11]. This is a relatively strict failure criterion compared to other definitions found in literature. This is because a maximum voltage drop of 10% allows for small deviations in power output but guarantees the necessary stable performance for smart structures. So, failure is not a complete (mechanical) breakdown of a specimen, only a reduction of designed voltage. Therefore, the term **degradation** is often used to describe the reduction of designed performance.

Four variables are found to have a negative influence on the piezoelectric material properties. Each will be discussed separately.

2.2. Ageing

Describing the time dependent change of the piezoelectric properties, the two terms ageing and degradation are often misused. Degradation is caused by external influences and normally implies detrimental change to a necessary property of the device or material. Where ageing is defined as a positive or negative spontaneous change of a property with time without external influences [51]. For piezoelectric related materials this means that ageing is not associated with external stresses. However, ageing influences the the performance of the piezoceramic and this has to be taken in account when investigating the degradation of piezoelectric energy harvesters. The piezoelectric coefficient d_{31} , is found to age at -4.4% per time decade (for PZT-5H) [13]. Similar ageing rate, of -3.9% per decade, is reported by Morgan Electronics for the d_{33} coefficient of PZT-5H [34].

$$\text{Ageing rate} = \frac{1}{\log(t_1) - \log(t_2)} \frac{p_2 - p_1}{p_1} \quad (2.1)$$

According to the logarithmic degradation, in formula 2.1, the piezoelectric charge coefficient (d_{31}) degrades 10% after 188 days, assuming -4.4% aging rate. Where t_1 and t_2 are the number of days after polarisation and p_1 and p_2 the piezoelectric parameters. So, the ageing can not be neglected in future reliability studies.

Ageing of piezoceramic materials

The depolarisation of piezoceramic materials is a logarithmic function of time.

There are two ways to compensate for the ageing in experimental researches, a reference beam is suggested for compensating environmental variations. Second option is to leave the samples for an extended amount of time after polarisation, so that the natural ageing will be negligible during the experiment. The linear semi-logarithmic behaviour means that, the largest degree of degradation occurs just after the polarisation of the piezoceramic. Leaving the samples for 60 days with a -4% decay of d_{31} per decade, will result in only a 0.2% further decay over an 8 day experiment.

So, there are two ways to compensate for the ageing effects during experimental tests. Firstly, using a reference beam that is not being cycled. Secondly, resting the test sample for an extended time, to reduce ageing effect.

2.3. Temperature

The piezoelectric structure changes at the Curie temperature from piezoelectric to non-piezoelectric form, losing the piezoelectric properties. M.Gall et.al. found that PZT cantilevers at elevated temperatures produced a lower electrical charge at the same strain levels. And the static fracture strength decreases at higher temperatures [12]. Figure 2.1, shows the effect of temperature and maximum strain on piezoceramic cantilevers. Higher strains and temperatures result in early failure.

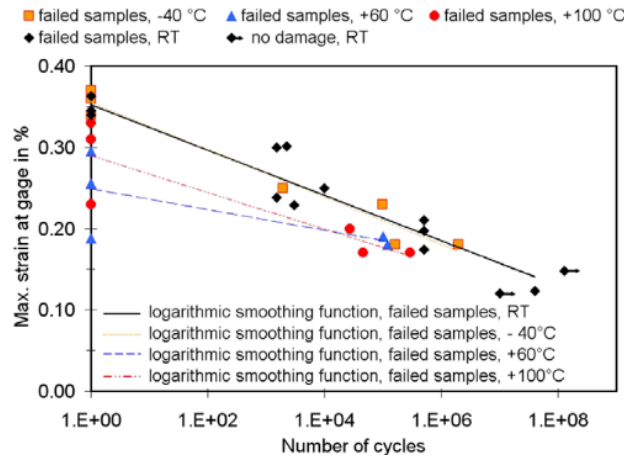


Figure 2.1: Tensile fatigue test at different temperatures showing temperature degradation. A sample is considered failed when the power output is less than 90% of the initial power. [12]

Temperatures below freezing point up to $-40\text{ }^{\circ}\text{C}$ show to have no degradation on the power output [6]. MEMS scale PVEH's using thin film PZT have a decreased temperature dependence due to the more constraint domain motions with the smaller grain size [23].

The value of the piezoelectric charge constant (d_{33}) is always a trade-off with the Currie temperature of the material. Figure 2.2, shows the d_{33} for most commercially available piezoelectric materials as function of their Currie Temperature. The best piezoelectric properties are found for materials with low Curie temperatures. The highlighted state of the art material is made of Bismuth Scandate (BiScO_3) and Lead Titanate (PbTiO_3) developed in 2001.

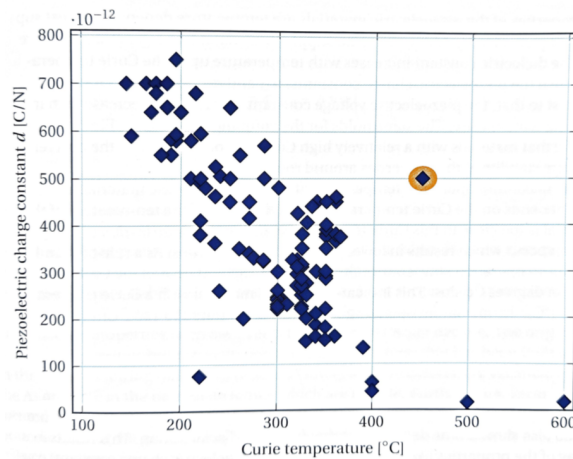


Figure 2.2: Piezoelectric charge constant in relation with the Curie temperature for various piezoelectric ceramics. [17]

Last but not least, increase of temperature softens the epoxy glue between the piezoceramic layers and the electrical contacts. The induced softening of the epoxy matrix and adhesive leads to a decrease of strain transmitted to the piezoceramic material. This reduces the resonant frequency and the power output. There might be even a chance of delamination of the composite piezoceramic cantilever. This effect is found to occur around $120\text{ }^{\circ}\text{C}$ [12, 23]. As a rule of thumb the maximum operating temperature should not be higher than half the Curie temperature in degrees Celsius [17]. Curie temperature (T_c) of the piezo ceramic (PZT508) used in the experimental research (chapter 4.5) is $208\text{ }^{\circ}\text{C}$.



Thermal degradation

Thermal degradation occurs at elevated temperatures above the Curie temperature, the temperature where the material depolarises and loses the piezoelectric properties. Secondly for composite cantilevers, elevated temperatures softens the epoxy glue reducing the resonant frequency and strain transmitted to the piezoceramic material.

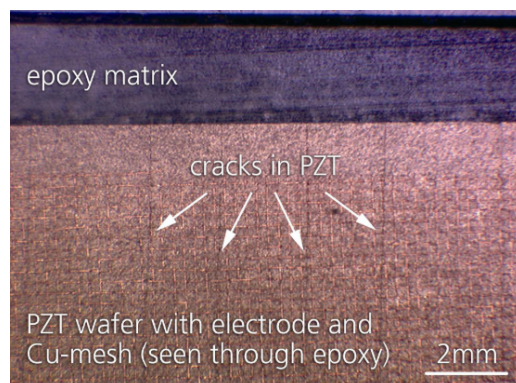
2.4. Humidity

No research has been found on the effect of humidity on piezoelectric cantilevers for energy harvesting. However, there are experiments done on multi layer piezoelectric actuators. The lifetime in 80% relative humidity was 2 to 3 decades shorter than that at 10% relative humidity[56]. P.Pertsch et.al. also writes about humidity driven degradation processes in multi layer piezoelectric actuators[41]. Suggesting that high relative humidity will cause degradation of the power output of the PVEH. In MEMS applications humidity is disastrous because of stiction [19]. This is induced by capillary forces acting on the surfaces coming into contact to each other. Therefore it is recommended to have the piezoelectric energy harvesting mechanism in a closed system.

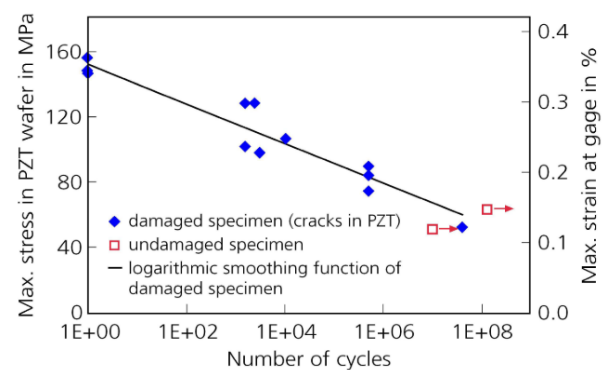
2.5. Mechanical strain

With the goal to maximise the power output piezoelectric cantilevers are deformed to the limits of the material stresses. It is found that the degradation of the PVEH is mainly caused by the mechanical cyclic loading [8, 11, 42, 43, 58, 62, 63]. M.Gall and B.Thielicke used a four-point cyclic tensile bending test to describe the degradation as function of the applied strain. The larger the strain in piezoceramic the more electrical charge is generated. But after 2000 cycles at 0.3% strain the electrical charge has declined by 14%, due to the mechanical degradation of the piezoceramic [11].

Figure 2.3b expresses the number of cycles a sample survives before failure occurs(90% of initial voltage). The number of cycles a sample survives is dependent on the applied strain. For this sample the quasi-static fracture strain is 0.35%. Almost immediate failure occurs at this strain. As expected lower strain levels results in higher number of cycles before failure. Samples that are cycled over 10^8 cycles at a maximum strain of 0.12% showed less than 10% reduction of initial performance. In real life applications that operate for example at 30Hz this means only an operational lifetime 39 days. This emphasises the importance of not over straining the piezoelectric ceramic in order to yield maximum output.



(a) Microcrack in piezoceramic layer. [11]



(b) Failure (90% of initial voltage) of PZT patches as function of number of cycles under tensile loading at room temperature [11]

Figure 2.3: Influence of mechanical strain on piezoceramic cantilevers

The degradation of the piezoelectric ceramic is primarily caused by microcracks resulting from the strain in the material [39]. Most microcracks occur at the high-strain areas, where the strain is largest [43]. For a cantilever that is uniform in width and thickness, area near the clamped fixed end is most prone to the microcracks. The experimental test with bimorph harvesters, energy harvesters with a piezoelectric layer in compression and tension, show that micro-cracking is primarily occurring in the

tensional layer. A 80% drop of capacitance is found in the tensile layer, caused by microcracks located at 20% percent of the length from the clamped-end of the cantilever [43]. This is proven by stereo microscopy visual inspections of the sample [11], see Figure 2.3a.

Mechanical degradation

Degradation of piezoceramic cantilevers is primarily caused by tensional strain, resulting in microcracks, lowering the eigen frequency and piezoelectric properties.

The microcracks in the piezoceramic reduces the coupling factor (k_{31}) and changes the dynamic behaviour of the cantilever. Therefore this can be used as a measure for degradation. The microcracks reduce the stiffness of the cantilever beam, influencing the resonant frequency. This frequency shift is often more detrimental than the change in piezoelectric properties [42], since the cantilevers are designed to operate at specific frequencies, that causes the cantilever beam to resonate efficiently. Frequency shifts of 4-8Hz are found in [42]. Similar frequency shifts are found in other literature [24, 43, 63]. It is important to note that the most significant frequency shift occurs within the first cycles.

2.6. Other practical considerations

For fabricating piezoelectric energy harvesters there are some basic considerations that can be kept in mind for improving the reliability and safety.

Making the electrical connections to the electrodes of the piezoceramic cantilever can be challenging. Soldering, glueing and tape are most commonly used to make electrical contact. Each has his benefits and considerations. Conducting double-sided tape has the weakest contacts and over time the conducting capabilities get lost. Gluing the wires is done with conducting epoxy, having strong bonding and excellent conduction. However, the epoxy is difficult to apply on small surfaces and expensive. 7 grams of conducting epoxy is 90 to 130,- euro. Last but not least, soldering is most often used. During the soldering it is important to make sure the piezoceramic material does not exceed the Curie temperature and depolarise. Three tricks can minimise the chance of depolarisation. First, pre-tin the stripped wires with low melting temperature solder and the stripping length should be at least 2 times the wire diameter. Secondly, use a clean pre-tinned soldering iron with a low thermal mass. Thirdly, use the lowest possible temperature setting to prevent thermal(shock) damage. Soldering is the primary choice based on the flexibility, ease of operation, low-cost and ability to form reliable contacts. The quality and reliability of the solder joints can be assessed by IPC-A-610 standard "Acceptability of Electronic Assemblies". In general the wetting angles should not exceed 90 degrees, for reliable solder connections. Figure 2.4 schematically summarises basic guidelines for a reliable soldering.

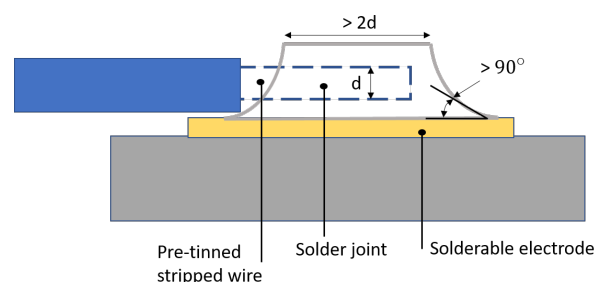


Figure 2.4: Schematic drawing of a solder joint with basic guidelines for reliable soldering connection. Adapted from: [17]

Environmental and health issues of lead (Pb) are well-known, disposal and recycling of devices containing lead-based piezoceramic materials is of great concern. The Restriction of Hazardous Substances (RoHS 2002/95/EC) of China and Europe restricts hazardous substances used in electronic devices, including lead. Since, no alternative material is available, PZT ceramics have been exempted from European RoHS regulation. Two lead-free materials are available: Barium Titanate ($BaTiO_3$) and Bismuth Sodium Titanate (BNT). However, none of the lead-free piezoelectric materials are ready to fully replace the PZT-based materials. Because, of their poorer piezoelectric properties.

Geometric Design Principles for Reliable Cantilever Piezoelectric Energy Harvesters

This chapter elaborates on the findings of a literature study. This is based on the the paper *A Review of Design Principles for Reliable Cantilever Piezoelectric Vibration Energy Harvesting*¹, that has been presented at the IEEE conference on Delft on the 6th of November 2019.

¹By J.A.Brans, T.W.A. Blad and N.Tolou. Delft 2019

3.1. Introduction

The previous chapter 1.4, summarised the most common failure mechanisms of Piezoelectric Vibration Energy Harvesters (PVEH's). The most dominant degradation of piezoceramic cantilevers for vibration energy harvesting is the mechanical cyclic loading [8, 11, 42, 43, 58, 62, 63]. This chapter reviews design principles found in literature that improve the mechanical reliability of PVEH's. The goal of this chapter is to present an overview of design principles for improving piezoelectric cantilever beams operational lifetime, by limiting strain and strain concentrations. Keeping in mind the consequences on the change of efficiency by the modification of geometric design for improved mechanical reliability. Hence, the research question for this chapter is: What design principles exist in literature for increased mechanical reliability of cantilever beam piezoelectric energy harvesters?

3.2. Classification of literature

Classification of the found literature is done according to the principle the strain is minimised to improve reliability, since tensional strain is the dominant failure cause of rectangular PVEH's. To the writers' knowledge all existing principles found in literature can be included within this strain based classification. This classification is made to differentiate and compare various design principles relative to conventional rectangular cantilevers. The three strain design principles that are identified to categorise literature are schematically depicted in Figure 3.1.

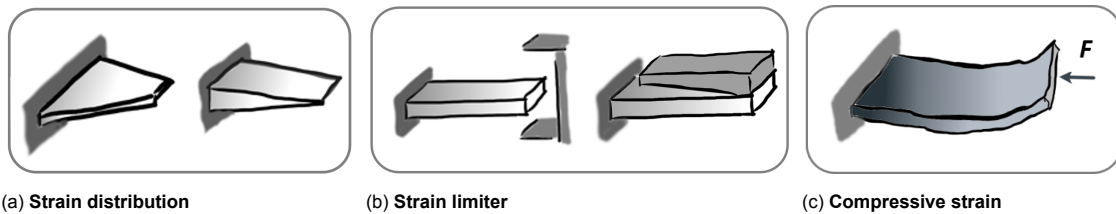


Figure 3.1: Categorized design principles for strain reduction improving piezoelectric vibration energy harvesters

a. Strain distribution:

The first category is the strain distribution over the cantilever beam. Stress concentrations are here minimised, and strain is more even distributed by tapering the cantilever. The goal is to have a homogeneous distribution of strain over the cross section or surface area of the piezoelectric cantilever.

b. Strain limitation:

Limiting the deformation assures that the strain does not exceed the maximum fracture strain and therefore prevents it from breaking. The strain limitation can be achieved by limiting the amplitude of the cantilever movement.

c. Compressive strain:

Operation in compressive strain reduces the maximum tensional strain in the piezoceramic. This can be achieved by pre-compression of the piezoceramic material on the substrate.

To evaluate the three design principles a relative comparison is made with the conventional single degree of freedom rectangular cantilever. Therefore, more complicated structures and multi degree of freedom energy harvesting mechanisms are excluded in this research. However, the single degree of freedom cantilever is often the basis of more complicated structures. Therefore, findings for increased reliability of single degree of freedom cantilevers can lead to increased reliability of more complicated structures as well.

3.3. Strain distribution

Conventional rectangular cantilever designs are limited by the maximum strain; hence, it is difficult to obtain larger electrical output power by increasing the deflection [45]. Increasing the lifetime and electrical output power of the piezoelectric cantilever beam can be achieved by reducing stress concentrations over the piezoceramic, and therefore allowing a higher average strain over the piezoelectric material. This can be achieved by distributing the strain over the area or cross section, see Figure 3.2

Area strain homogenisation

Glynne-Jones.P, Beeby.S.P and White.N.M. where the first writing about a tapered piezoelectric cantilever beams for strain homogenisation [13]. To quantify how well the stress is distributed over the area the average strain can be defined along the length axis and thickness. L.Matue and F.Moll analytically compared rectangular cantilevers with tapered cantilevers, he found that the average strain of the rectangular cantilever is 75% of the triangular cantilever average strain with identical load and active area [31]. Therefore, a triangular cantilever can generate more electrical power per unit area.

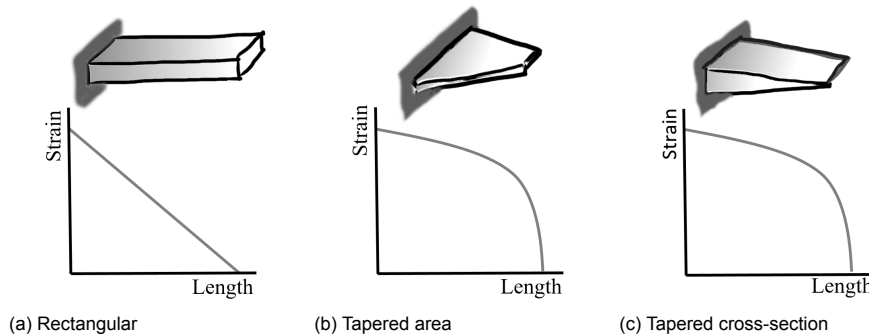


Figure 3.2: **Strain homogenisation over top layer area and cross-section along the length of a cantilever beam. The deflection is applied downwards at the free-end.**

Roundy et al. claims that a triangular cantilever can supply twice the energy per unit volume PZT than a rectangular cantilever [47]. Bakker et al. investigated the shape effects by comparing rectangular and triangular cantilever PVEH's [4]. For the comparison he kept the PZT volume, natural frequency, proofmass and maximum strain constant. He calculated a theoretical 50% higher electrical power output compared to a rectangular design. In reality, the experiments show a 30% increase. This difference can be attributed to the uncertainties in manufacturing and inaccuracies in dimensions or material properties. Also neglecting of dynamics in bonding layer and assumption of linear spring behaviour result in a difference of theoretical and experimental results.

In reaction of the study from Baker [4] with macro scale design PVEH Jung-Hyun Park, et.al. conducted a similar study on micro machined cantilevers. Both samples had a same thickness and proofmass. The eigenfrequency of the cantilevers were 128.1 Hz and 117.3 Hz, respectively for the rectangular beam and triangular beam. The dimensions were 3x2x0.5 mm (LxWxH), and the trapezoidal cantilever had a reduced width of 1mm. He concluded that with an equal PZT surface area (1mm^2) of the trapezoidal shape cantilever 39% more power is harvested compared to a rectangular design [40]. It could be concluded that scaling to micro scale yields similar advantages obtained by strain homogenisation.

So, a triangular surface shape is preferred over rectangular and trapezoidal shapes [7, 21, 31, 33, 45, 65]. This is because of the resulting uniform stress distribution over the cantilever, assuming no edge effects exist [14]. The more uniform strain distribution can be seen in Figure 3.2 in comparison with a rectangular cantilever. The stress concentrations near the fixed end are reduced and the effective strain area increased. This suggests that the operational lifetime of the tapered PVEH is longer than the rectangular cantilevers. However, no lifetime or experimental failure tests were performed to the writers knowledge. Most experimental test focus on the electrical power generation. Since, tapered cantilevers have not only higher reliability but also a higher power density [4, 7, 10, 14, 15, 38, 44, 45, 50].

Important to notice is that the tapered shaped area is only advantageous when dealing with long slender cantilevers. If the length-width ratio is smaller than 1, the tapered beams deliver less output power. With a length-width ratio of 1/3, 25% less output can be generated compared with a non-tapered beam with the same area and thickness [22].

Cross-section strain homogenisation

Also the thickness can be varied for strain homogenisation. A profile that does not compromise the effective active area is a rectangular beam with an elliptical or tapered cross-section [27, 45]. This cross-section also reduces the stress at the fixed-end of the cantilever since the thickness of the material is greater. S. Mehraeen et al. [32] was the first optimising the cross-section instead of using a linear tapered beam. The cantilever used in experiments is made by a tapered substrate covered with thin film piezoelectric material. However, fabrication of bulk cross-section tapered cantilevers is challenging with the conventional production methods. Therefore, these piezoceramic cantilevers are less common. These shape principles distribute the strain over the beam surface and hence, the life cycles of the energy harvester will increase without compromising the generated electrical power [45].

Strain distribution

Tapered cantilevers are preferred over rectangular cantilevers for their higher power output per unit area, due to the strain homogenisation.

3.4. Strain limitation

A mechanical stopper is used to limit the deflection of the cantilever beam, therefore limiting the stress due to the reduced deformation. This design concept is especially useful for shock environments and random vibrations to prevent the cantilever bend above its fracture strength [54]. In specific, for PVEH's that are designed to have low natural frequencies are most prone to shock environments due to their low stiffness of cantilever beam. The lower stiffness allows larger deformations when subjected to shocks. The maximum shock magnitude that a cantilever beam can survive decreases linearly with the natural frequency of the energy harvesters [55, 60]. A mechanical stopper is also a strategy to increase the bandwidth. With increasing frequency (frequency-up sweep) the cantilever amplitude is limited further by the mechanical stopper causing non-linear oscillations [5, 53]. Yielding in an increased power output over a wider frequency bandwidth. On the contrary, with decreasing frequencies, this appears not to work [5]. Also, the maximum power output drops due to the limitation on vibration amplitude.

Mechanical stopper

Often the mechanical stopper architecture is combined with the encapsulation package that protects the PVEH not only from shocks but also from other environmental influences, for example moisture and dust.

The challenge that brings a mechanical stopper is that it induces extra stresses at other zones other than the anchor point where failure is most common [25, 29], see Fig 3.3a. Z.Wang et al. [60] reports the reliability of shock protection structures including the stress induced due to the impact of the proof mass and mechanical stopper. He showed that the mechanical stopper causes significant stresses at the junction between the cantilever and the seismic mass. Fig 3.3b depicts the stress induced due to the impact of the cantilever mass with the mechanical stopper. When the free-end tip hits the package, the inertia causes the seismic mass to continue moving, deforming the cantilever in an S-shape. Fig 3.3c is the shape of the cantilever after impact. After impact, the cantilever beam vibrates along several normal modes which can also lead to stress concentrations [59]. This dynamic behaviour is highly non-linear and may result in earlier fatigue-induced failure in the cantilever beam. The S-shape

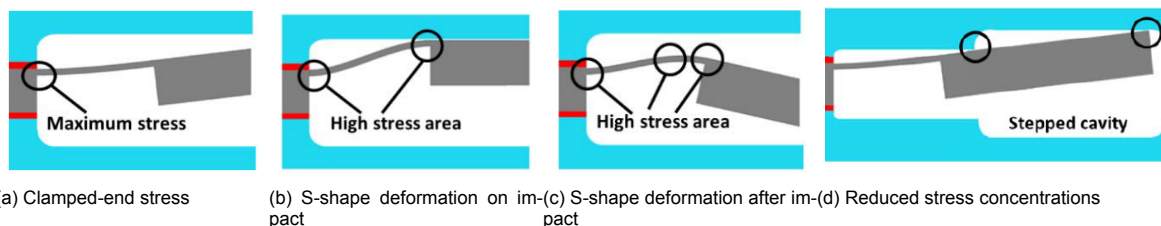


Figure 3.3: Identification of stress locations on excited cantilever beam limited by a mechanical stopper. Adapted from [60]

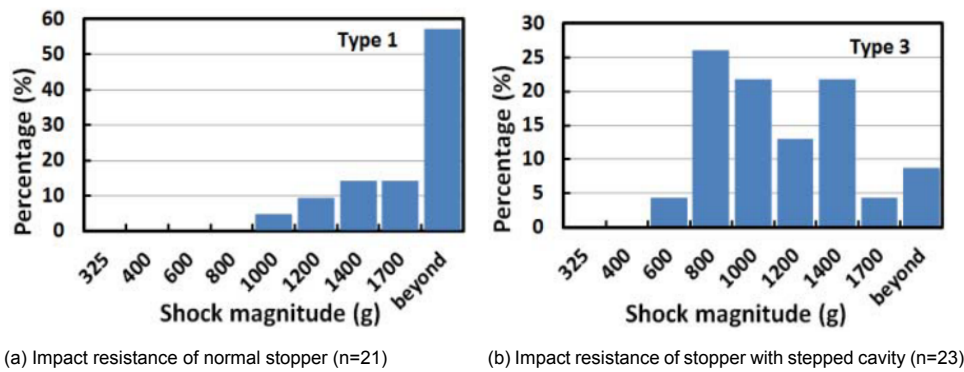


Figure 3.4: **Statistical results of critical shock magnitudes of piezoelectric vibration harvesters with a beam thickness of 50 micrometer. The shock duration is kept constant at 0.7ms. [60]**

deformation implies a second disadvantage, next to the extra stress concentrations. The top layer at the clamped-end of the cantilever beam is in compression and the remainder in tension due to the S-shape deformation. The different strain regions on the same piezoelectric layer cancel the positive charge by the negative charge generated. The opposite also occurs at the bottom piezoelectric layer. As a consequence, the voltage output almost halves compared to a PVEH without a mechanical stopper even though they operate with the same amplitude [29].

Z.Wang et al. proposes the design concept of a stepped cavity as a mechanical stopper, seen in Fig 3.3d, reducing the S-shaped deformation of the cantilever. Experimental results prove the increased shock reliability of the stepped cavity, due to the more constant deformation. Non stepped cavity samples are tested to shocks till 600g, resulting in 70% of the 21 samples that break. Compared to samples with a stepped cavity only 30% of the samples break [60]. Moreover, 60% of the stepped stoppers survived 1700g, while only 4% of the samples without stopper survived 1700g [46].

Proofmass stoppers

Another mechanical stopper design that does not use the external package as deformation limiter is a proofmass in a L-shape, see Fig 3.5. This improves the energy density and reduces the resonance frequency by efficiently increasing the proof mass [26]. This proofmass architecture is used to block the amplitude and to prevent S-shape deformations of the cantilever beam. S.Roundy proposed having on both sides of cantilever the the proofmass limiter[49]. It is expected that the proofmass limiter architecture will increase the shock reliability as well. However, it is discussed in [26] that the bond of the proofmass and the cantilever beam was rather weak resulting in a loss of bonding and failure of the PVEH.

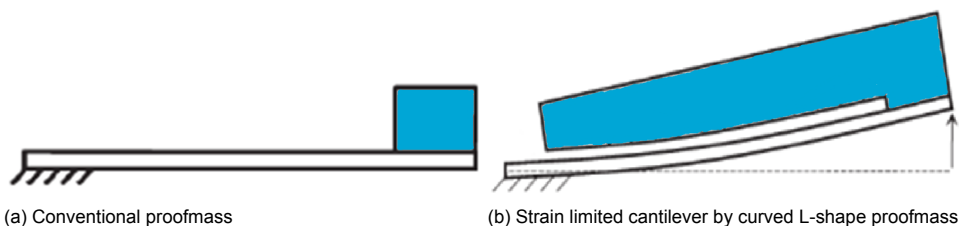


Figure 3.5: **Proof mass stopper design attached to cantilever beam limiting the strain in the cantilever beam. Adapted from [26]**

Strain Limitation

Experimental research in literature shows that strain limitation improves the shock resilience of piezoelectric cantilevers, under the condition no s-shape deformations occur.

3.5. Compressive strain

It is known that most energy harvesters fail due to tensile stress rather than compressive stress [43, 47]. The cyclic loading in compressive strain causes less micro cracking in the piezoelectric, hence increasing the operational lifetime.

M.Gall and B.Thielicke [11] uses a four-point bending test, to measure compressive degradation in PZT patches. It is found that no mechanical damage is detected up to -0.6% strain in quasi-static and cyclic testing (10^5 cycles). Where the same sample would have a quasi-static fracture strength of 0.35% in tensional strain. The decrease of the electrical capacitance under compressive loading suggest that the depolarisation of the ceramic is the cause of decreased performance [11]. This is emphasised by the fact that re-polarisation yields the initial performance. So, compressive cycling of the PZT patch causes reversible electric depolarisation. But this phenomenon is reversible unlike the microcracks in tensional operation.

Energy harvesting in compressive strain can be achieved by pre-loading the piezoelectric layer [37]. Internal compressive stress is achieved by differences between thermal expansion coefficients of the substrate layer and piezoceramic [28]. Some commercially available piezoelectric ceramics configurations exist. THUNDER (Thin Unimorph Driver) is made with substrates of stainless steel and a top layer of aluminium [16, 36]. The other configuration, Lipca-C2, is made of fibreglass and carbon composite layers. The third configuration is named: RAINBOW (reduced and internally biased oxide wafer). All show enhanced strain capabilities [61][35]. Other than the internal compressive loading's external spring loaded configurations are also possible. Schwartz R.W et al. [52] increased the electrical mechanical response by adding elongated springs to pre-load a THUNDER actuator. By adjusting the pre-loading the natural frequency can be changed, increasing the frequency bandwidth [47].

3.6. Discussion







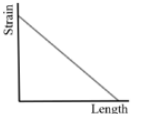

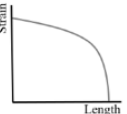
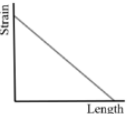
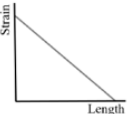
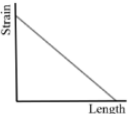
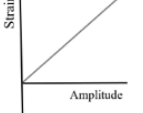
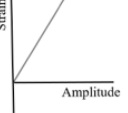
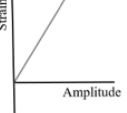
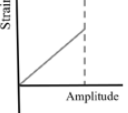
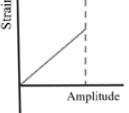
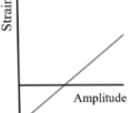
Comparative overview of strain design principles

To summarise the reliability design improvements found in literature, each design principle is evaluated in a comparative Table 3.1. Each design principle is compared against a rectangular cantilever by seven criteria. To begin with the used strain principle. The second and third row visualises the strain along the length of the cantilever and the strain as function of the amplitude, respectively. For the strain-length graph, the strain is measured along the length of the top layer of the cantilever when a fixed downwards amplitude is applied. And for the strain-amplitude graph, the strain is measured at the top layer clamped-end with increasing amplitude. Both graphs show what happens with the strain for each particular design principle. For the strain limitation principle it is assumed, that s-shape deformation is prevented. The amplitude-strain graph for strain distribution design principle is steeper, due to the increased stiffness. The strain limitation is visualised by a shorter strain-amplitude slope. And the slope of compressive strain shifted down, since the PZT is subjected to a compressive force.

The last four criteria in the table are being compared with plus/minus criteria relative to the rectangular cantilever. Where the scale of assessment runs from --, -, o, +, ++. A decrease of performance scores "--" or "-" and an increase of performance scores "+" or "++". The relative decrease or increase compared to the rectangular cantilever determines the single or double math symbol. No relative change is indicated by "o". A negative sign does not imply a negative performance. For example, a decrease of natural frequency is not particularly bad.

The first criteria is the electrical power then can be generated over the area, defining the effectiveness the piezoelectric cantilever converts mechanical energy to electrical energy. For strain homogenised area's the power output is higher due to the larger average strain relative to the rectangular cantilever. For the strain limiting design principles the piezoelectric power output does not change since the geometry of the cantilever does not change. And for the piezoceramic under pre-loading, the piezoelectric coupling is lower since compressive deformation yields less electrical energy output. The frequency bandwidth only increases for strain limitation designs principles, in specific with increasing frequencies (frequency-up sweep). The natural frequency increases with the increased stiffness or with addition of proofmass. Therefore, the distributed strain principle and proofmass limiter has a positive sign. The strain limited design has no relative change. And the compressive strain principle has a

Table 3.1: Comparative overview of design principles for improved PVEH Reliability. The fixed deflection is applied in downwards direction and strain measured at clamped-end top layer or over the length of the cantilever. The performance is expressed by a increase or decrease relative to the rectangular cantilever.

						
Strain principle	none	Strain distribution	Strain distribution	Strain limitation	Strain limitation	Compressive strain
Strain-length graph						
Strain-amplitude graph						
Electrical power/area	o	+	+	o	o	o
Frequency bandwidth	o	o	o	+	+	o
Natural frequency	o	+	+	o	+	+
Impact resistance	o	+	+	++	++	+

higher natural frequency since these cantilevers are often thicker. The impact resistance for all design principles increase relative to the rectangular cantilever, due to the change in stiffness or deformation limitation.

Application of the design principles

The proposed design principles are a guiding concept for engineers during a design process. It emphasises the importance to take in account, in a early design phase, the strain that is induced during operation. Optimising a cantilever structure by homogenising and limiting the strain will result in a longer operational lifetime of the PVEH. The reliability should be stated in the requirements, so it is taken into account during the whole design process.

The design principles can also be combined or integrated in existing energy harvesting devices. Often the rectangular cantilever VEH can be replaced by a tapered design. Important is to keep in mind the increase of stiffness with tapered geometries [18, 38], and therefore lead to a higher natural frequency. This can be compensated by reducing the width/length ratio, the thickness or increasing the proof mass [2]. For the application of the design principles Table 3.1 can be used as reference.

Important to notice is that reliability is not only a function of geometric design principles, in other words the strain. Surface finish of the piezoceramic and ageing properties [13, 34] cannot be neglected. Also environmental influences have a impact on the reliability of the device as well. For example shocks, temperature, moisture and dust reduce the lifetime drastically. Therefore, it is always recommended to have an encapsulation around the energy harvesting devices. Often the inside of the casing is vacuum to reduce damping effects for increased electrical power output. However, this is sometime more detrimental due to the larger deformations.

3.7. Conclusion

In this chapter geometric design principles to improve the mechanical reliability have been addressed. Micro cracking is identified as the number one failure mode for piezoelectric vibration energy harvesters (PVEH) based on cantilevers. The cause for microcracking are tensional strains at strain concentrations and deformations larger than the fracture limit. It was shown that the operational lifetime of the PVEH's is a function of the maximum strain applied.

Design principles for improving mechanical reliability

Strain distribution, strain limitation and compressive strain are found in literature to improve the mechanical reliability of piezoceramic cantilevers. Interestingly no experimental research has been found on the reliability of tapered cantilevers.

The three strain focused geometric design principles are evaluated relative to an one degree of freedom rectangular cantilever and the way strain is optimised for increased operational lifetime. First, the strain distribution design principle that effectively homogenises the strain over the cantilever. The theoretical average strain in the piezoceramic layer is 25% lower in the rectangular cantilever beam compared to a triangular shaped cantilever with the same maximum strain, yielding also a higher electrical output. Secondly, a stepped mechanical limiter and curved L-shape proof mass are effective strain limitation design principles. Since, they prevent too large strains and s-shape formations. Thirdly, operation in compressive strain reduces the tensile strain and therefore the chance of micro cracks. Overall, it can be concluded that these three design principles should be taken into account in an early design phase.

4

Experimental study to tapered cantilever energy harvesters

4

Based on the findings of the previous chapters an experimental research is conducted towards the reliability of tapered piezoceramic cantilevers. This chapter shows the first experimental research on the reliability of tapered cantilevers.

Reliability of Tapered Bimorph Piezoelectric Energy Harvesters - an Experimental Study

J.A.Brans, T.W.A.Blad, T.R.Mahon, W.A.Groen and N.Tolou

Abstract— Cantilever piezoelectric energy harvesting from ambient vibrations is a viable solution for powering wireless sensors and low-power electronics. However, the greatest issue preventing these systems from being widely used is their poor reliability. With the aim to maximise their power output, the devices are often operated close the fracture strength, which results in cracks in the brittle piezoceramic layer. Tapered cantilevers are suggested to improve the mechanical reliability. A relative comparison is made between tapered piezoelectric cantilevers and conventional rectangular cantilevers in terms of reliability and power output. Tensional strains causing fractures show serious reduction of power output and eigenfrequency. Moreover, for large accelerations causing deflections lower than the fracture strength, electrical degradation takes place. Experiments show that tapered cantilevers have a higher power output per unit area.

Keywords—Mechanical reliability, PZT, vibration energy harvester, tapered cantilever

I. INTRODUCTION

Vibration energy harvesting provides long term alternatives to replaceable batteries across a number of applications. The most attractive applications are found in environments where battery replacement is expensive, inconvenient and/or prohibited by regulations. Examples of such applications are medical implants such as pacemakers or sensors for the internet of things.

The working principle of piezoelectric vibration energy harvesting is based on the piezoelectric effect. The piezoelectric ceramic material converts mechanical strain to electrical power that can be used to power small (wireless) devices. The piezoelectric effect results from pressure on ceramic crystals yielding an electric potential. Most vibration energy harvesters are based on one degree of freedom cantilever beam spring structure [1–3].

However, piezoelectric vibration energy harvesters (PVEH's) suffers from low reliability and high dependency of excitation in resonance frequency. With the aim to gain maximum energy output the piezoelectric vibrational energy harvesters are operated at their maximum deformation, resulting in fractures in the piezoceramic layer where strain is the largest. In practice, high reliability is required for their desired applications.

Prior arts suggest three ways to improve the reliability of the PVEH's[4]; use stoppers to limit the strain, apply compressive strain at the piezoceramic by the composite and thirdly tapering the piezoelectric cantilevers. The first design principle, limiting the strain, shows experimentally improved shock resistance[5–7]. Strain distribution design principle is suggested by multiple researches to improve the lifetime of



Fig. 1: Three bimorph tapered piezoelectric cantilevers shaped by abrasive water cooled cutting for reliability and power output experiments.

the PVEH's [8–10]. However, previous work on the reliability of tapered piezoelectric cantilevers is only theoretically investigated. To the authors knowledge experimental research is lagging.

The goal of this research is to explore the influence of tapering on the reliability and power output of piezoelectric cantilevers. This research proposes tapered Lead Zirconate Titanate (PZT) cantilevers for PVEH for improving the reliability. The experimental research objective is to find the influence of tapering on the reliability and power output for piezoelectric energy harvesting.

In Section II the experimental method and test setup are explained. The results from the experiments are presented in Sections IV and V. Section VI compares the findings and evaluates the results. The conclusions are drawn in section VII.

II. METHOD

Piezoceramic samples

The samples used for the experiments are bimorph Morgan Advanced Ceramics High Performance PZT-508. These are chosen for two reasons. First of all, for their high reliability and efficient energy harvesting properties. Secondly, because of the bimorph structure and parallel polarisation. This makes it possible to distinguish power output between the top and bottom layers of the piezoelectric cantilever. The properties and dimensions of the three cantilevers are listed in Table I. Where L , w and t are the dimensions of the cantilever. L_0 is the free length of the cantilever. The mass and capacitance of the free vibrating area are given by m_0 and C_{p0} .

TABLE I: Properties and parameters of PZT508 samples

	Rectangular cantilever	50% tapered cantilever	100% tapered cantilever
L	47.0 mm	47.0 mm	47.0 mm
L_0	34.0 mm	34.0 mm	34.0 mm
w	4.0-4.0 mm	4.0-2.0 mm	4.0-0.0 mm
t	0.8 mm	0.8 mm	0.8 mm
m_0	$0.950 \pm 0.005g$	$0.737 \pm 0.021g$	$0.634 \pm 0.015g$
C_{p0}	$28.0 \pm 1.17nF$	$18.8 \pm 0.64nF$	$15.5 \pm 0.83nF$

Two different taperings of the conventional rectangular piezoceramic cantilever are made to find relationships between the degree of tapering, the power output and reliability. The 50% tapered and 100% tapered PZT cantilevers are shaped by water cooled abrasive diamond cutting (Struers Secotom-10). This shaping process is preferred over laser cutting or sawing, because of the low shear stresses and minimal temperature effects. In order to verify the constancy of the shaped samples the individual masses and capacitance are measured, see table I. In total there are 21 samples, 7 for each shape. No large deviations are found, therefore all samples are accepted for the reliability test.

Test setup

A schematic drawing of the setup can be found in Figure 2. Vibration Exciter type 4809 and amplifier of Brüel and Kjær are used for generating vibrations. The data is acquired by a National Instruments BNC compact DAQ 9215 and processed in Matlab with the Data Acquisition toolbox. The shaker is feedback controlled for constant peak accelerations at the base of the PZT cantilever. The acceleration is measured by PCB accelerometer model Y356A32. The input frequency and amplitude of the shaker is generated by a Keysight 33220A function generator. The deflection of the piezoceramic cantilever is measured by two Keyence LK-H052 and LK-H022 laser distance sensors. The power output of each piezoelectric layer is measured over a decade resistance box.

Experimental method

The experimental method can be divided in two parts. The quasi-static deformation and dynamic deformation experiments. Before each experiment the PZT cantilevers are characterised by a frequency and resistance sweep as a reference baseline. A resistance sweep from 100 Ω to 200 $k\Omega$ is performed, at the conditions of 1g constant peak acceleration and at the eigenfrequency of the cantilever. The matched optimal resistance for each tapered cantilever is used in further experiments. In order to quantify the power output over the frequency spectrum a frequency sweep from 300Hz to 730 Hz is performed with a resolution of 2 Hz at 1g constant peak acceleration. The power output of each layer is calculated over the optimal resistance for 1 second. The total average power output for each frequency is the sum of both layers. As an extra verification the deflection is also measured. With this

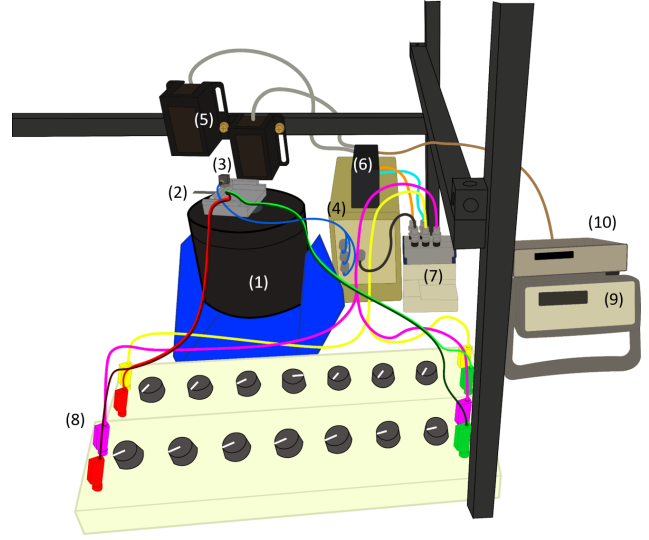


Fig. 2: Illustrated figure of the vibration test setup for clearly depicting the individual components and wire connections. With the following hardware present: (1) Shaker, (2) Piezo cantilever, (3) Accelerometer, (4) Accelerometer signal conditioner, (5) Laser distance meter, (6) Laser distance controller, (7) DAQ, (8) Resistance box, (9) Function generator, (10) Power supply

data a reference baseline is set for the intact PZT cantilevers.

A quasi-static deformation experiment is performed on the three different PZT cantilevers to identify the static fracture strength. A PI linear stage(M505) with Futek force sensor is used for the force deflection test setup. The PZT cantilevers are clamped at the base with the same aluminium clamping being used in other experiments. The piezoceramic cantilevers are deformed by a sphere ball ($\varnothing 0.5mm$) with a point of application 4mm from the tip. The point of application could not be exactly at the tip, due to the lack of area at the tip of 100% tapered cantilevers and the lateral shift of the point of application during deformation. As an extra verification an audio recording of the fracture is made during the measurement. After the quasi-static deformation experiment a same frequency sweep as before the quasi-static deformation is performed. In order evaluate the severity of fractures in the material.

The last experiment is conducted to achieve deformations equal to the quasi-static deformation caused by vibrations. In order to achieve these large deformations, a tip proofmass of 0.88 gram is added at the tip. The new frequency and optimal resistance of the PZT cantilevers with proofmass are found by a frequency and resistance sweep. The power output at the frequency sweep is measured from 50 to 200 Hz at 1g acceleration. Deforming the PZT samples to large deformations an acceleration sweep is performed from 1 to 35g at the eigenfrequency and optimal resistance. During the measurement deflection and voltage output are measured.

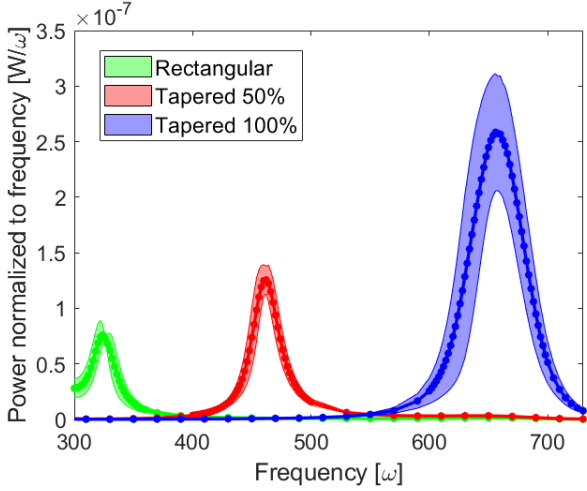


Fig. 3: Frequency sweep at 1g constant maximum acceleration showing the eigenfrequency of the three different cantilevers ($n=7$). The power output is normalised by the frequency of the cantilever for relative power comparison.

III. CHARACTERISATION

Optimal resistance

The matched resistance can be found analytically by equation 1.

$$R = \frac{1}{\omega C} \quad (1)$$

Where ω is the eigenfrequency in open loop in rad/s and C the capacitance in nF). The analytical optimal resistance for the rectangular, 50% tapered and 100% tapered cantilever are respectively 16.9, 18.4 and 16.6 $k\Omega$.

The optimal resistances of the tapered cantilevers are experimentally found by performing the resistance sweep at the respective open loop eigenfrequency. Experiments show that the optimal resistance are at 28, 43 and 21 $k\Omega$ for the rectangular, 50% tapered and 100% tapered cantilever respectively.

Normalised power output

The respective power output of the three cantilevers is identified by a frequency sweep. To make a fair comparison between the different eigenfrequencies of the cantilevers, the power output of the energy harvester is normalised by the input power and frequency. Since, the input vibrational power of the shaker scales proportionally with the input frequency ($P \propto \omega$) and input acceleration ($P \propto a$) [11]. The power output normalisation is done by equation 2.

$$P_{norm} = \frac{P}{\omega a} \quad (2)$$

Where ω is the frequency and a the peak acceleration at the clamping. Since the acceleration is kept constant the normalisation is done by dividing the power by the frequency. The results of the frequency sweep can be found in Figure 3. The shaded areas represent standard deviation of the measurement. It can be seen that the 100% tapered

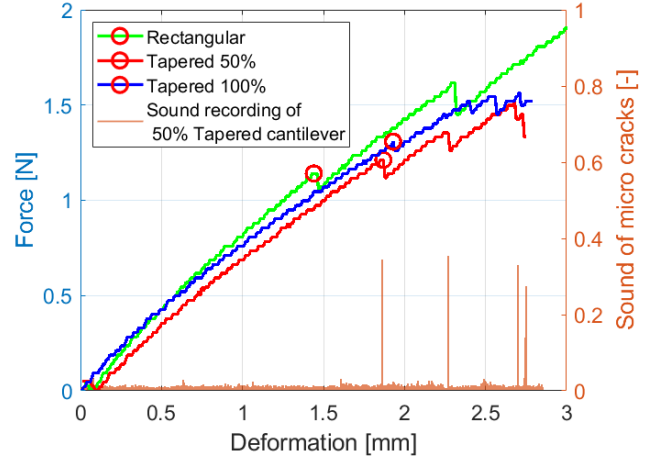


Fig. 4: Force-deflection curve at static deformations initiating cracks in ceramic material shown by the red circle markers that is audible shown in this graph by the red audio peaks.

cantilever generates significantly more power compared to the conventional rectangular cantilevers. Tapered cantilevers generate more power per unit area therefore less deformation is needed to harvest the same power as rectangular cantilevers.

The resulting displacements of the tip and base the deformations are measured. The following deformations at eigenfrequency are found for respectively the rectangular, 50% tapered and 100% tapered cantilevers, 0.018 ± 0.003 mm 0.029 ± 0.001 mm and 0.037 ± 0.04 mm.

IV. QUASI-STATIC DEFORMATIONS

Quasi-static deformation experiment

Figure 4 depicts the results of the quasi-static deformation experiment. The first internal crack at a static deformation occurs around 1.4mm. This can be seen in the graph by the sudden drop of the blocking force. Larger strain levels lead to increased cracking. During the experiment the occurrence of the cracks was also audible, indicated by the red spiked line at the bottom of Figure 4.

Fig 5 shows a frequency sweep showing the destructive consequences of internal cracks in the material. The power output drops significantly. Moreover, the eigenfrequency drops approximately with 10%. Important is to realise that in practice, the eigenfrequency does not longer match with the input frequency of the application. This causes a power output reduction of at least 50% for the application.

Since the experiments are done with a bimorph parallel poled cantilever, the voltage output of the top and bottom layer can be compared. The piezoceramic layer deformed in tension has a voltage output of half the voltage output of the layer deformed in compression. The lower voltage output at the top piezo layer can be related to the fractures in the material.

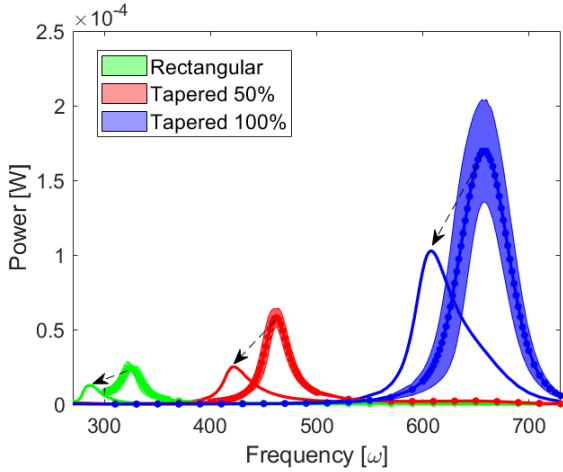


Fig. 5: Frequency sweep at 1g showing the drop in eigen frequency and power output of the three different tapered samples after quasi-static deformation.

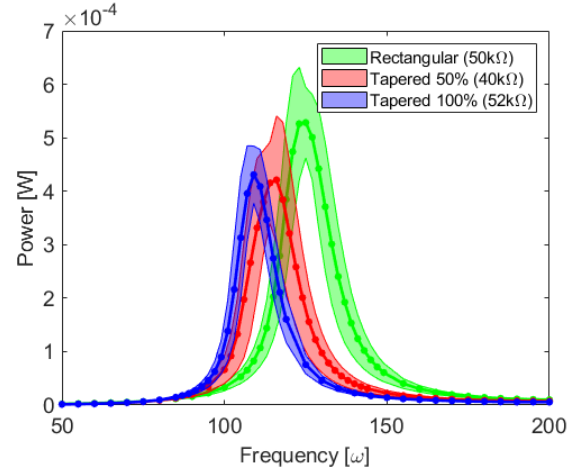


Fig. 6: Frequency Sweep at 1g constant peak acceleration with a proofmass of 0.88 gram at the tip of the PZT cantilevers. n=3

V. DYNAMIC DEFORMATIONS

A. Mechanical Degradation

In energy harvesting applications, the piezoceramic cantilevers are not subjected to static deformations. To find the mechanical degradation of the piezoceramic cantilever under dynamic vibrations an acceleration sweep is performed. Figure 6 shows the respective eigenfrequencies of the PZT cantilevers with tip proofmass. Due to the added mass the eigenfrequencies are lower and power output increases.

Results of the acceleration sweep can be found in Figure 7. Three observations are made. First, the fracture behaviour can be observed at accelerations larger than 20g. This is in line with deformations larger than the static fracture deformations shown in Figure 4. Secondly, the 100% tapered cantilevers deform less compared to the rectangular and 50% tapered cantilevers for increasing accelerations. Third, the deformations gradually flattens out by increasing accelerations. This is due to the shift in eigenfrequency caused by the fractures in ceramic material. The quality factors for the rectangular, 50% tapered and 100% tapered decreases from 10.5 ± 0.07 , 10.4 ± 0.07 and 8.0 ± 0.05 to 2.3 ± 0.7 , 1.2 ± 0.5 and 1.8 ± 0.6 respectively. Based on these results one would expect a power output that is proportional to the deformation.

Power output at large deformations

However, it is found that before fracture of the PZT ceramic takes place already some electrical degradation occurs. Figure 8, shows the power output by acceleration. At peak accelerations around 5-10g the power output does not increase further. Looking at the voltage output of the piezoceramic cantilever it can be seen that the voltage drops at maximum deflection. In other words, larger deformations do not yield more electrical power output.

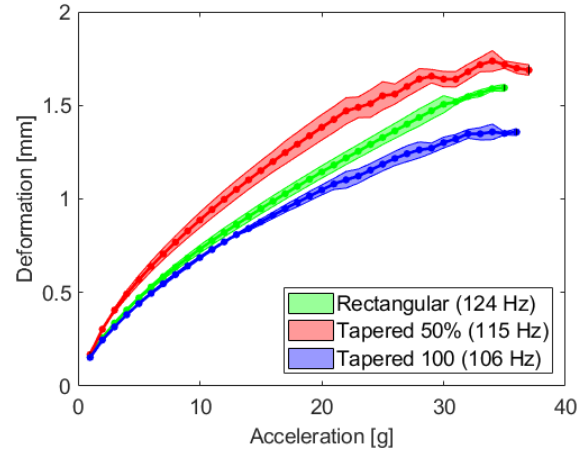


Fig. 7: Acceleration sweep at eigenfrequency showing the gradually levelling of the maximum deformation due to induced fractures in the PZT ceramic material. n=3

VI. DISCUSSION

Fracture induced dynamics

Experiments show that fractures in the ceramic material lowers the eigenfrequency. This can be explained by the reduction of stiffness after fracture. The reduction of stiffness can be observed in the force-deflection graph. Additionally, the cracks in the piezoceramic material cause a softening effect of the cantilever. The microcracks act as a hinge, with lower stiffness than the surrounding ceramic material. This causes a geometric non-linearity in the PZT cantilever. The effect can be seen in Figure 5.

Power output at large deformations

For small accelerations the PZT cantilevers show to have an expected power output proportional to the increase of acceleration. However, the power output drop at large accelerations seen in Figure 8 could not be explained with the performed measurements. The voltage drop suggests

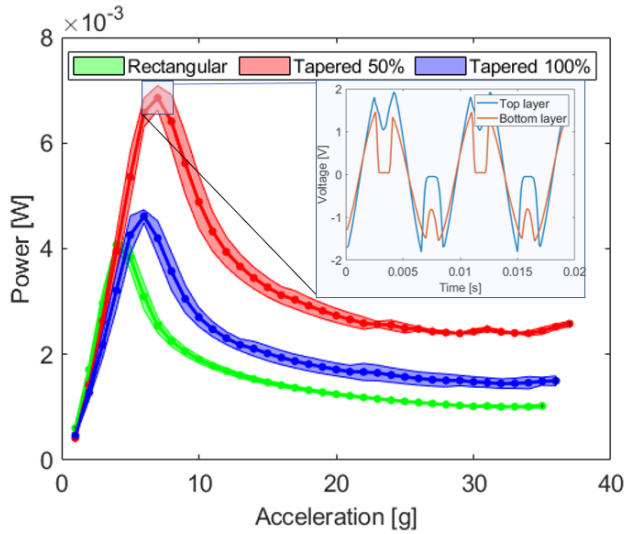


Fig. 8: Electrical power output at eigenfrequency for increasing accelerations. The peak of the electrical power output of the 50% tapered cantilever is highlighted by a graph showing the respective voltage output for 2 cycles.

that the electrical contacts of the ceramic layers opens and short circuit the voltage. The studies of P.Pillatsch [12, 13] measured capacitance to detect broken electrical contacts. In the deflected state a drop of capacitance should be measured. However, no drop of capacitance is measured in the fractured samples used in the experiments. This suggests that the electrodes on the PZT cantilevers stays intact during the experiments.

Future recommendations

Three recommendations are given for future research. First, abrasive cutting of PZT samples is the preferred method for shaping PZT cantilevers. Secondly, sound recording could be used in experiments to identify the event of fractures in PZT bimorph cantilevers. Finally, the power output from the acceleration sweep could not yet been fully explained by the preformed experiments. Future research is required to find the underlying cause of the drop of the voltage output at deformations smaller than the fracture strength.

VII. CONCLUSION

This paper presents experiments on the degradation of piezoelectric cantilevers for application of energy harvesting. It can also be concluded that tapered cantilevers generate more power per unit area. Therefore less deformation is needed to harvest the same power as rectangular cantilevers. The static deformation at which the cantilevers fracture is found. The fractured PZT cantilevers show a significant reduction of eigenfrequency and power output, due to the reduced stiffness caused by the fractures. Interestingly it is found that, dynamically deforming the PZT cantilevers at eigenfrequency show a power drop that occurs before fracture of the piezoceramic material takes place. This dramatically reduces the power output for larger deformations. This

effect can not be explained by the performed experiments. Further research is needed to find the underlying cause of the voltage drop.

REFERENCES

- [1] S.P. Beeby, R.N. Torah, and M.J. Tudor. "Kinetic energy harvesting". In: *Energy Harvesting for Autonomous systems*. Ed. by Neil Beeby Stephen; White. January. Artech House, 2010. Chap. 4, pp. 91–134. ISBN: 978-1-59693-718-5.
- [2] Steven R Anton and Henry A Sodano -. "A review of power harvesting using piezoelectric materials (2003-2006)". In: *Smart Materials and Structures* 16 (2007). DOI: 10.1088/0964-1726/16/3/R01.
- [3] Tom J. Kazmierski and Steve Beeby. *Energy Harvesting Systems : Principles, Modelling and Applications*. 2011, p. 101. ISBN: 9781441975652. DOI: 10.1007/978-1-4419-7566-9.
- [4] J.A. Brans, T.W.A. Blad, and N. Tolou. "A Review of Design Principles for Improved Mechanical Reliability of Cantilever Piezoelectric Vibration Harvesters". In: *Institute of Electrical and Electronics Engineers (IEEE)*, Feb. 2020, pp. 408–415. DOI: 10.1109/iccma46720.2019.8988762.
- [5] Ziyang Wang et al. "Shock Reliability of Vacuum-Packaged Piezoelectric Vibration Harvester for Automotive Application". In: *Journal of Microelectromechanical Systems* 23.3 (June 2014), pp. 539–548. ISSN: 1057-7157. DOI: 10.1109/JMEMS.2013.2291010.
- [6] M. Renaud et al. "Improved mechanical reliability of MEMS piezoelectric vibration energy harvesters for automotive applications". In: *2014 IEEE 27th International Conference on Micro Electro Mechanical Systems (MEMS)*. IEEE, Jan. 2014, pp. 568–571. ISBN: 978-1-4799-3509-3. DOI: 10.1109/MEMSYS.2014.6765704.
- [7] Wen G. Li, Siyuan He, and Shudong Yu. "Improving power density of a cantilever piezoelectric power harvester through a curved L-shaped proof mass". In: *IEEE Transactions on Industrial Electronics* 57.3 (2010), pp. 868–876. ISSN: 02780046. DOI: 10.1109/TIE.2009.2030761.
- [8] S. Roundy et al. "Improving Power Output for Vibration-Based Energy Scavengers". In: *IEEE Pervasive Computing* 4.1 (Jan. 2005), pp. 28–36. ISSN: 1536-1268. DOI: 10.1109/MPRV.2005.14.
- [9] P Glynne-Jones, S P Beeby, and N M White. *A method to determine the ageing rate of thick-film PZT layers*. Tech. rep. 2001, pp. 663–670.
- [10] Jessy Baker, Shad Roundy, and Prof Paul Wright. "Alternative Geometries for Increasing Power Density in Vibration Energy Scavenging for Wireless Sensor Networks". In: *3rd International Energy Conversion Engineering Conference* (2005). ISSN: 2005-5617. DOI: 10.2514/6.2005-5617.

- [11] Paul D. Mitcheson et al. “Energy harvesting from human and machine motion for wireless electronic devices”. In: *Proceedings of the IEEE* 96.9 (2008), pp. 1457–1486. ISSN: 00189219. DOI: 10.1109/JPROC.2008.927494.
- [12] P. Pillatsch et al. “Degradation of piezoelectric materials for energy harvesting applications”. In: *Journal of Physics: Conference Series* 557.1 (2014). ISSN: 17426596. DOI: 10.1088/1742-6596/557/1/012129.
- [13] P. Pillatsch et al. “Degradation of bimorph piezoelectric bending beams in energy harvesting applications”. In: *Smart Materials and Structures* 26 (2017). DOI: 10.1088/1361-665X/aa5a5d.

5

Discussion

The results of this research are discussed in this chapter. A critical view is given on the relevance of the results, generalisation and the limitations of the of the results with the given assumptions. Finally, a reflection is given on the research activities that contributed to the results.

5.1. Relevance

Theoretically piezoelectric vibration energy harvesting show to have great potential replacing batteries. Making replacement of batteries unnecessary, reducing the maintenance costs. However, industries are restrained in using piezoelectrics for energy harvesting because of the brittleness of the material and high demands of customers on the reliability. This research confirms worries of the industry. Results show the severity of too large deformations in the material on the significant drop of power output.

This research has contributed to a more reliable piezoelectric vibrational energy harvester. This will be the first step towards higher reliability of self powered autonomous devices, bringing piezoelectric energy harvesting closer to the implementation in industry.

5.2. Generalisation & Limitations

The assumptions that were made in this thesis constrain the applicability of the results. Most important limitations are listed below, and some thoughts about their impact and validity are shared.

The power output experiments are performed only on sinusoidal input frequencies and over simple resistance. First, for real world applications the ambient vibrations are mostly chaotic. Therefore, the efficiency of the piezoceramic cantilevers will be significantly lower. Secondly, the energy harvester will be connected to an electrical circuit, probably consisting of a rectifier, resistances and capacitors. However, in the academic world the sinusoidal input frequencies and simple electrical circuits are still the preferred way to benchmark piezoceramic energy harvesters.

Quasi-static deformations and dynamic excitation's are used to damage the piezoceramic cantilevers and find the influence on the dynamics. In real world applications the piezoceramic cantilevers will not only suffer from these excitation's. It will probably be more likely that impacts are the cause of piezoceramic degradation.

The conclusions are drawn for a specific material with excellent material properties compared to other piezoceramic cantilevers. This generalisation can be questioned. There exist great variety in other piezoceramic cantilevers on the market. Since, most cantilevers are composites they are build of various layers. Therefore, it is not possible to draw generalised conclusions on the absolute values of the results. However, relative comparisons between the three tapered design can be made.

5.3. Reflection

For a project taking months to complete, it is learned that, it is most important to focus on the process and enjoyment rather than the results. The project has been mostly curiosity driven, dealing with challenges is most important. A brief reflection on these challenges will be given.

Starting with the beginning of the project, forming a research objective and creating an overview of the state of the art in the field of energy harvesting was challenging. Discussions with colleagues and fellow students helped in finding the real challenges in the field of piezoelectric energy harvesting. Which bring us to the reliability part of the research. During bachelor and master projects no attention has been paid to durability or reliability. Most prototypes survived only the testing day, if you were lucky. This research challenged the researchers to think two steps forward, preventing loss of piezoceramic samples due to unnecessary mistakes.

The development of the experimental setup is considered a strong point of the research. Much thought has been given to the choice of sensors and equipment, this payed out when doing the experiments. This is shown by the ability to capture high frequencies and at the same time extremely low amplitudes. Also, the piezoelectric samples have been made with great care. Which is shown by there outstanding properties. Compared to other researches this research differentiates itself from other researches concerning the great sample size that has been used. Last but not least, the biggest lesson learned is when having vibrations, 3D printed materials act as rubber. The system as a whole should be considered as a combination of individual springs acting together. Changing the 3D printed

materials to aluminium counterparts solved this problem. All with all new skills were acquired, including setting up an experiment, academic writing, conducting a literature review, being critical and open at your own results and managing your own project.

Still there are challenges ahead, while measurements did not always yield into directly explainable results. However, the activities contributed to the process of creating more insights. In Figure 5.1 an overview is given of the main research activities. Three attempts will be highlighted. Firstly, an experimental impact setup has been made. The initial goal was to use this for developing impact energy harvesting mechanisms or impact testing of piezoceramic cantilevers. Eventually, shakers ended up to be more consistent for the research objective. Nevertheless, this developed impact setup could be of great value for future reliability testing of mechanical stoppers. Secondly, attempts have been made to develop a model finite element model in Matlab by partial differential equations, as can be found in Appendix G. Initially the choice for using Matlab instead of Comsol or Ansys programming, was that it would give more insight in what is happening with the math behind it. The main challenge was to define the initial conditions and the electrical boundary conditions for the piezoceramic layer. Effectively, this side path gave an understanding of the multiphysic properties of piezoelectrics. Finally, an attempt has been made to analytically calculate the eigenfrequency of the tapered cantilevers based on the material properties. Interestingly, the resulting equation shows that the eigenfrequency of tapered cantilevers without proofmass is the same as rectangular cantilevers. Which is in contradiction with the results of the experiments.

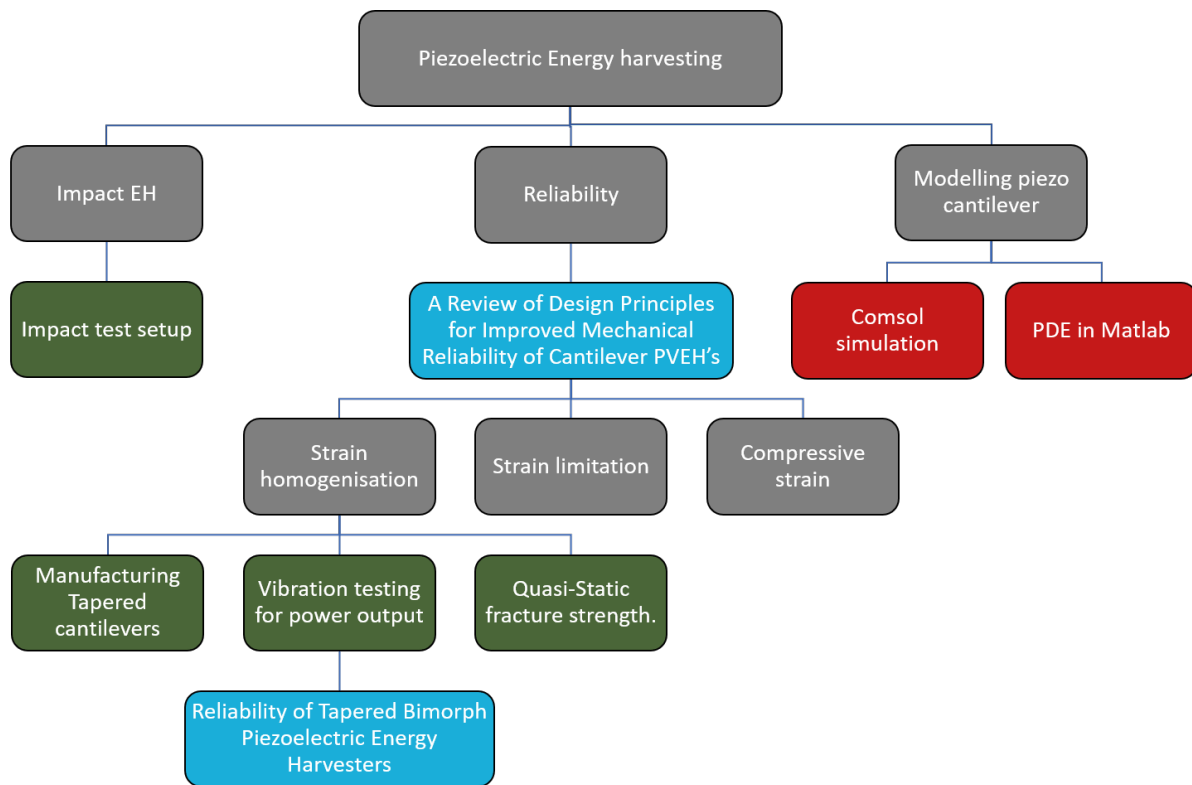


Figure 5.1: Flow chart of research activities and achievements. Red boxes indicates numerical and simulation work. The green boxes indicates experimental research and practical activities. The blue boxes show the resulting articles of the research activities.

6

Conclusions

All the findings and answers to the research questions are given in this chapter. First, the findings on the sub questions will be presented. Secondly, some recommendations are given for the two main stakeholders of the research. Finally, some future research recommendations are given for fellow bachelor and master students.

6.1. Conclusions

The research objective of this thesis was to improve the reliability of piezoceramic cantilever energy harvesters. The failure mechanisms are identified and specific design principles are given for engineers to improve reliability. All in all, it can be concluded that tapered cantilevers are a reliable replacement for conventional rectangular piezoceramic cantilevers without sacrificing power output. The research questions will be answered below:

What are the main failure causes of piezoceramic degradation?

Micro cracking is identified as the number one degradation mechanism for PVEH's. The cause for microcracks are tensional strain and deformations larger than the fracture strength. It is found that the operational lifetime of the PVEH's is a function of the maximum applied strain. Other degradation mechanisms are ageing, high relative humidity and temperatures above the Curie temperature.

What geometric design principles are used in literature to increase the reliability of PVEH's?

All design principles for improved mechanical reliability can be classified by three strain principles: strain distribution, strain limitation or strain inversion. An overview has been made to evaluate the geometric design principles relative to a conventional one degree of freedom rectangular piezoceramic cantilever. First, strain distribution design principle effectively homogenises the strain over the cantilever by tapering the cantilever. Theoretically the average strain in the rectangular cantilever is 25% lower compared to a triangular cantilever with the same maximum strain, therefore yielding also a higher electrical output. Secondly, materials with pre-stressed compressive strain show to have a higher tolerance to deformations. This is in line with the compressive strain design principle. Thirdly, a mechanical limiter and blocking proofmass are effective strain limitation design principles. Especially for operating environments which are prone to impacts and low frequency energy harvesters. Overall, it can be concluded that the three design principles contribute to the development for more reliable energy harvesters.

What is the influence of tapering of PZT cantilevers on the power output and reliability

Long slender PZT tapered cantilevers have a higher power density per unit area compared to the conventional rectangular cantilevers. Therefore the tapered cantilevers can be less deformed compared to the conventional rectangular cantilevers for the same power output. Which is beneficial for the reliability for vibrational energy harvesting. Experiments show that deformations larger than the fracture strength of the PZT ceramic cause fractures in the brittle material. This causes a drop of eigenfrequency and voltage output, resulting in a serious reduction of power output for the application.

6.2. Recommendations

There are two main stakeholders in this research project: the engineers and researchers. The recommendations will be specified for both parties.

In the engineering aspect it can be kept short. For development of future energy harvesters higher power densities can be achieved by using tapered cantilevers. Knowledge of the environmental operating conditions is important for setting the reliability requirements. When impacts are likely to happen, it is recommended to include also mechanical stoppers in the design. The fracture strength of PZT cantilevers should also be a constraint in energy harvesting design. The goal for enhancing the power output of piezoelectric energy harvesters is not meaningful without taking material strength into consideration in the design process. Last but not least, development of very sophisticated energy harvesters will be worthless, when it fails to deliver the designed performance.

In the research aspect, only the tip of the ice berg is shown. More research is required for improving the reliability of piezoceramic cantilevers. It is recommended to look at the cause that influences the drop of power output for large accelerations, before fracture occurs. Secondly, for on the long term, a replacement material for the PZT cantilevers that do not contain lead is required. Current replacement

materials do not come close to the piezoelectric properties of PZT. And are therefore not yet a suitable replacement. Other recommended future research projects are listed in the next section.

Finally, some more general and practical recommendations are listed below that could be helpful for future work.

- Abrasive cutting is the preferred method to shape PZT materials.
- Soldering electrical connections to PZT cantilevers is recommended above using double sided conducting tape or conductive epoxy glue.
- Use 3D printing for developing and prototyping. However, when it comes to testing consider using other materials.
- Experimentally testing is often more convenient than using simulation programs.
- Always question yourself; "if what you see is what you get". Validate your results. Are they consistent with what you expected?
- Do not save time on building a test setup. Eventually, you will regret not having an trustworthy and easy to use experimental test-setup.
- When you are new in piezoelectric field it can be hard to understand the multiphysics material behaviour of piezoelectrics. Recommended is to start with reading books, for example: "An Introduction to Piezoelectric Materials and Applications" or "Piezoelectric Energy Harvesting: Modelling and Application".

6.3. Future research recommendations

Below some interesting future researches are listed. The possible projects are separated for Bachelor and Master students.

Bachelor projects

- Automated frequency and resistance sweep to find the optimum settings for the highest power output.
Challenges: Automate resistance sweep and control
- Piezoelectric step counter. How many steps did a cow or human make?
Challenges: Low frequency, electronic system design and use the harvester simultaneously for sensing (counting steps).
- Ortho-planar springs
Challenge: Deal with s-shape deformations. Segmented electrodes could be the solution.
- What is the preferred clamping design or method in terms of reliability and power output for piezoceramic cantilevers?
Challenges: Literature research what is currently being used. And experimentally compare various clamping designs

Master projects

- Research the potential of piezoelectric impact energy harvesting by a zero stiffness compliant mechanism that translates low frequency large amplitudes to high frequency low amplitude vibrations.
- Develop a segmented piezoelectric energy harvester that allows s-shaped deformations. Challenges: Manufacturing techniques.
- Micromachined PZT cantilever based on SOI structure for low frequency vibration energy harvesting. Challenges: The trade-off between miniaturisation and resonance frequency.
- Investigate the reliability of magnetic stoppers for shock environments. It is assumed that the magnetic forces instead of physical contact improves the operational lifetime of the piezoelectric VEH. Challenges: build a representative energy harvesting system where the right conclusions could be drawn for comparison of mechanical stoppers.
- Develop circular ortho-planar piezoelectric structures for vibrational energy harvesters.
Challenges: deal with s-shape deformations and optimisation of energy density.

Acknowledgements

I am fortunate to have many friends that are supporting me in my work. Most of them are approached, some of them many times, with questions or for good discussions about the topic. I apologise for not mentioning them all.

A few persons played a major role in making this research happen. In no specific order, I would like to thank my supervisors Thijs Blad and Nima Tolou. Nima Tolou for his inspiring course on compliant mechanisms, sparking my interest in vibration energy harvesting. Thijs Blad for being supportive throughout the whole project and open for questions any time. I could not have wished for a better supervisor.

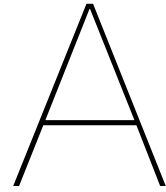
I would like to thank Pim Groen and Tadhg, from the aerospace faculty, for supplying me with the piezoceramic cantilevers and practical information regarding PZT cantilevers.

Other people I would like to acknowledge that have been contributing to this research and helped me in the process of building my experimental test setup are the technical support staff of PME. I really appreciate the advice they gave on all the practical things of the experiments. We students might be good in solving equations, but you guys really know how to turn those equations into something physical.

Secondly, I would like to thank the "Squad" for providing almost infinitely supplies of caffeine and cookies. Giving me a daily rhythm and positive feedback.

Not to mention, all the people I got to know while studying in Delft. Especially, students from the fraternities Sint Jansbrug and Slopend. You demonstrated that student life encompasses much more than the curriculum one is ought to complete. Every single one of you should know I am sincerely grateful for the memories we share.

I would like to thank my family, in specific my parents, for the support during the project and prior years making this possible. Last but not least, I owe my gratitude to my beloved girlfriend, Femke Luijten. I cannot express how much I appreciate your mental support to bring the subject to a successful ending.



Literature paper

Included in this appendix is the original literature review, that has been presented at the 7th International Conference on Control, Mechatronics and Automation (ICCMA) conference in Delft on 6th of november 2019.

A Review of Design Principles for Improved Mechanical Reliability of Cantilever Piezoelectric Vibration Energy Harvesters

J.A. Brans

Biomechanical Engineering
Technical University of Delft
Delft, The Netherlands
j.a.brans@student.tudelft.nl

T.W.A. Blad

High-Tech Engineering
Technical University of Delft
Delft, The Netherlands
t.w.a.blad@tudelft.nl

N. Tolou

High-Tech Engineering
Technical University of Delft
Delft, The Netherlands
n.tolou@tudelft.nl

Abstract—Vibration energy harvesters based on piezoceramics can provide a sustainable source of energy for low-power electronics. The greatest issue preventing these systems from being widely used is their poor reliability. With the aim to maximise their power output, the devices are often operated close the point of yielding, which results in microcracks and fatigue in the piezoceramic layer. This paper offers a comparative review of design principles that aim to improve the reliability of piezoelectric vibration energy harvesters. Three different design principles are investigated with the focus on strain limitation. The results show that strain homogenisation, strain limitation and compressive strains can be effective design principles to increase reliability without sacrificing efficiency.

Keywords- Mechanical reliability, piezoelectric, vibration energy harvester, MEMS

I. INTRODUCTION

Increasing interests in the internet of things and small medical implants requires a new way of providing power [1, 2]. Nowadays, most autonomous devices rely on battery power. The use of conventional batteries implies disadvantages, such as the finite energy supply. Therefore, continuous replacement is necessary increasing the maintenance cost. The replacement is often impractical for difficult to reach applications, for example in Tire Pressure Monitoring Systems (TPMS) [3, 4] or artificial cardiac pacemakers [5]. Moreover, batteries are made of chemical resources and demand a large footprint on the device. The rotary and bio-implanted applications or other low power electronic devices could be powered by vibration ambient energy, diminishing the disadvantages of batteries and leading to new possibilities. Along with the rapid development of low-power integrated circuits the energy harvesting generators are expected to give rise to an era of self-powered autonomous devices [6].

Piezoelectric vibration energy harvesters (PVEH's) are a promising mechanism to harvest vibration ambient energy. The piezoelectric ceramic material converts mechanical strain to electrical power that can be used to power small (wireless) devices. The piezoelectric effect results from pressure on ceramic crystals yielding an electric potential. Most vibration energy harvesters are based on one degree of freedom cantilever beam spring structure [7], actuated in 31-mode [8, 9]. This piezoelectric cantilever architecture has promising potential to power for example Tire Pressure Monitor Systems (TPMS) to provide infinite energy [10], eliminating the need for battery replacement.

In previous work, the reliability of the device is often not considered during the design process [6]. With the goal of gaining maximum output power the cantilevers are operating at the limits of the material stresses of the piezoceramic. Therefore, this is a major factor in the reduced lifetime of the energy harvesting devices. Especially, for powering low power sensors, high reliability of the energy harvester is required.

However, to date, a comparative evaluation of design principles for improved mechanical reliability of PVEH is lacking in literature. Prior art experimental test show the importance of mechanical cyclic loading [11–17]. The issue with reliability is that it doesn't matter how sophisticated the devices are, it becomes useless when it fails to deliver the designed performance during the desired lifetime. Hence, the research question is: What design principles exist in literature for increased mechanical reliability of cantilever beam piezoelectric energy harvesters?

The goal of this review is to present an overview of design principles for improving piezoelectric cantilever beams operational lifetime, by limiting strain and strain

concentrations. Therefore, the causes of failure of PVEH's have to be understood. From the results the design principles can be evaluated, increasing operational lifetime expectancy of vibration energy harvesters. Keeping in mind the consequences on the change of efficiency by the modification of geometric design for improved mechanical reliability.

In section II Failure causes, the failure modes and underlying failure causes of a rectangular cantilever are identified. With this in mind three different design principles to increase the reliability of PVEH's are evaluated in section III Design principles. Section IV Discussion compares and evaluates the results. Finishing with the conclusions that can be drawn.

II. FAILURE CAUSES

A. Reliability and failure definition

Reliability is defined as the ability of the device to perform its designed function in terms of years/cycles of operational lifetime [18]. The probability of success is inversely related to the probability of failure: $P(\text{Reliability}) = 1 - P(\text{Failure})$. Understanding the failure modes creates, therefore, an understanding of the reliability of the device. In the field of energy harvesting, there are different definitions of failure found in literature [17, 19–21]. M.Gall et al. regarded a specimen as failed if the sensor voltage dropped below 90% of the initial state value [21][17]. This is a relatively strict failure criterion compared to other definitions found in literature. This is because a maximum voltage drop of 10% allows for small deviations in power output but guarantees the necessary stable performance for smart structures. So, failure is not a complete (mechanical) breakdown of a specimen, only a reduction of designed voltage. Therefore, the term degradation is often used to describe the reduction of designed performance.

B. Degradation analysis single DoF cantilever beam

It is found that the degradation of the PVEH is mainly caused by the mechanical cyclic loading [11–17]. M.Gall and B.Thielicke used a four-point cyclic tensile bending test to describe the degradation as function of the applied strain. The larger the strain in piezoceramic the more electrical charge is generated. But after 2000 cycles at 0.3% strain the electrical charge has declined by 14%, due to the mechanical degradation of the piezoceramic [17]. Figure 1 expresses the number of cycles a sample survives before failure (90% of initial voltage) occurs. The number of cycles a sample survives is dependent on the applied strain. For this sample the quasi-static fracture strain is 0.35%. Almost immediate failure occurs at this strain. As expected lower strain levels results in higher number of cycles before failure. Samples that are cycled over 10^8 cycles at a maximum strain of 0.12% showed less than 10% reduction of initial performance. In real life applications that operate for example at 30Hz this means only an operational lifetime 39 days. This emphasises the importance of not over straining the piezoelectric ceramic in order to yield maximum output.

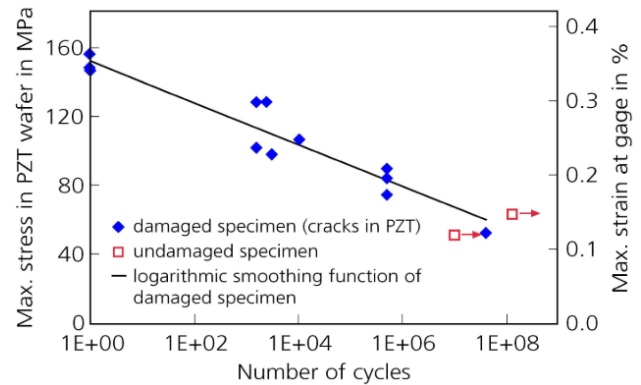


Fig. 1: Failure (90% of initial voltage) of PZT patches as function of number of cycles under tensile loading at room temperature [17]

The degradation of the piezoelectric ceramic is primarily caused by microcracks resulting from the strain in the material [22]. Most microcracks occur at the high-strain areas, where the strain is largest [13]. For a cantilever that is uniform in width and thickness, area near the clamped fixed end is most prone to the microcracks. The experimental test with bimorph harvesters, energy harvesters with a piezoelectric layer in compression and tension, show that micro-cracking is primarily occurring in the tensional layer. An 80% drop of capacitance is found in the tensile layer, caused by microcracks located at 20% percent of the length from the clamped-end of the cantilever [13]. This is proven by stereo microscopy visual inspections of the sample [21].

The microcracks in the piezoceramic reduces the coupling factor (k_{31}) and changes the dynamic behaviour of the cantilever. Therefore this can be used as a measure for degradation. The microcracks reduce the stiffness of the cantilever beam, influencing the resonant frequency. This frequency shift is often more detrimental than the change in piezoelectric properties [12], since the cantilevers are designed to operate at specific frequencies, that causes the cantilever beam to resonate efficiently. Frequency shifts of 4-8 Hz are found in [12]. Similar frequency shifts are found in other literature [13, 15, 23]. It is important to note that the most significant frequency shift occurs within the first cycles.

To summarise, micro cracking is the main failure mode, caused by too large deformations and tensional strain concentrations.

C. Classification of design for reliability principles

Classification of the literature is done according the principle the strain is minimised to improve reliability, since tensional strain is the dominant failure cause of rectangular PVEH's. To the writers knowledge all existing principles found in literature can be included within this strain based classification. This classification is made to differentiate and compare various design principles relative to conventional rectangular cantilevers. The three strain design principles that are identified to categorise literature are:

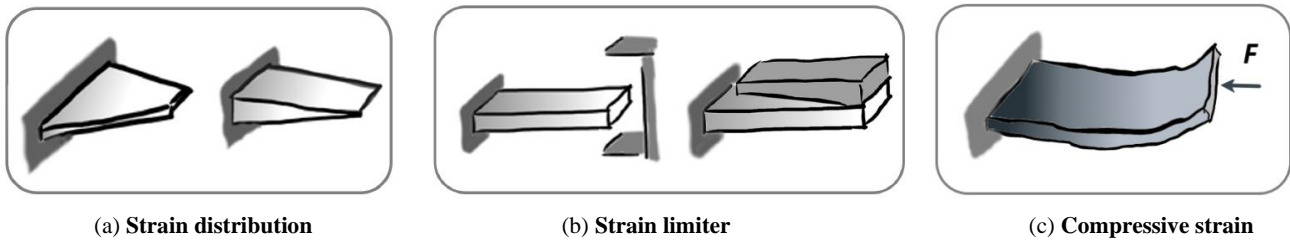


Fig. 2: Categorized design principles for strain reduction improving piezoelectric vibration energy harvesters

1) *Strain distribution:*

The first category is the strain distribution over the cantilever beam. Stress concentrations are here minimised, and strain is more even distributed. The goal is to have a homogeneous distribution of strain over the cross section or surface area of the piezoelectric cantilever.

2) *Strain limitation:*

Limiting the deformation assures that the strain does not exceed the maximum yield strain and therefore prevents it from breaking. The strain limitation can be achieved by limiting the amplitude of the cantilever movement.

3) *Compressive strain:*

Operation in compressive strain reduces the maximum tensional strain in the piezoceramic.

Each principle is schematically depicted in Figure 2. Each will be elaborated one by one in the next section Design Principles.

III. DESIGN PRINCIPLES

A. Strain distribution

1) *Area strain homogenisation:*

Conventional rectangular cantilever designs are limited by the maximum strain; hence, it is difficult to obtain larger electrical output power by increasing the deflection [24]. Increasing the lifetime and electrical output power of the piezoelectric cantilever beam can be achieved by reducing stress concentrations over the piezoceramic, and therefore allowing a higher average strain over the piezoelectric material. Analytically the average strain can be defined along the length axis and thickness described in [25]. L. Matue and F. Moll analytically compared rectangular cantilevers with tapered cantilevers, he found that the average strain of the rectangular cantilever is 75% of the triangular cantilever average strain with identical load and active area [25]. Therefore, a triangular cantilever can generate more electrical power per unit area.

Glynne-Jones. P, Beeby. S P and White. N M where the first writing about a tapered cantilever beam for strain homogenisation [26]. Roundy et al. claims that a triangular cantilever can supply twice the energy per unit volume PZT than a rectangular cantilever [27]. Bakker et al. investigated the shape effects by comparing rectangular and triangular cantilever PVEH's [28]. For the comparison he kept the PZT

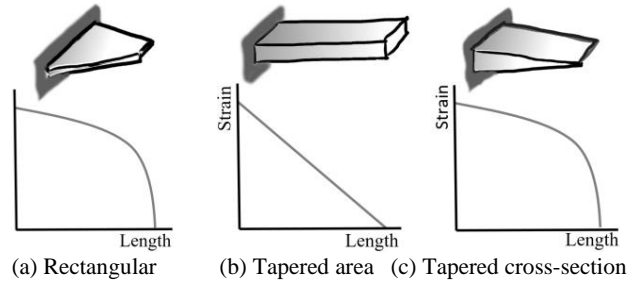


Fig. 3: Strain homogenisation over top layer area and cross-section along the length of a cantilever beam. The deflection is applied downwards at the free-end.

volume, natural frequency, proofmass and maximum strain constant. He calculated a theoretical 50% higher electrical power output compared to a rectangular design. In reality, the experiments show a 30% increase. This difference can be attributed to the uncertainties in manufacturing and inaccuracies in dimensions or material properties. Also neglecting dynamics in bonding layer and assumption of linear spring behaviour result in a difference of theoretical and experimental results. In reaction of the study from Baker [28] with macro scale design PVEH Jung-Hyun Park, et. al. conducted a similar study on micro machined cantilevers. Both samples had a same thickness and proofmass. The eigenfrequency of the cantilevers were 128.1 Hz and 117.3 Hz, respectively for the rectangular beam and triangular beam. The dimensions were 3x2x0.5 mm (LxWxH), and the trapezoidal cantilever had a reduced width of 1mm. He concluded that with an equal PZT surface area (1 mm²) of the trapezoidal shape cantilever 39% more power is harvested compared to a rectangular design [29]. It could be concluded that scaling to micro scale yields similar advantages obtained by strain homogenisation.

So, a triangular surface shape is preferred over rectangular and trapezoidal shapes [24, 25, 30–33]. This is because of the resulting uniform stress distribution over the cantilever, assuming no edge effects exist [34]. The more uniform strain distribution can be seen in Figure 3 in comparison with a rectangular cantilever. The stress concentrations near the fixed end are reduced and the effective strain area increased. This suggests that the operational lifetime of the tapered

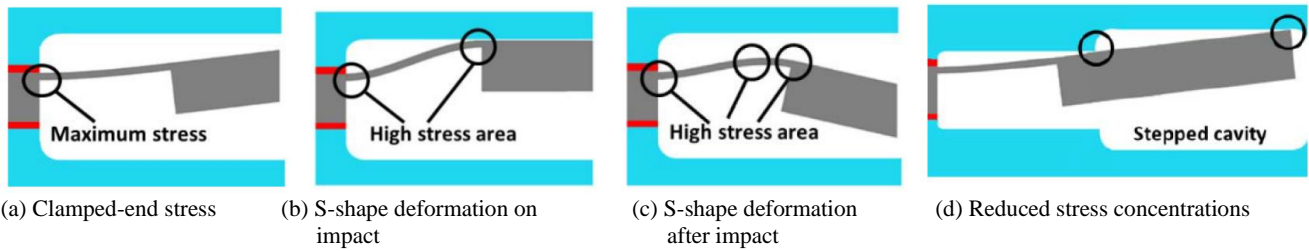


Fig. 4: Identification of stress locations on excited cantilever beam limited by a mechanical stopper. Adapted from [43]

PVEH is longer than the rectangular cantilevers. However, no lifetime or experimental failure tests were performed to the writers knowledge. Most experimental test focus on the electrical power generation. Since, tapered cantilevers have not only higher reliability but also a higher power density [24, 28, 30, 34–39].

Important to notice is that the tapered shaped area is only advantageous when dealing with long slender cantilevers. If the length-width ratio is smaller than 1, the tapered beams deliver less output power. With a length-width ratio of 1/3, 25% less output can be generated compared with a non-tapered beam with the same area and thickness [40].

2) Cross-section strain homogenisation:

Also the thickness can be varied for strain homogenisation. A profile that does not compromise the effective active area is a rectangular beam with an elliptical or tapered cross-section [24, 41]. This cross-section also reduces the stress at the fixed end of the cantilever since the thickness of the material is greater. S. Mehraeen et al. [42] was the first optimising the cross-section instead of using a linear tapered beam. Frank Goldschmidtboeing and Peter Woias [35] introduced the relative mean curvature κ_0 characterising the stress homogeneity, expressed in Equation 1.

$$\kappa' = \frac{|\kappa_{mean}|}{|\kappa_{max}|} \quad (1)$$

Where κ_{mean} is the mean curvature at the bottom of the piezoelectric and κ_{max} is the maximum curvature. There is a perfect homogeneous strain over the surface when $\kappa = 1$. These shape principles distribute the stress and fatigue over the beam surface and hence, the life cycles of the energy harvester will increase without compromising the generated electrical power [24].

B. Strain limitation

1) Mechanical stopper:

A mechanical stopper is used to limit the deflection of the cantilever beam, therefore limiting the stress due to the reduced deformation. This design concept is especially useful for shock environments and random vibrations to prevent the cantilever bend above its fracture strength [44]. In specific, for PVEH's that are designed to have low natural frequencies are most prone to shock environments due to their low

stiffness of cantilever beam. The lower stiffness allows larger deformations when subjected to shocks. The maximum shock magnitude that a cantilever beam can survive decreases linearly with the natural frequency of the energy harvesters [43, 45]. Often the mechanical stopper architecture is combined with the encapsulation package that protects the PVEH not only from shocks but also from other environmental influences, for example moisture and dust.

A mechanical stopper is also a strategy to increase the bandwidth. With increasing frequency (frequency-up sweep) the cantilever amplitude is excited further by the mechanical stopper causing non-linear oscillations [7, 46]. Yielding in an increased power output over a wider frequency bandwidth. On the contrary, with decreasing frequencies, this appears not to work [7]. Also, the maximum power output drops due to the limitation on vibration amplitude.

The problem of a mechanical stopper is that it induces extra stresses at other zones other than the anchor point where failure is most common [47, 48], see Fig 4a. Z.Wang et al. [43] reports the reliability of shock protection structures including the stress induced due to the impact of the proof mass and mechanical stopper. He showed that the mechanical stopper causes significant stresses at the junction between the cantilever and the seismic mass. Fig 4b depicts the stress induced due to the impact of the cantilever mass with the mechanical stopper. When the free-end tip hits the package, the inertia causes the seismic mass to continue moving, deforming the cantilever in an S-shape. Fig 4c is the shape of the cantilever after impact. After impact, the cantilever beam vibrates along several normal modes which can also lead to stress concentrations [3]. This dynamic behaviour is highly non-linear and may result in earlier fatigue-induced failure in the cantilever beam. The S-shape deformation implies a second disadvantage, next to the extra stress concentrations. The top layer at the clamped-end of the cantilever beam is in compression and the remainder in tension due to the S-shape deformation. The different strain regions on the same piezoelectric layer cancel the positive charge by the negative charge generated. The opposite also occurs at the bottom piezoelectric layer. As a consequence, the voltage output almost halves compared to a PVEH without a mechanical stopper even though they operate with the same amplitude [48].

Z.Wang et al. proposes the design concept of a stepped cavity as a mechanical stopper, seen in Fig 4d, reducing the

S-shaped deformation of the cantilever. Experimental results prove the increased shock reliability of the stepped cavity, due to the more constant deformation. Non stepped cavity samples are tested to shocks till 600g, resulting in 70% of the 21 samples that break. Compared to samples with a stepped cavity only 30% of the samples break [43]. Moreover, 60% of the stepped stoppers survived 1700g, while only 4% of the samples without stopper survived 1700g [49].

2) Proofmass stoppers:

Another mechanical stopper design that does not use the external package as deformation limiter is a proofmass in a L-shape, see Fig 5. This improves the energy density and reduces the resonance frequency by efficiently increasing the proof mass [50]. This proofmass architecture is used to block the amplitude and to prevent S-shape deformations of the cantilever beam. S.Roundy proposed having on both sides of cantilever the proofmass limiter [51]. It is expected that the proofmass limiter architecture will increase the shock reliability as well. However, it is discussed in [50] that the bond of the proofmass and the cantilever beam was rather weak resulting in a loss of bonding and failure of the PVEH.

C. Operation in compressive strain

It is known that most energy harvesters fail due to tensile stress rather than compressive stress [13, 27]. The cyclic loading in compressive strain causes less micro cracking in the piezoelectric, hence increasing the operational lifetime.

M.Gall and B.Thielicke [17] uses a four-point bending test, to measure compressive degradation in PZT patches. It is found that no mechanical damage is detected up to -0.6% strain in quasi-static and cyclic testing (10^5 cycles). Where the same sample would have a quasi-static fracture strength of 0.35% in tensional strain. The decrease of the electrical capacitance under compressive loading suggest that the depolarisation of the ceramic is the cause of decreased performance [17]. This is emphasised by the fact that repolarisation yields the initial performance. So, compressive cycling of the PZT patch causes reversible electric depolarisation. But this phenomenon is reversible unlike the microcracks in tensional operation.

Energy harvesting in compressive strain can be achieved by preloading the piezoelectric layer [52]. Internal compressive stress is achieved by differences between thermal expansion coefficients of the substrate layer and piezoceramic [53]. Some commercially available piezoelectric ceramics configurations exist. THUNDER (Thin Unimorph Driver) is made with substrates of stainless steel and a top layer of aluminium [54, 55]. The other configuration, Lipca-C2, is made of fibreglass and carbon composite layers. The third configuration is named: RAINBOW (reduced and internally biased oxide wafer). All show enhanced strain capabilities [56, 57]. Other than the internal compressive loading's external spring loaded configurations are also possible. Schwartz R.W et al. [58] increased the electrical mechanical response by adding

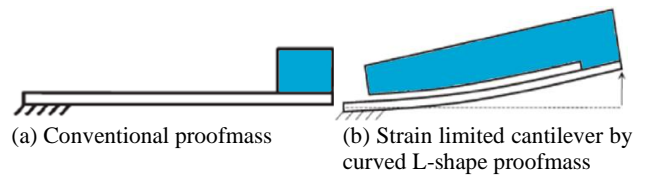


Fig. 5: **Proof mass stopper design attached to cantilever beam limiting the strain in the cantilever beam.** Adapted from [50]

elongated springs to pre-load a THUNDER actuator. By adjusting the preloading the natural frequency can be changed, increasing the frequency bandwidth [27]. A phenomenon that is not understood is that the initial RMS voltage of the tensile layer is ~ 1.75 times bigger than the initial voltage in the compressive layer of a bimorph [13].

IV. DISCUSSION




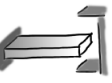


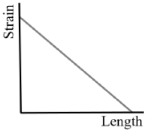
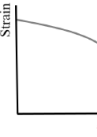

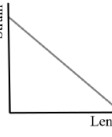
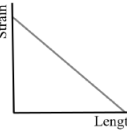
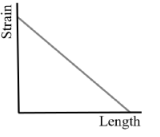
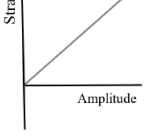
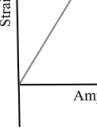
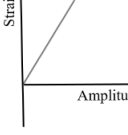
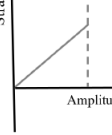
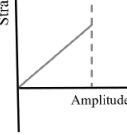
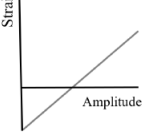
A. Comparative overview of strain design principles

To summarise the reliability design improvements found in literature, each design principle is evaluated in a comparative Table I. Each design principle is compared against a rectangular cantilever by seven criteria. To begin with the used strain principle. The second and third row visualises the strain along the length of the cantilever and the strain as function of the amplitude, respectively. For the strain length graph, the strain is measured along the length of the top layer of the cantilever when a fixed downwards amplitude is applied. And for the strain-amplitude graph, the strain is measured at the top layer clamped-end with increasing amplitude. Both graphs show what happens with the strain for each particular design principle. For the strain limitation principle it is assumed, that S-shape deformation is prevented. The amplitude-strain graph for strain distribution design principle is steeper, due to the increased stiffness. The strain limitation is visualised by a shorter strain-amplitude slope. And the slope of compressive strain shifted down, since the PZT is subjected to a compressive force.

The last four criteria in the table are being compared with plus/minus criteria relative to the rectangular cantilever. Where the scale of assessment runs from - -, -, \circ , +, ++. A decrease of performance scores - or - and an increase of performance scores + or ++. The relative decrease or increase compared to the rectangular cantilever determines the single or double math symbol. No relative change is indicated by \circ . A negative sign does not imply a negative performance, for example a decrease of natural frequency is not particularly bad.

The first criteria is the electrical power than can be generated over the area, defining the effectiveness the piezoelectric cantilever converts mechanical energy to electrical energy. For strain homogenised area's the power output is higher due to the larger average strain relative to the rectangular cantilever. For the strain limiting design principles the piezoelectric power output does not change

TABLE I: Comparative overview of design principles for improved PVEH Reliability. The fixed deflection is applied in downwards direction and strain measured at clamped-end top layer or over the length of the cantilever. The performance is expressed by an increase or decrease relative to the rectangular cantilever.

						
Strain principle	none	Strain distribution	Strain distribution	Strain limitation	Strain limitation	Compressive strain
Strain-length graph						
Strain-amplitude graph						
Electrical power/area	o	+	+	o	o	o
Frequency bandwidth	o	o	o	+	+	o
Natural frequency	o	+	+	o	+	+
Impact resistance	o	+	+	++	++	+

since the geometry of the cantilever does not change. And for the piezoceramic under pre-loading, the piezoelectric coupling is lower since compressive deformation yields less electrical energy output. The frequency bandwidth only increases for strain limitation designs principles, in specific with increasing frequencies (frequency-up sweep).

The natural frequency increases with the increased stiffness or with addition of proofmass. Therefore, the distributed strain principle and proofmass limiter has a positive sign. The strain limited design has no relative change. And the compressive strain principle has a higher natural frequency since these cantilevers are often thicker.

The impact resistance for all design principles increase relative to the rectangular cantilever, due to the change of stiffness or deformation limitation.

B. Application of the design principles

The proposed design principles from section III Results are a guiding concept for engineers during a design process. It emphasises the importance to take in account, in an early design phase, the strain that is induced during operation. Optimising a cantilever structure by homogenising and limiting the strain will result in a longer operational lifetime of the PVEH. The reliability should be stated in the requirements, so it is taken into account during the whole design process.

The design principles can also be combined or integrated in existing energy harvesting devices. Often the rectangular cantilever PVEH can be replaced by a tapered design. Important is to keep in mind the increase of stiffness with tapered geometries [37, 59], and therefore lead to a higher natural frequency. This can be compensated by reducing the width/length ratio, the thickness or increasing the proof mass [60]. For the application of the design principles Table I can be used as reference.

Important to notice is that reliability is not only a function of geometric design principles, in other words the strain. Surface finish of the piezoceramic and ageing properties [26, 61] cannot be neglected. Also environmental influences have an impact on the reliability of the device as well. For example shocks, temperature, moisture and dust reduce the lifetime drastically. Therefore, it is always recommended to have an encapsulation around the energy harvesting devices. Often the inside of the casing is vacuum to reduce damping effects for increased electrical power output. However, this is sometime more detrimental due to the larger deformations.

C. Future research

In literature the reliability focus on pure bending, but real life operation is often in random frequencies and shock environments. The influence higher frequency modes of bending and torsion can be investigated. Including lamb wave propagation due to impact.

To the writers knowledge no experimental research is done on the reliability of tapered cantilevers. It is only assumed by literature that it is more reliable.

Finally, for future research it is important that the reliability is reported of newly developed PVEH's. By reporting the voltage or charge degradation as function of number of cycles.

V. CONCLUSION

In this work geometric design principles to improve the mechanical reliability have been addressed. Micro-cracking is identified as the number one failure mode for piezoelectric vibration energy harvesters (PVEH) based on cantilevers. The cause for microcracks are tensional strains at strain concentrations and deformations larger than the elastic limit. It was shown that the operational lifetime of the PVEHs is a function of the maximum strain applied.

Three strain focused geometric design principles are evaluated relative to an one degree of freedom rectangular cantilever and the way strain is optimised for increased operational lifetime. First, the strain distribution design principle that effectively homogenises the strain over the cantilever. The theoretical average strain in the piezoceramic layer is 25% lower in the rectangular cantilever beam compared to a triangular shaped cantilever with the same maximum strain, yielding also a higher electrical output. Secondly, a stepped mechanical limiter and curved L-shape proof mass are effective strain limitation design principles. Since, they prevent too large strains and S-shape formations. Thirdly, operation in compressive strain reduces the tensile strain and therefore the chance of micro cracks. Overall, it can be concluded that these three design principles should be taken into account in an early design phase.

REFERENCES

- [1] Yen Kheng Tan. Energy harvesting autonomous sensor systems: design, analysis and practical implementation. Taylor & Francis Group, LLC, 2013. ISBN: 9781439894354.
- [2] Edwar Romero. Powering Biomedical Devices. Academic Press, 2013, p. 62. ISBN: 9780124077836. DOI: 10.1016/C2012-0-06126-1.
- [3] R. van Schaijk et al. "A MEMS vibration energy harvester for automotive applications". In: ed. By Ulrich Schmid, Josfffdfffd Luis S'anchez de Rojas Aldavero, and Monika Leester-Schaedel. Vol. 8763. International Society for Optics and Photonics, May 2013, p. 876305. DOI: 10.1117/12.2016916.
- [4] Shad Roundy et al. Method for generating electric energy in a tyre. Oct. 2010.
- [5] Mir Imran. Energy harvesting mechanism for medical devices. Sept. 2009.
- [6] Zhengbao Yang et al. Review: High-Performance Piezoelectric Energy Harvesters and Their Applications. 2018. DOI: 10.1016/j.joule.2018.03.011.
- [7] S.P. Beeby, R.N. Torah, and M.J. Tudor. "Kinetic energy harvesting". In: Energy Harvesting for Autonomous systems. Ed. by Neil Beeby Stephen; White. January. Artech House, 2010. Chap. 4, pp. 91–134. ISBN: 978-1-59693-718-5.
- [8] Steven R Anton and Henry A Sodano -. "A review of power harvesting using piezoelectric materials (2003-2006)". In: Smart Materials and Structures 16 (2007). DOI: 10.1088/0964-1726/16/3/R01.
- [9] Learn Wang Tom J. Kazmierski. Energy Harvesting Systems : Principles, Modelling and Applications. 2011, p. 101. ISBN: 9781441975652. DOI: 10.1007/978-1-4419-7566-9.
- [10] Geon-Tae Hwang et al. "Self-Powered Cardiac Pacemaker Enabled by Flexible Single Crystalline PMNPT Piezoelectric Energy Harvester". In: Advanced Materials 26.28 (July 2014), pp. 4880–4887. ISSN: 09359648. DOI: 10.1002/adma.201400562.
- [11] Markys G Cain et al. Degradation of Piezoelectric Materials. Tech. rep. January. Teddington, Middlesex, TW11 0LW, UK: National Physical Laboratory Management Ltd, 1999. DOI: 10.1109/ICMB.2011.54.
- [12] P. Pillatsch et al. "Degradation of piezoelectric materials for energy harvesting applications". In: Journal of Physics: Conference Series 557.1 (2014). ISSN: 17426596. DOI: 10.1088/1742-6596/557/1/012129.
- [13] P Pillatsch et al. "Degradation of bimorph piezoelectric bending beams in energy harvesting applications". In: (2017). DOI: 10.1088/1361-665X/aa5a5d.
- [14] Y. Tsujiura et al. "Reliability of vibration energy harvesters of metal-based PZT thin films". In: Journal of Physics: Conference Series 557.1 (2014), pp. 3–8. ISSN: 17426596. DOI: 10.1088/1742-6596/557/1/012096.
- [15] Y. H. Yang et al. "The Reliability Testing and Fatigue Behavior Study of Micro Piezoelectric Energy Harvester". In: Volume 2: Mechanics and Behavior of Active Materials; Structural Health Monitoring; Bioinspired Smart Materials and Systems; Energy Harvesting; Emerging Technologies. ASME, Sept.2018, V002T07A006. ISBN: 978-0-7918-5195-1. DOI: 10.1115/SMASIS2018-8022.
- [16] C Wilson, A Ormeggi, and M Narbutovskih. "Fracture testing of silicon microcantilever beams". In: Journal of Applied Physics 79 (1996), p. 5840. DOI: 10.1063/1.361102.
- [17] Monika Gall and Barbel Thielicke. "Life-span investigations of piezoceramic patch sensors and actuators". In: ed. by Marcelo J. Dapino. Vol. 6526. International Society for Optics and Photonics, Apr. 2007, 65260P. DOI: 10.1117/12.714756.
- [18] Definition of reliability in English by Oxford Dictionaries.
- [19] S Mall and J M Coleman. Monotonic and fatigue loading behavior of quasi-isotropic graphite/epoxy laminate embedded with piezoelectric sensor. Tech. rep. 1998, pp. 822–832.
- [20] Jirawat Thongrueng, Toshio Tsuchiya, and Kunihiko Nagata. "Lifetime and Degradation Mechanism of Multilayer Ceramic Actuator". In: Japanese Journal of Applied Physics 37 (1998).
- [21] Monika Gall, Barbel Thielicke, and Ingo Schmidt. "Integrity of piezoceramic patch transducers under cyclic loading at different temperatures". In: Smart Materials and Structures 18.10 (2009). DOI: 10.1088/0964-1726/18/10/104009.
- [22] Mitsuhiro Okayasu, Go Ozeki, and Mamoru Mizuno. "Fatigue failure characteristics of lead zirconate titanate piezoelectric ceramics". In: Journal of the European Ceramic Society 30.3 (Feb. 2010), pp. 713–725. ISSN: 0955-2219. DOI: 10.1016/J.JEURCERAMSOC.2009.09.014.
- [23] Eric J. Kjolsing and Michael D. Todd. "The effects of damage accumulation in optimizing a piezoelectric energy harvester configuration". In: Sensors and Smart Structures Technologies for Civil, Mechanical, and Aerospace Systems 2018. Ed. by Hoon Sohn. SPIE, Mar. 2018, p. 102. ISBN: 9781510616929. DOI: 10.1117/12.2283053.
- [24] Tamil Selvan Ramadoss, Hilaal Alam, and Prof Ramakrishna Seeram. "Profile Geometric Effect of Cantilever Piezoelectric Device Using Flexural Mechanism". In: September (2018).
- [25] Loreto Mateu and Francesc Moll. "Optimum Piezoelectric Bending Beam Structures for Energy Harvesting using Shoe Inserts". In: Journal of Intelligent Material Systems and Structures 16.10 (Oct. 2005), pp. 835–845. ISSN: 1045-389X. DOI: 10.1177/1045389X05055280.
- [26] P Glynn-Jones, S P Beeby, and N M White. A method to determine the ageing rate of thick-film PZT layers. Tech. rep. 2001, pp. 663–670.
- [27] S. Roundy et al. "Improving Power Output for Vibration-Based Energy Scavengers". In: IEEE Pervasive Computing 4.1 (Jan. 2005), pp. 28–36. ISSN: 1536-1268. DOI: 10.1109/MPRV.2005.14.
- [28] Jessy Baker, Shad Roundy, and Prof Paul Wright. "Alternative Geometries for Increasing Power Density in Vibration Energy Scavenging for Wireless Sensor Networks". In: 3rd International Energy Conversion Engineering Conference (2005). ISSN: 2005-5617. DOI: 10.2514/6.2005-5617.
- [29] Jung Hyun Park et al. "Analysis of stress distribution in piezoelectric MEMS energy harvester using shaped cantilever structure". In: Ferroelectrics 409.1 (2010), pp. 55–61. ISSN: 00150193. DOI: 10.1080/00150193.2010.487125.
- [30] E. Brusa et al. "Analytical characterization and experimental validation of performances of piezoelectric vibration energy scavengers". In: ed. by Ulrich Schmid. Vol. 7362. International Society for Optics and Photonics, May 2009, p. 736204. DOI: 10.1117/12.821425.
- [31] Guangyi Zhang et al. "A low frequency piezoelectric energy harvester with trapezoidal cantilever beam: theory and experiment". In: Microsystem Technologies 23 (2017), pp. 3457–3466. DOI: 10.1007/s00542-016-3224-5.
- [32] Lei Jin et al. "The effect of different shapes of cantilever beam in piezoelectric energy harvesters on their electrical output". In: Microsystem Technologies 23 (2017), pp. 4805–4814. DOI: 10.1007/s00542-016-3261-0.

- [33] Seyed Mohammad et al. "Multi-objective shape design optimization of piezoelectric energy harvester using artificial immune system". In: *Microsystem Technologies* 22 (2016), pp. 2435–2446. DOI: 10.1007/s00542-015-2605-5.
- [34] P. Glynn-Jones, S.P. Beeby, and N.M. White. "Towards a piezoelectric vibration-powered microgenerator". In: *IEE Proceedings - Science, Measurement and Technology* 148.2 (2001), pp. 68–72. ISSN: 13502344. DOI: 10.1049/ip-smt:20010323.
- [35] Frank; Goldschmidtboeing and Peter Woias. "Characterization of different beam shapes for piezoelectric energy harvesting". In: *Journal of Micromechanics and Microengineering* (2008). DOI: 10.1088/0960-1317/18/10/104013.
- [36] John M Dietl and Ephraim Garcia. "Beam Shape Optimization for Power Harvesting". In: *Journal of Intelligent Material Systems and Structures* 21.6 (2010), pp. 633–646. DOI: 10.1177/1045389X10365094.
- [37] Asan G A Muthalif and N H Diyana Nordin. "Optimal piezoelectric beam shape for single and broadband vibration energy harvesting: Modeling, simulation and experimental results". In: *Mechanical Systems and Signal Processing* 54-55 (2014), pp. 417–426. DOI: 10.1016/j.ymsp.2014.07.014.
- [38] S Srinivasulu Raju, M Umamathy, and G Uma. "Design and analysis of high output piezoelectric energy harvester using non uniform beam Design and analysis of high output piezoelectric energy harvester using non uniform beam". In: (2018). DOI: 10.1080/15376494.2018.1472341.
- [39] Mohammed Salim et al. "New simulation approach for tuneable trapezoidal and rectangular piezoelectric bimorph energy harvesters". In: *Microsystem Technologies* 23 (2017), pp. 2097–2106. DOI: 10.1007/s00542-016-2999-8.
- [40] T M Kamel et al. "Effect of length/width ratio of tapered beams on the performance of piezoelectric energy harvesters". In: (2013). DOI: 10.1088/0964-1726/22/7/075015.
- [41] Yabin Liao et al. "Improving the performance of a piezoelectric energy harvester using a variable thickness beam". In: *MATERIALS AND STRUCTURES Smart Mater. Struct* 19 (2010), pp. 105020–105034. DOI: 10.1088/0964-1726/19/10/105020.
- [42] S. Mehraeen, S. Jagannathan, and K.A. Corzine. "Energy Harvesting From Vibration With Alternate Scavenging Circuitry and Tapered Cantilever Beam". In: *IEEE Transactions on Industrial Electronics* 57.3 (Mar. 2010), pp. 820–830. ISSN: 0278-0046. DOI: 10.1109/TIE.2009.2037652.
- [43] Ziyang Wang et al. "Shock Reliability of Vacuum- Packaged Piezoelectric Vibration Harvester for Automotive Application". In: *Journal of Microelectromechanical Systems* 23.3 (June 2014), pp. 539–548. ISSN: 1057-7157. DOI: 10.1109/JMEMS.2013.2291010.
- [44] V T Srikar and Stephen D Senturia. "The reliability of microelectromechanical systems (MEMS) in shock environments". In: 11.3 (2002), pp. 206–214.
- [45] W. T. Thomson and M. D Dahleh. *Theory of Vibration With Applications*. Tech. rep. New Jersey: Englewood Cliffs, 1998.
- [46] M. S M Soliman et al. "A wideband vibration-based energy harvester". In: *Journal of Micromechanics and Microengineering* 18.11 (2008). ISSN: 09601317. DOI: 10.1088/0960-1317/18/11/115021.
- [47] K Komai, K Minoshima, and S Inoue. "Fracture and fatigue behavior of single crystal silicon microelements and nanoscopic AFM damage evaluation". Tech. rep. 1998, pp. 30–37.
- [48] Kuok H. Mak et al. "Performance of a cantilever piezoelectric energy harvester impacting a bump stop". In: *Journal of Sound and Vibration* 330 (2011), pp. 6184–6202. ISSN: 0022460X. DOI: 10.1016/j.jsv.2011.07.008.
- [49] M. Renaud et al. "Improved mechanical reliability of MEMS piezoelectric vibration energy harvesters for automotive applications". In: 2014 IEEE 27th International Conference on Micro Electro Mechanical Systems (MEMS). IEEE, Jan. 2014, pp. 568–571. ISBN: 978-1-4799-3509-3. DOI: 10.1109/MEMSYS.2014.6765704.
- [50] Wen G. Li, Siyuan He, and Shudong Yu. "Improving power density of a cantilever piezoelectric power harvester through a curved L-shaped proof mass". In: *IEEE Transactions on Industrial Electronics* 57.3 (2010), pp. 868–876. ISSN: 02780046. DOI: 10.1109/TIE.2009.2030761.
- [51] Shadrach Joseph Roundy. "Energy Scavenging for Wireless Sensor Nodes with a Focus on Vibration to Electricity Conversion". PhD thesis. THE UNIVERSITY OF CALIFORNIA, BERKELEY, 1996.
- [52] Karla M. Mossi et al. "Prestressed curved actuators: characterization and modeling of their piezoelectric behavior". In: August (2003), p. 423. DOI: 10.1117/12.484749.
- [53] Zdenfffdffdk Majer et al. "Optimization of Design Parameters of Fracture Resistant Piezoelectric Vibration Energy Harvester". In: *Key Engineering Materials* 774 (Aug. 2018), pp. 416–422. DOI: 10.4028/www.scientific.net/kem.774.416.
- [54] Richard F Hellbaum, Robert G Bryant, and Robert L Fox. *Thin layer composite unimorph ferroelectric driver and sensor*. Apr. 1995.
- [55] Karla M Mossi, Gregory V Selby, and Robert G Bryant. "Thin-layer composite unimorph ferroelectric driver and sensor properties". In: *Materials Letters* 35.1-2 (Apr. 1998), pp. 39–49. ISSN: 0167-577X. DOI: 10.1016/S0167-577X(97)00214-0.
- [56] R Wieman and Rc Smith. "Displacement models for THUNDER actuators having general loads and boundary conditions". In: *Signal Processing and Control in Smart Structures August 2001* (2001), pp. 252–263. ISSN: 0277-786X. DOI: 10.1117/12.436479.
- [57] Karla M. Mossi and Richard P. Bishop. "Characterization of different types of high-performance THUNDER actuators". In: July 1999 (1999), pp. 43–52. DOI: 10.1117/12.352812.
- [58] R.W. Schwartz and M. Narayanan. "Development of high performance stress-biased actuators through the incorporation of mechanical pre-loads". In: *Sensors and Actuators A: Physical* 101.3 (Oct. 2002), pp. 322–331. ISSN: 0924-4247. DOI: 10.1016/S0924-4247(02)00263-7.
- [59] Rouhollah Hosseini and Mohsen Hamed. "An investigation into resonant frequency of trapezoidal Vshaped cantilever piezoelectric energy harvester". In: *Microsystem Technologies* 22 (2016), pp. 1127–1134. DOI: 10.1007/s00542-015-2583-7.
- [60] Abdul Hafiz Alameh et al. "Effects of proof mass geometry on piezoelectric vibration energy harvesters". In: *Sensors (Switzerland)* 18.5 (2018). ISSN: 14248220. DOI: 10.3390/s18051584.
- [61] Morgan. *Piezoelectric Ceramics Data Book for Designers*.

A

B

Conference

On the 8th of November, I had the honor to present my literature review on the ICCMA conference. A three minute pitch has been given followed by a poster presentation. The conference poster and certificate are attached in this Appendix. The poster presentation session resulted in interesting discussions for applications of fellow researchers in different research fields.

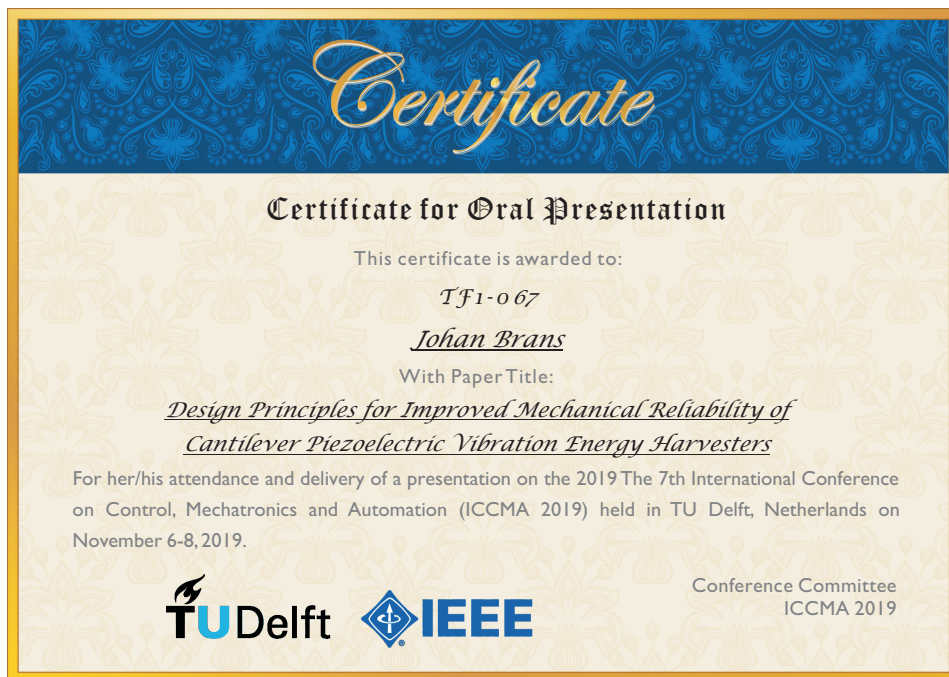


Figure B.1: Conference certificate for oral presentation

Energy Harvesting:

Reliability design principles for piezoelectric cantilevers

J.A.Brans, T.W.A.Blad & N.Tolou
 Delft University of Technology
 Department of High-Tech Engineering

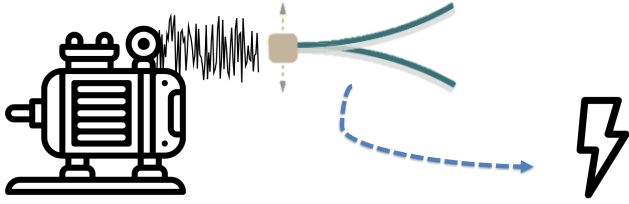


Figure 1: Application of Energy harvesting for Internet of Things

Background

Piezoelectric vibrational energy harvesters (PVEH) use ambient vibration energy, for example from electric motors, to **power small sensors**. The greatest issue preventing these systems from being widely used is their **poor reliability**. Gaining maximum output power the cantilevers are operating at the **limits of the material stresses** of the piezoceramic. Therefore, this is a major factor in the reduced lifetime.

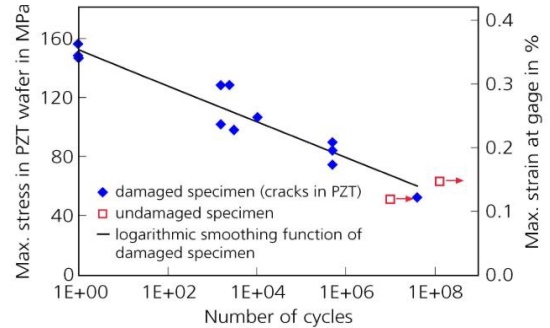


Figure 2: Failure (90% of initial voltage) of PZT as function of the number of cycles under tensile loading. [1]

Objective

Present a **literature overview of design principles** for improving piezoelectric cantilever beams operational lifetime, by limiting strain and strain concentrations.

Results

Three different design principles are investigated with the focus on strain limitation. A comparison of the design principles is made relative to the conventional rectangular cantilever, shown in Table 1.

Strain principle	none	Strain distribution	Strain distribution	Strain limitation	Strain limitation	Compressive strain
Strain-length graph						
Strain-amplitude graph						
Electrical power/area	o	+	+	o	o	o
Frequency bandwidth	o	o	o	+	+	o
Natural frequency	o	+	+	o	+	+
Impact resistance	o	+	+	++	++	+

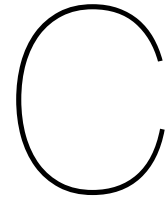
TABLE 1: Comparative overview of design principles for improved reliability. The performance is expressed by an increase or decrease relative to the rectangular cantilever.

Conclusion

Strain homogenisation, strain limitation and compressive strains can be effective design principles to **increase reliability without sacrificing efficiency**.

Future Research

Experimentally prove to what degree tapered energy harvesters are more reliable relative to conventional rectangular cantilevers.



Clamping design

The dynamics of mounting energy harvesters on shakers is often underestimated. This appendix elaborates further on the dynamics of the shaker and clamping mechanism. Technical drawings of the clamping design are added with some design considerations.

Dynamics of clamping

At the preliminary experimental tests a 3D printed clamping has been used. It is found out that this is not recommended, because of the low stiffness of PLA filament. Figure C.2 shows a frequency sweep at 1g of a same piezoceramic cantilever clamped in the aluminium clamping and 3D printed clamping. It can be concluded that the aluminium clamping is favourable. The 3D printed clamping has multiple modes in the frequency range measured resulting in a undefinable eigen frequency of the piezoceramic cantilever.

3D printed clamping versus aluminium clamping

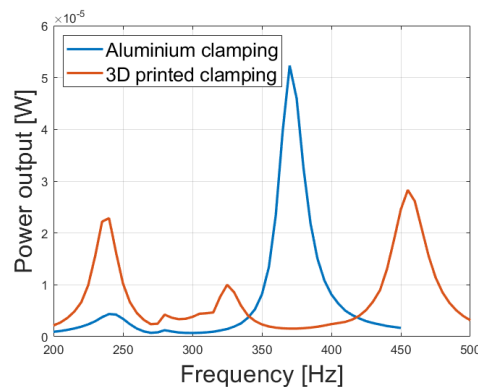


Figure C.1: Frequency sweep of rectangular cantilever for different clamping materials

To make the difference between the two clampings more clear a transfer function has been made from a frequency sweep with constant electrical power input. The transfer function is constructed by dividing the amplitude of the voltage output from the piezo cantilever (V_{piezo}) by the amplitude of the acceleration measured at the clamping from the piezo (A_{clamp}) or the acceleration of the shaker (A_{shaker}). Evaluating the transfer functions of Figure C.2a and C.2b shows that the 3D printed clamping has more peaks, yielding more uncertainties and controlling of the shaker at constant acceleration more difficult.

Difference of the transfer functions of figure C.2b represent the dynamic effects between the locations of the accelerometers.

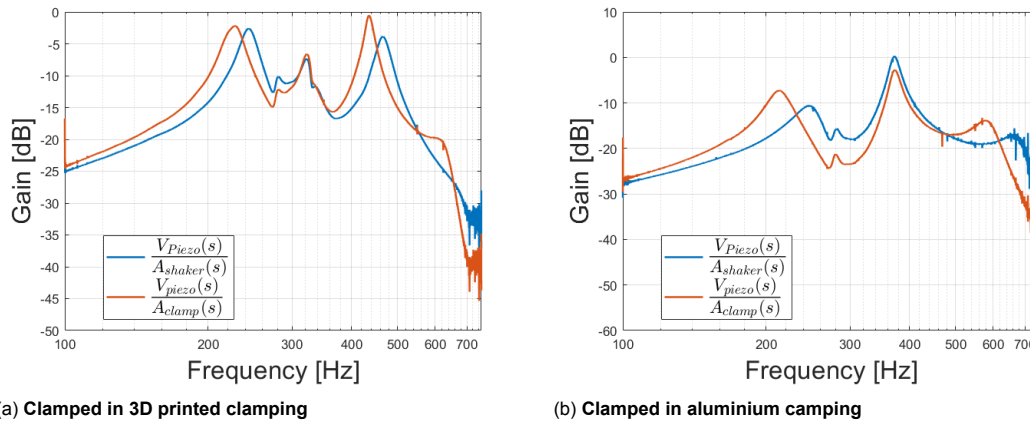


Figure C.2: Transfer functions

Shaker horizontal vs vertical

As can be seen in Figure C.2b there are still two undesirable peaks in the transfer functions in the frequency bandwidth 200-300 Hz. An attempt has been made to get rid of the peaks by tilting the shaker to an horizontal position instead of the vertical position. Figure C.3 shows the resulting transfer function. It can be seen that tilting the shaker to horizontal position does not solve the problem. Therefore, the choice has been made to keep the shaker vertical.

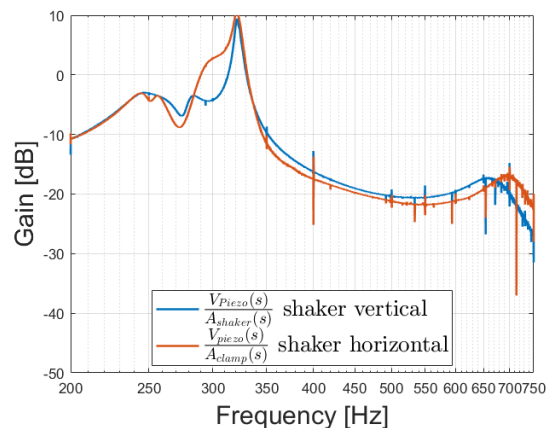


Figure C.3: Transfer function of power output piezoelectric cantilever with shaker horizontal versus vertical. With the aim to shift the eigen frequency of the system to lower frequency regime.

Repeatability of clamping

The repeatability of the clamping mechanism is tested by performing a frequency sweep over the same sample multiple times, while it is fixed and loosened before and after each frequency sweep. A fixed torque of 0.3 Nm is used for the screws fixing the clamping, ensuring a constant clamping stiffness. The repeatability has been measured over multiple days to include also the time variance of the measurement, results can be found in figure C.4. The standard deviation found for the eigen frequencies for the three samples is 1.0 Hz with a sample size of 7. It is expected that the standard deviation could have been lower, if the resolution of frequency sweep was smaller. However, all tests are performed with a frequency resolution of 1Hz for frequency sweeps.

Geometry

The clamping mechanism is made from aluminium and shaped in a milling process. The dimensions are in millimetres with a tolerance of 0.1mm unless otherwise specified. The drawings are given in

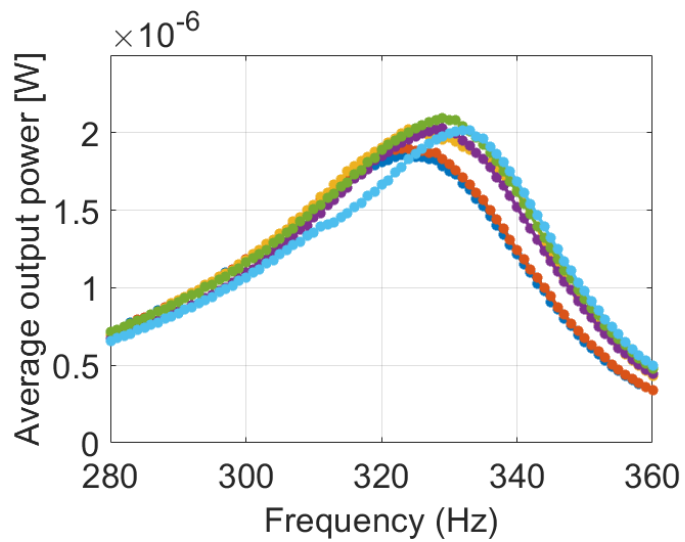


Figure C.4: Repeatability of clamping

Figure C.5 and Figure C.6. Important dimensions are the distance of the clamping area to the square block where the piezo cantilever is placed against, ensuring constant free length of the cantilevers. A small recess in the clamping area relative to the sides where the top part rests, ensures optimal contact area with the piezo cantilever and top clamping.

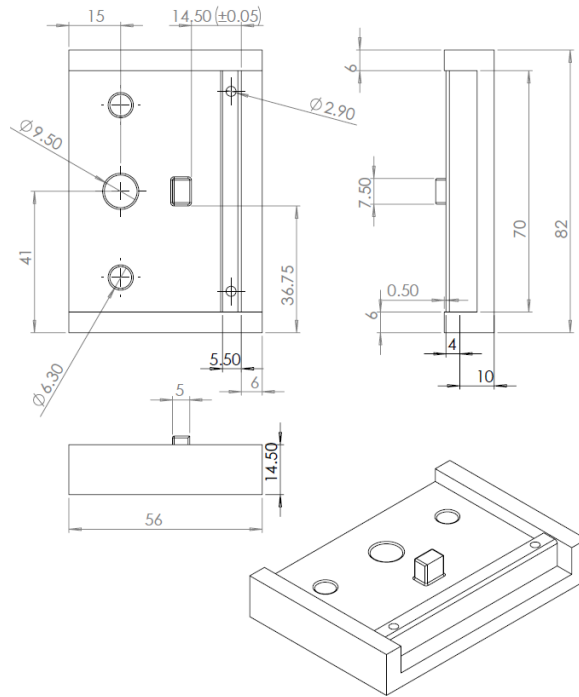


Figure C.5: Technical drawing of aluminium clamping base. With one large hole(9.5mm) for fixing the clamping to the shaker, a rectangular cube positioned 14.50 mm from the free-end clamping ensuring constant free length of the cantilever and two screw holes for fixing the top clamping.

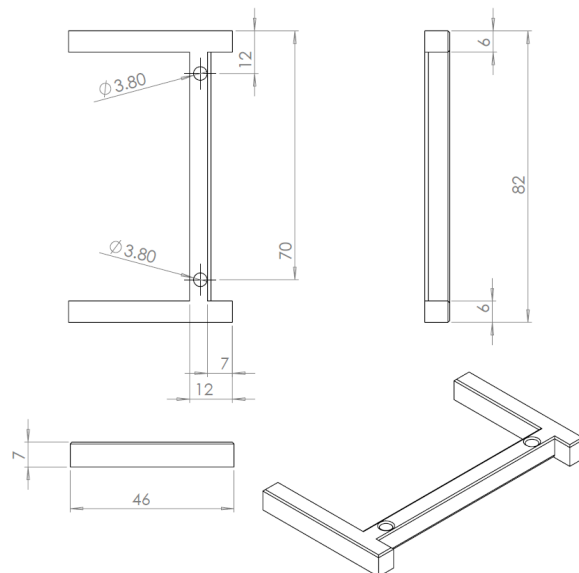
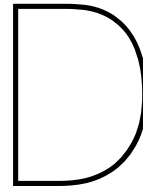


Figure C.6: Technical drawing of aluminium clamping top with two screw holes for fixing on the clamping base.



Electrical circuit

Electrical circuit

The electrical circuit is drawn below in Figure D.1. Over the piezoelectric layers a resistance is placed to calculate the power output. The voltage is differential measured by a NI data acquisition system. The variable resistance are used to find the optimal resistance over the piezo.

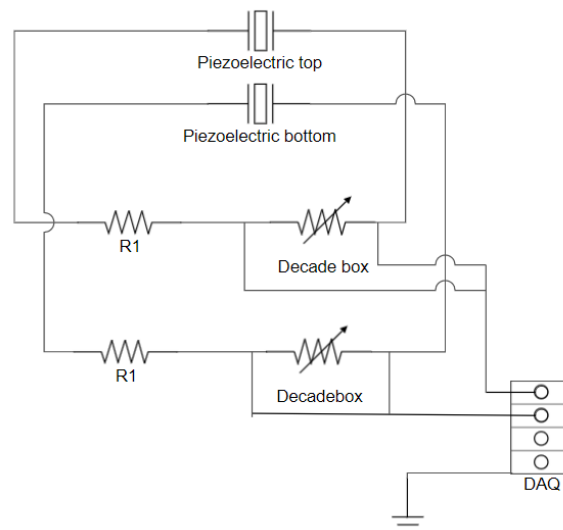


Figure D.1: **Electrical circuit for measuring the voltage output of the piezoceramic. With a variable resistance for the optimal resistance.**

Voltage distributor

For the lifetime experiments the voltages the piezoceramic cantilever outputs are out of range for the data acquisition system (DAQ). The range voltage range that can be measured by the DAQ is -10V to 10V. To measure the large voltage outputs of the piezo a voltage distributor is made. The voltage distributor is designed to lower the voltage output by a factor dependent on the combination of the resistance R1 and the decade box.

Effective resistance

A resistance is placed over the piezo to measure the voltage output, and calculate the power over the resistance. Important to consider is that the data acquisition system has also an internal resistance. For large resistances over the piezo the effective resistance will change, due to the parallel connected DAQ resistance. Figure D.2, depicts the relative error of the resistance over the piezo. For resistances lower than 10kOhm the relative error is below the 5%. Therefore the effective resistance should be taken into account for the calculations.

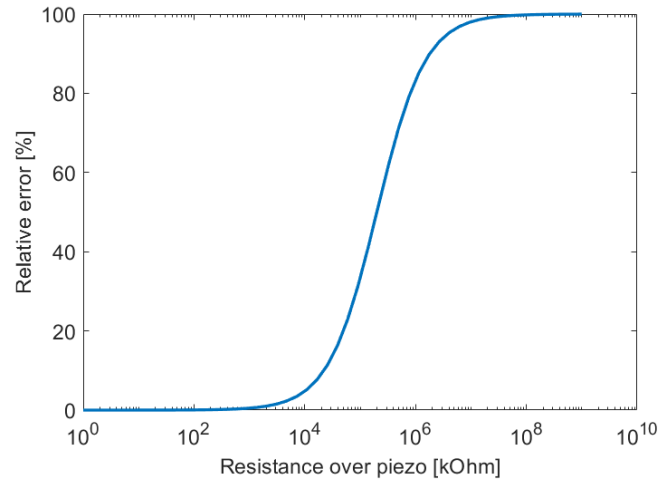
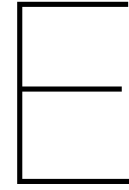


Figure D.2: Graph showing the influence of the internal resistance (200kOhm) of the DAQ on the effective resistance over the piezo.



Test samples

E

Sample data from supplier

Table E.1: Manufacture data of PZT508

Properties	Symbol	PZT508	Unit
Relative permittivity	ϵ_{r33}^T	3900	
Dielectric loss	$\tan \delta$	0.02	
Coupling Factors	k_ρ	0.71	
	k_{15}	0.72	
	k_{31}	0.41	
	k_{33}	-0.75	
Charge Constants/ Strain constants	d_{33}	720	$\times 10^{-12} C/N$
	d_{31}	-315	$\times 10^{-12} C/Norm/V$
	d_h	90	$\times 10^{-12} C/N$
	d_{15}	750	$\times 10^{-12} C/Norm.V$
Voltage constants/ Stress constants	g_{33}	18.5	$\times 10^{-3} Vm/N$
	g_{31}	-9	$\times 10^{-3} Vm/N$
	g_h	0.5	$\times 10^{-3} Vm/N$
Frequency constants	N_ρ	1950	Hz.m
	N_1	1420	Hz.m
	N_3	1880	Hz.m
Quality factor	Q_m	55	
Compliance	S_{33}^E	22	$\times 10^{-12} m^2/N$
	S_{11}^E	16.4	$\times 10^{-12} m^2/N$
	S_{33}^D	8.8	$\times 10^{-12} m^2/N$
	S_{11}^D	13.9	$\times 10^{-12} m^2/N$
	Y_{33}^E	4.9	$\times 10^{10} \{10\} N/m^2$
	Y_{11}^E	6.1	$\times 10^{10} \{10\} N/m^2$
	Y_{33}^D	11	$\times 10^{10} \{10\} N/m^2$
	Y_{11}^D	7	$\times 10^{10} \{10\} N/m^2$
Density	ρ	7900	kg/m^3
Curie Temperature	T_c	208	$^\circ C$

Sample data measured

All samples that have been used in this research have been coded, by a letter and number combination, to keep track of the experimental history. To make sure broken samples are not mixed up with non-broken samples.

Table E.2: Measured data of the rectangular, tapered and triangular cantilevers.

Tapered	Mass [Kg]	Capacitance Top [nf]	Capacitance bottom [nf]	Free vibration mass [Kg]	Effective mass [kg]
R1	0.980	39.7	43	0.709	0.158
R2	0.975			0.705	0.157
R3	0.991	38.05	39.20	0.717	0.160
R4	0.974	39.86	40.19	0.705	0.157
R5	0.976	38.55	39.22	0.706	0.157
R6	0.979			0.708	0.158
R10	0.985	42.74	41.82	0.713	0.159
R11	0.983	38.62	38.62	0.711	0.159
R12	0.990	39.57	39.01	0.716	0.160
R13	0.978	40.62	40.84	0.707	0.158
R14	0.985	40.66	40.78	0.713	0.159
R15	0.981	39.73	39.12	0.710	0.158
R16	0.977	40.11	38.6	0.707	0.158
R17	0.974	39.05	40.37	0.705	0.157

Table E.3: Measured properties 50% tapered samples

Tapered	Mass [Kg]	Capacitance Top [nf]	Capacitance bottom [nf]	Free vibration mass [Kg]	Effective mass [kg]
T1	0.702	29.1	29.5	0.431	0.072
T2	0.711	29.6	30	0.440	0.074
T3	0.727	29.2	28.8	0.456	0.076
T4	0.733	29.6	29.3	0.462	0.077
T5	0.752	29.7	31.00	0.481	0.080
T6	0.755	29.5	30.3	0.484	0.081
T7	0.756	30.5	30.3	0.485	0.081
T8	0.760	29.6	28.3	0.489	0.082
T9	0.738	30.2	29.8	0.467	0.078

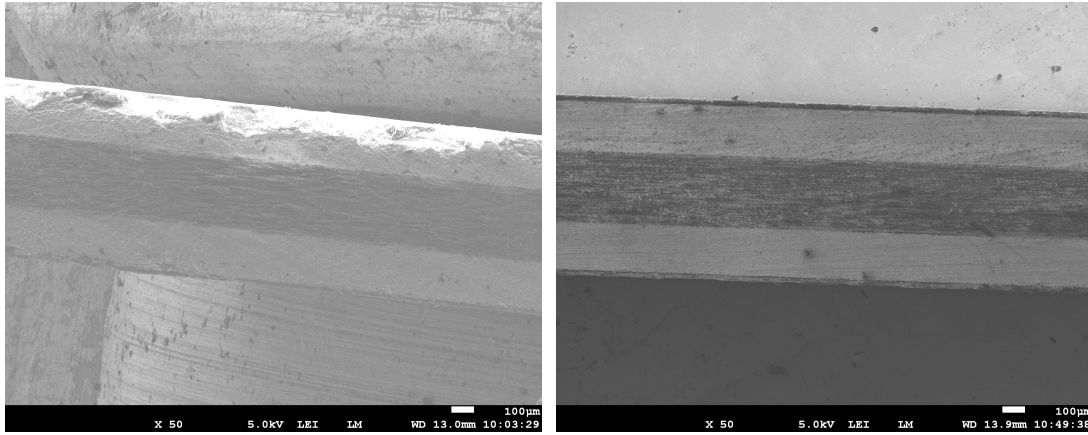
Table E.4: Measured properties %100 tapered cantilevers

Triangular	Mass [Kg]	Capacitance Top [nf]	Capacitance bottom [nf]	Free vibration mass [Kg]	Effective mass [kg]
D1	0.610	25.06	24.46	0.339	0.039
D2	0.615	24.84	23.8	0.344	0.040
D3	0.618	24.5	23.9	0.347	0.040
D4	0.635	25.3	25.6	0.364	0.042
D5	0.641	26.3	25.00	0.370	0.043
D6	0.644	26.8	25	0.373	0.043
D7	0.646	25	24.5	0.375	0.043
D8	0.649	25.2	26.5	0.378	0.043
D9	0.648	26.2	25.7	0.377	0.043

Cutting effects on tapered samples

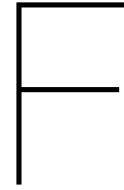
Analysing the samples by Scanning Electron Microscopy (SEM) visualises the effect of the cutting process on the cutted edge. Figure E.1a depicts a tapered sample where the cutted cross section shows defects at the bottom layer. Grinding the sides removes the superficial defects, the results can be seen in Figure E.1b. This shows the importance of polishing the sides for minimising defects.

In hindsight, it is advised to not fully taper the cantilevers for two reasons. First of all, it is hard to manufacture a 100% tapered tip. Secondly, the tip is very brittle. Therefore it is difficult to add a proofmass if necessary.



(a) Scanning Electron Microscope image from the cutted cross-section of a tapered sample

(b) Scanning Electron Microscope image from the cutted and grinded cross-section.



Test protocols experiments

To make sure the experiments can be reproduced and all samples undergo the same testing procedure three protocols are written and used for consistent experiments.

Protocol 1: Sample preparation

To shape the standard sized samples to tapered sizes an abrasive diamond cutting table is used. Laser cut PLA mold ensures constant geometries and safe cutting of the rectangular samples.

Procedures

1. Place the diamond cut-off wheel in the machine.
2. Visually inspect the samples on defects.
3. Place the piezoelectric cantilever in the mold for desired shape.
4. Fix the guidance bar at the distance from the abrasive saw equal to the width of the mold.
5. Switch on the Struers cutting machine; switch on the water cooling; set motorspeed on 1450 RPM.
6. Slowly move the mold with sample through the cutting wheel while keeping constant pushing force.
7. Switch off the machine.
8. Clean the sample by paper towel and store in a storage box preventing damage in transportation.
9. Clean the machine and workspace

Validation:

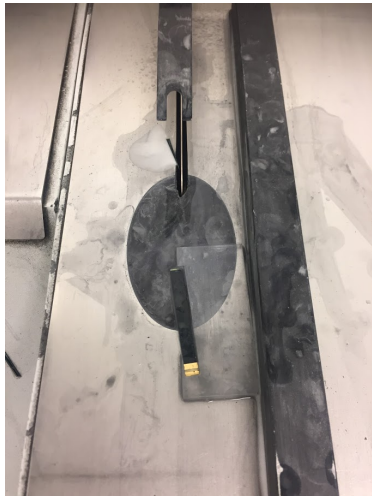
1. Measure the weight of the individual samples.
2. Measure the capacitance of the samples at 100Hz with an LCR meter.
3. Measure the length of the samples

Equipment:

Part	Specifications	unit
Struers secotom-10 precise cutting machine	Rotation speed	300-5000 RPM
	Rotation speed resolution	100 RPM
	Positioning	0-4mm (up-down)
	Max cutting sizes	60 mm dia. or 160 x 50 mm
	Cooling	800 ml/mim
Stuers Diamond cut-off wheel M1D20	Size	203 mm dia. x 0.6 mm

Table F.1: Specifications Shaker test setup





(a) Sample holder for abrasive cutting on cutting table



(b) Diamond precise abrasive cutting machine

Safety:

- Protective glasses
- Nitrile disposable protective gloves

Protocol 2: force deflection

Procedures

1. Screw the aluminium clamping to the Thorlabs structure.
2. Fix the piezocantilever in the clamping with 0.3Nm. Check if the free length of the cantilever is 34 mm.
3. Place the force deflection stage so that the the ball tip will apply a deformation at 28mm from the clamped end on the cantilever.
4. Slowly move the force deflection ball tip to the cantilever until a force is measured.
5. Place a microphone close to the cantilever.
6. Start audio recording and the experiment with the following settings: 2.75mm deformation, max force 3N, deformation increments of 0.01mm.
7. Retract the ball tip until it is not in contact with the cantilever, and remove the cantilever.
8. Save the data with the name tag of the tested cantilever, date and time.

Validation:

1. Use sound recording to validate cracks that are measured by a drop of force.
2. Validate the applied deformation by a laser distance meter.

Equipment:

Part	Specifications	unit
Force deflection setup	Deformation range	0-50mm
	Deformation resolution	0.1 μm
	Force range	0-45 N
	Laser sensor range	0-200mm
Ball bearing tip	Size	203 mm dia. x 0.6 mm

Table F.2: Specifications Shaker test setup

- Force deflection setup.
- 3D laser printed clamping.
- Ball bearing tip with screw-thread for deformation setup.

Safety:

Personal protective equipment(PPE) is not required.

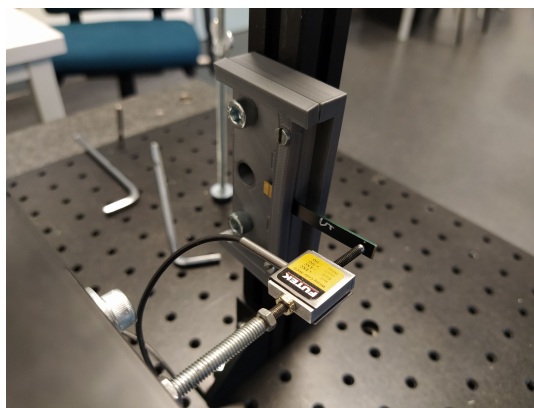


Figure F.3: Detail of force deflection setup: ball bearing tip with force sensor place at 28mm from clamped end on the cantilever

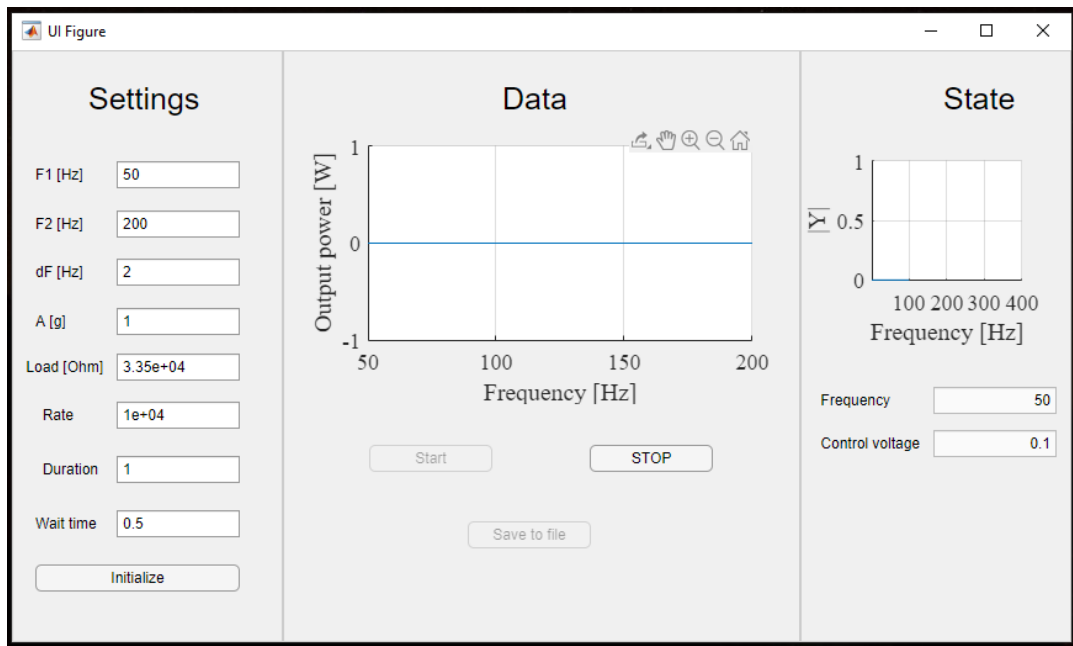


Figure F.4: Graphical user interface for frequency sweep. On the left side the experimental parameters can be given. In the middle of the GUI a real time plot is given from the measured data. On the right side the current states of the setting are shown

Protocol 3: Shaker

Procedures:

1. Switch on the shaker amplifier(0.5gain), voltage source for laser sensor, function generator and PCB accelerometer controller.
2. Place the piezo cantilever in the clamping mechanism with the brown electrical cables to the top.
3. Screw the clamping to 0.3Nm.
4. Connect the brown cables to the BNC connectors which are labelled top. Connect the yellow cables to the BNC connectors labelled bottom.
5. Place the shaker underneath both laser distant sensors. Verify if both are measuring in range by looking at the Keyence controller. "FFFFFFF" means that the position of the shaker is not correct relative to the laser sensors.
6. Set the desired resistance on both resistance decade boxes.
7. Check if the PCB accelerometer controller is finished calibrating. So, no red fault indication red is on.
8. Start the desired experiment from your Matlab code. (Resistance sweep, Frequency sweep, fatigue measurement)
9. Save the data with the name tag of the cantilever, the data, time and type of experiment.
10. Analyse the results before making changes to the setup.
11. Remove the cantilever by disconnecting the four cables; unscrewing the clamp; place the sample in a storage box to prevent damaging.
12. Switch of the amplifier, voltage source, function generator and accelerometer controller.

Validation:

Specifications test setup

Part	Specifications	unit
Shaker Type 4809	Frequency range	10-20.000 Hz
	Max acceleration	75 g
	Max Displacement	8 mm
	Resonant frequency shaker	20.000 Hz
NI DAQ	Measurement resolution	16 bit
	Impedance of DAQ	200 kOhm
	Sample rate	100 kS/s/ch
	Analog measurement range	±10 V
PCB Accelerometer	Frequency range accelerometer (±5%)	1Hz - 4kHz
	Frequency range accelerometer (±10%)	0.7 to 5000 Hz
	Sensitivity accelerometer	(± 10%) 100mV/g
	Measurement range accelerometer	± 50 g
	Resonant frequency accelerometer	≥25 kHz
Keyence laser sensor	Sampling cycle laser sensors	1 - 392 kHz (2.55-1000 μs)
	Measurement range laser sensor base	±3 mm ±0.12
	Measurement range laser sensor tip	±10 mm ±0.39
	Sampling frequency	1 - 392 kHz
	spot diameter	ø25 μm
ELC Resistance decade box	Resistance range	1 ohm - 1 Mohm
	Accuracy	1%
	Resolution	1 ohm height

Table F.3: Specifications Shaker test setup

Limitations of setup

Limitation	unit
Actuation acceleration range	± 50 g
Actuation frequency range	10 - 20.000 Hz
Actuation amplitude	±3mm
Max sampling frequency	5kHz

Table F.4: Specifications whole setup

Safety:

Personal protective equipment(PPE) is not required. The laser distance meters are of type class II, therefore no extra protection is needed.



Figure F.5: Photo of shaker test setup



Partial differential equations

Constitutive equations

Since, the piezoelectric material is ceramic Hooks law applies for the elastic behaviour.

$$-\nabla \cdot \sigma = f \tag{G.1}$$

Where σ is the stress tensor and f the body force vector. The electrostatic behaviours can be described by the Gauss' Law

$$\nabla \cdot D = \rho \tag{G.2}$$

Where D is is the electric displacement and ρ the distributed free charge. Both partial differential equations (PDE) can be written in a single equation.

$$-\nabla \cdot \begin{Bmatrix} \sigma \\ D \end{Bmatrix} = \begin{Bmatrix} f \\ -\rho \end{Bmatrix} \tag{G.3}$$

It is assumed that the strains remain small so that linear elastic constitutive relations apply. Also, the material is assumed to be isotropic. For the 2D plane stress case, the constitutive relations may be written in matrix form:

For our 2D application the plane stress conditions apply, $\sigma_{31} = \sigma_{13} = \sigma_{32} = \sigma_{23} = \sigma_{33} = 0$

$$\begin{Bmatrix} \sigma_{11} \\ \sigma_{22} \\ \sigma_{12} \\ D_1 \\ D_2 \end{Bmatrix} = \begin{bmatrix} C_{11} & C_{12} & e_{11} & e_{31} \\ C_{12} & C_{22} & e_{13} & e_{33} \\ C_{12} & e_{14} & e_{34} & \\ e_{11} & e_{13} & e_{14} & -\mathcal{E}_1 \\ e_{31} & e_{33} & e_{34} & -\mathcal{E}_2 \end{bmatrix} \begin{Bmatrix} \epsilon_{11} \\ \epsilon_{22} \\ \gamma_{12} \\ -E_1 \\ -E_2 \end{Bmatrix} \tag{G.4}$$

The strain vector can be written in terms of the x-displacement, ∂u and y displacement, ∂v .

$$\begin{Bmatrix} \epsilon_{11} \\ \epsilon_{22} \\ \gamma_{12} \end{Bmatrix} = \begin{Bmatrix} \frac{\partial u}{\partial x} \\ \frac{\partial v}{\partial y} \\ \frac{\partial u}{\partial y} + \frac{\partial v}{\partial x} \end{Bmatrix} \tag{G.5}$$

The electrical field can be written by the electrical potential $\partial \phi$.

$$\begin{Bmatrix} E_1 \\ E_2 \end{Bmatrix} = - \begin{Bmatrix} \frac{\partial \phi}{\partial x} \\ \frac{\partial \phi}{\partial y} \end{Bmatrix} \tag{G.6}$$



The constitutive equation can be written as.

$$\begin{aligned} S &= s^E T + d' E \\ D &= d T + \epsilon^T E \end{aligned} \quad (\text{G.7})$$

S is the strain tensor.

T is the stress tensor.

E is the electric field vector.

D is the electric displacement vector.

s^E is the elastic compliance matrix when subjected to a constant electric field.

d is the piezoelectric constant matrix.

ϵ^T is the permittivity measured at a constant stress.

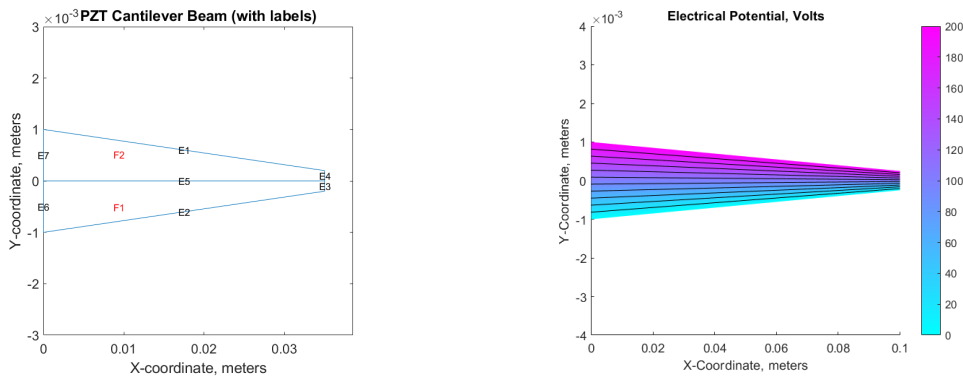
Matlab

2D tapered cantilever with applied voltage

With the above equations a piezoelectric cantilever can be simulated, with the help of the Matlab function *creatPDE*. For now we consider a 2D unimorph cantilever beam. The geometry and boundary conditions are given in Figure G.1. The following material properties were used:

- $E = 2.0 \times 10^9 \text{ N/m}^2$
- $\nu = 0.29$
- $G = 0.775 \times 10^9 \text{ N/m}^2$
- $d_{31} = 2.2 \times 10^{-11} \text{ C/N}$
- $d_{33} = -3.0 \times 10^{-11} \text{ C/N}$

The edges and faces of the geometry are labelled to define boundary conditions to the geometry.



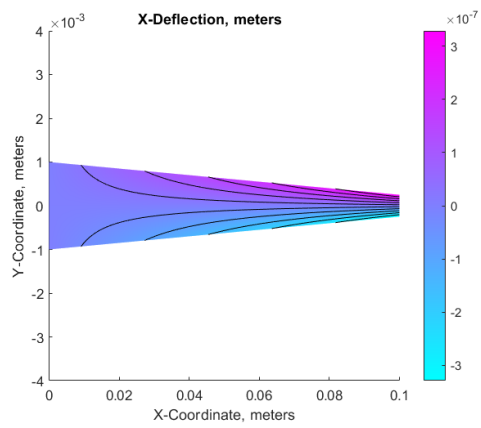
(a) The defined geometry with labels to define the boundary conditions (b) Plot showing the defined initial electrical boundary condition of 200 Volts on the top layer

Figure G.1: Initial conditions

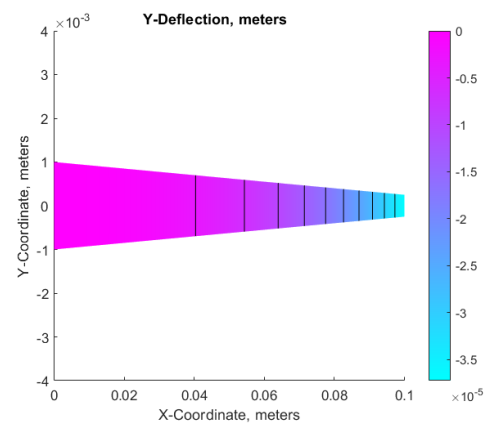
Figures G.2a and G.2b show the results of the simulation with an applied voltage potential. This is a relatively easy multi physics problem since it has a static solution. The results can be verified by analytical calculations.

2D tapered cantilever with applied deformation

An attempt has been made to change the initial boundary condition to a applied deformation. The initial deformation is found by solving the eigenvalue problem giving the nodal positions of the cantilever in deflected state. This deflected state is then used for solving the partial differential equations. So far, the problem could be solved. However, great difficulty is found by setting the electrical boundary conditions at the top and bottom layers. Therefore no solution could be found for the direct piezoelectric effect.

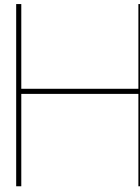


(a) The resulting deflection in x direction



(b) The resulting deflection in y direction

G



Mechanical analytical background

Eigenfrequency dependency

To maximise the output power of the piezoelectric energy harvester, the cantilever type piezoelectric energy harvesters are operated in a mechanical resonance frequency (eigenfrequency). Therefore, design of the eigenfrequency for the application is important. To analytically find the eigenfrequencies of cantilevers the following assumptions are made:

- Undamped cantilever
- Equally distributed mass over the beam
- Transverse free vibration
- The neutral surface does not change in length and normals to the neutral surface remain normal. Hence, the deflections are small.

Euler–Bernoulli beam differential equation (H.1) is used as basis to determine the eigen frequencies.

$$-EI \frac{\partial^4 y}{\partial x^4} = \rho \frac{\partial^2 y}{\partial t^2} \quad (\text{H.1})$$

With E , I and ρ the Young's modulus, second moment of area and the mass per unit length respectively. With four boundary conditions the solution of the boundary value problem can be found. Assumed zero displacement and slope at the fixed and zero bending moment and zero shear force at the free-end of the cantilever, yields the following boundary conditions.

$$y(0) = 0 \quad \left. \frac{dy}{dx} \right|_{x=L} = 0 \quad (\text{H.2a})$$

$$\left. \frac{d^2 y}{dx^2} \right|_{x=L} = 0 \quad \left. \frac{d^3 y}{dx^3} \right|_{x=L} = 0 \quad (\text{H.2b})$$

Suppose a quarter cosine wave solution for y .

$$y(x) = Y_0 \left[1 - \cos\left(\frac{\pi x}{2L}\right) \right] \quad \frac{dy}{dx} = Y_0 \left(\frac{\pi}{2L}\right) \sin\left(\frac{\pi x}{2L}\right) \quad (\text{H.3a})$$

$$\frac{d^2 y}{dx^2} = Y_0 \left(\frac{\pi}{2L}\right)^2 \cos\left(\frac{\pi x}{2L}\right) \quad \frac{d^3 y}{dx^3} = -Y_0 \left(\frac{\pi}{2L}\right)^3 \sin\left(\frac{\pi x}{2L}\right) \quad (\text{H.3b})$$

This solution meets all the boundary conditions except for the zero stress at the free end. As an approximation for the deflected shape the solution is accepted.

The Rayleigh-Ritz numerical method is used to find an approximation of an eigenvalue problem that is difficult to solve analytically. Therefore, the total kinetic and potential energy have to be determined.

The total kinetic energy is

$$T = \frac{1}{2} \omega_n^2 \int_0^L \rho_L(x) (y)^2 dx \quad (\text{H.4a})$$

$$T = \frac{1}{2} \omega_n^2 \int_0^L \left[\rho_m h b(x) \left(Y_0 \left(1 - \cos \left(\frac{\pi x}{2L} \right) \right) \right)^2 \right] dx \quad (\text{H.4b})$$

$$T = \frac{1}{2} \omega_n^2 \rho_m h Y_0^2 \int_0^L \left[\left(b_0 - \Delta b \frac{x}{L} \right) \left(1 - 2 \cos \left(\frac{\pi x}{2L} \right) + \cos^2 \left(\frac{\pi x}{2L} \right) \right) \right] dx \quad (\text{H.4c})$$

$$T = \frac{1}{2} \rho_m \omega_n^2 h Y_0^2 \int_0^L \left[\left(b_0 - \Delta b \frac{x}{L} \right) \left(1 - 2 \cos \left(\frac{\pi x}{2L} \right) + \frac{1}{2} + \frac{1}{2} \cos \left(\frac{\pi x}{L} \right) \right) \right] dx \quad (\text{H.4d})$$

$$T = \frac{1}{2} \rho_m \omega_n^2 h Y_0^2 \int_0^L \left[\left(b_0 - \Delta b \frac{x}{L} \right) \left(\frac{3}{2} - 2 \cos \left(\frac{\pi x}{2L} \right) + \cos \left(\frac{\pi x}{L} \right) \right) \right] dx \quad (\text{H.4e})$$

$$T = \frac{1}{2} \rho_m \omega_n^2 h Y_0^2 \int_0^L \left[\frac{3}{2} b_0 - 2 b_0 \cos \left(\frac{\pi x}{2L} \right) + \frac{1}{2} b_0 \cos \left(\frac{\pi x}{L} \right) - \frac{3}{2} \Delta b \frac{x}{L} + 2 \Delta b \frac{x}{L} \cos \left(\frac{\pi x}{2L} \right) - \frac{1}{2} \Delta b \frac{x}{L} \cos \left(\frac{\pi x}{L} \right) \right] dx \quad (\text{H.4f})$$

$$T = \frac{1}{2} \rho_m \omega_n^2 h Y_0^2 \left[\frac{3}{2} b_0 x - \frac{4 L b_0}{\pi} \sin \left(\frac{\pi x}{2L} \right) + \frac{L b_0}{2\pi} \sin \left(\frac{\pi x}{L} \right) - \frac{3}{4} \Delta b \frac{x^2}{L} + 4 \Delta b \left(\frac{\pi x \sin \left(\frac{\pi x}{2L} \right) + 2L \cos \left(\frac{\pi x}{2L} \right)}{\pi^2} \right) - \frac{1}{2} \Delta b \left(\frac{\pi x \sin \left(\frac{\pi x}{L} \right) + L \cos \left(\frac{\pi x}{L} \right)}{\pi^2} \right) \right]_0^L \quad (\text{H.4g})$$

$$T = \frac{1}{2} \rho_m \omega_n^2 h Y_0^2 \left[\frac{3}{2} b_0 L - \frac{4 L b_0}{\pi} - \frac{3}{4} \Delta b L + 4 \Delta b \frac{L}{\pi} + \frac{1}{2} \Delta b \frac{L}{\pi} - 4 \Delta b \frac{2L}{\pi^2} + \frac{1}{2} \Delta b \frac{L}{\pi^2} - 4 \Delta b \frac{2L}{\pi^2} + \frac{1}{2} \Delta b \frac{L}{\pi^2} \right] \quad (\text{H.4h})$$

$$T = \frac{1}{4} \rho_m \omega_n^2 h Y_0^2 L \left[b_0 \left(3 - \frac{8}{\pi} \right) + \Delta b \left(-\frac{3}{4} + \frac{4}{\pi} \right) + \frac{\Delta b}{\pi^2} \left(\frac{1}{2} - 8 + \frac{1}{2} \right) \right] \quad (\text{H.4i})$$

$$T = \frac{1}{4} \rho_m \omega_n^2 Y_0^2 L \left[b_0 \left(3 - \frac{8}{\pi} \right) + \Delta b \left(-\frac{3}{4} + \frac{4}{\pi} \right) - 7 \frac{\Delta b}{\pi^2} \right] \quad (\text{H.4j})$$

The total potential energy is

$$P = \frac{EI(x)}{2} \int_0^L \left(\frac{d^2 y}{dx^2} \right)^2 dx \quad (\text{H.5a})$$

$$P = \frac{E}{2} \int_0^L \left[\frac{h^3}{12} \left(b_0 - \Delta b \frac{x}{L} \right) \left(y_0 \left(\frac{\pi}{2L} \right) \cos \left(\frac{\pi x}{2L} \right) \right)^2 \right] dx \quad (\text{H.5b})$$

$$P = \frac{E h^3}{24} \left[y_0 \left(\frac{\pi}{2L} \right) \right]^2 \int_0^L \left[\left(b_0 - \Delta b \frac{x}{L} \right) \left(\cos \left(\frac{\pi x}{2L} \right) \right)^2 \right] dx \quad (\text{H.5c})$$

$$P = \frac{E h^3}{24} y_0^2 \left(\frac{\pi}{2L} \right)^4 \int_0^L \left[\left(b_0 - \Delta b \frac{x}{L} \right) \frac{1}{2} \left(1 + \cos \left(\frac{\pi x}{L} \right) \right) \right] dx \quad (\text{H.5d})$$

$$P = \frac{E h^3}{48} y_0^2 \left(\frac{\pi}{2L} \right)^4 \int_0^L \left[b_0 + b_0 \cos \left(\frac{\pi x}{L} \right) - \Delta b \frac{x}{L} - \Delta b \frac{x}{L} \cos \left(\frac{\pi x}{L} \right) \right] dx \quad (\text{H.5e})$$

$$P = \frac{E h^3}{48} y_0^2 \left(\frac{\pi}{2L} \right)^4 \left[b_0 x + b_0 \left(\frac{L}{\pi} \right) \sin \left(\frac{\pi x}{L} \right) - \frac{1}{2} \Delta b \frac{x^2}{L} - \frac{\Delta b}{\pi^2} \left(\pi x \sin \left(\frac{\pi x}{L} \right) + L \cos \left(\frac{\pi x}{L} \right) \right) \right]_0^L \quad (\text{H.5f})$$

$$P = \frac{E h^3}{48} y_0^2 L \left(\frac{\pi}{2L} \right)^4 \left[b_0 - \frac{1}{2} \Delta b + \frac{\Delta b}{\pi^2} \right] \quad (\text{H.5g})$$

By conservation of energy the potential and kinetic energy should be equal.

$$\frac{1}{4}\rho_m\omega_n^2hY_0^2L\left[b_0\left(3-\frac{8}{\pi}\right)+\Delta b\left(-\frac{3}{4}+\frac{4}{\pi}\right)-7\frac{\Delta b}{\pi^2}\right]=\frac{Eh^3}{48}Y_0^2L\left(\frac{\pi}{2L}\right)^4\left[b_0-\frac{1}{2}\Delta b+\frac{\Delta b}{\pi^2}\right] \quad (\text{H.6a})$$

$$\rho_m\omega_n^2\left[b_0\left(3-\frac{8}{\pi}\right)+\Delta b\left(-\frac{3}{4}+\frac{4}{\pi}\right)-7\frac{\Delta b}{\pi^2}\right]=\frac{Eh^2}{12}\left(\frac{\pi^4}{16L^4}\right)\left[b_0-\frac{1}{2}\Delta b+\frac{\Delta b}{\pi^2}\right] \quad (\text{H.6b})$$

$$\omega_n^2=\left(\frac{Eh^2\pi^4}{192\rho_mL^4}\right)\frac{\left[b_0-\frac{1}{2}\Delta b+\frac{\Delta b}{\pi^2}\right]}{\left[b_0\left(3-\frac{8}{\pi}\right)+\Delta b\left(-\frac{3}{4}+\frac{4}{\pi}\right)-7\frac{\Delta b}{\pi^2}\right]} \quad (\text{H.6c})$$

$$\omega_n=\left(\frac{\pi^2}{\sqrt{192}}\right)\sqrt{\left(\frac{Eh^2}{\rho_mL^4}\right)}\sqrt{\frac{\left[b_0-\frac{1}{2}\Delta b+\frac{\Delta b}{\pi^2}\right]}{\left[b_0\left(3-\frac{8}{\pi}\right)+\Delta b\left(-\frac{3}{4}+\frac{4}{\pi}\right)-7\frac{\Delta b}{\pi^2}\right]}} \quad (\text{H.6d})$$

Eigenfrequency rectangular cantilevers

For $\Delta b = 0$ the eigenfrequency in Hz of a rectangular cantilever can be found.

$$f_n=\left(\frac{1}{2\pi}\right)\left(\frac{\pi^2}{\sqrt{192}}\right)\sqrt{\left(\frac{Eh^2}{\rho_mL^4}\right)}\sqrt{\frac{[b_0]}{\left[b_0\left(3-\frac{8}{\pi}\right)\right]}} \quad (\text{H.7a})$$

$$f_n=\left(\frac{1}{2\pi}\right)\left(\frac{\pi^2}{\sqrt{192}}\right)\sqrt{\frac{1}{\left[\left(3-\frac{8}{\pi}\right)\right]}}\sqrt{\left(\frac{Eh^2}{\rho_mL^4}\right)} \quad (\text{H.7b})$$

$$f_n=\left(\frac{1}{2\pi}\right)1.05766\sqrt{\left(\frac{Eh^2}{\rho_mL^4}\right)} \quad (\text{H.7c})$$

$$(\text{H.7d})$$

This can be rewritten to

$$f_n\approx\left\{\frac{1}{2\pi}\right\}\left\{\frac{3.664}{L_0^2}\right\}\sqrt{\frac{EI}{\rho L}} \quad (\text{H.8})$$

Eigenfrequency of fully tapered cantilevers

For a fully tapered cantilever with $\Delta b = b_0$ the eigenfrequency can be calculated with the following formula.

$$f_n=\left(\frac{1}{2\pi}\right)\left(\frac{\pi^2}{\sqrt{192}}\right)\sqrt{\left(\frac{Eh^2}{\rho_mL^4}\right)}\sqrt{\frac{\left[b_0-\frac{1}{2}b_0+\frac{b_0}{\pi^2}\right]}{\left[b_0\left(3-\frac{8}{\pi}\right)+b_0\left(-\frac{3}{4}+\frac{4}{\pi}\right)-7\frac{b_0}{\pi^2}\right]}} \quad (\text{H.9a})$$

$$f_n=\left(\frac{1}{2\pi}\right)\left(\frac{\pi^2}{\sqrt{192}}\right)\sqrt{\frac{\left[\frac{1}{2}b_0+\frac{b_0}{\pi^2}\right]}{\left[\frac{9}{4}b_0-\frac{4}{\pi}b_0-\frac{7}{\pi^2}b_0\right]}}\sqrt{\left(\frac{Eh^2}{\rho_mL^4}\right)} \quad (\text{H.9b})$$

$$f_n=\left(\frac{1}{2\pi}\right)\left(\frac{\pi^2}{\sqrt{192}}\right)\sqrt{\frac{\left[\frac{1}{2}+\frac{1}{\pi^2}\right]}{\left[\frac{9}{4}-\frac{4}{\pi}-\frac{7}{\pi^2}\right]}}\sqrt{\left(\frac{Eh^2}{\rho_mL^4}\right)} \quad (\text{H.9c})$$

$$f_n=\left(\frac{1}{2\pi}\right)1.06790\sqrt{\left(\frac{Eh^2}{\rho_mL^4}\right)} \quad (\text{H.9d})$$

Comparing eigenfrequency of rectangular and tapered cantilevers

Comparing both formula's it can be found that the eigenfrequency of the tapered cantilevers is a factor 1.001 higher than the eigenfrequency of rectangular cantilevers.

$$\rho_m = m * l * h * b(x) \quad (\text{H.10a})$$

$$\rho_m = m * l * h * (b_0 - \Delta b \frac{x}{L}) \quad (\text{H.10b})$$

Eigenfrequency tapered cantilevers

Tapered cantilevers have a variable stiffness $EI(x)$ and a variable mass per unit length $\rho(x)$. So, the equation for the eigenfrequency changes as follows.

$$f_n \approx \left\{ \frac{1}{2\pi} \right\} \left\{ \frac{3.664}{L_0^2} \right\} \sqrt{\frac{EI(x)}{\rho_L(x)}} \quad (\text{H.11})$$

The second moment of inertia is defined as

$$I = \int \int y^2 dy dx \quad (\text{H.12})$$

Since the width varies over the length of the tapered cantilever the boundary conditions are a function of x . This is expressed by the initial width b_0 and the difference in width Δb .

$$I(x) = \int_{-\frac{b_0}{2} + \frac{\Delta b}{2} \frac{x}{L}}^{\frac{b_0}{2} - \frac{\Delta b}{2} \frac{x}{L}} \int_{-\frac{h}{2}}^{\frac{h}{2}} y^2 dy dx \quad (\text{H.13a})$$

$$I(x) = \int_{-\frac{b_0}{2} + \frac{\Delta b}{2} \frac{x}{L}}^{\frac{b_0}{2} - \frac{\Delta b}{2} \frac{x}{L}} \frac{h^3}{12} dx \quad (\text{H.13b})$$

$$I(x) = \frac{h^3}{12} \left(b_0 - \Delta b \frac{x}{L} \right) \quad (\text{H.13c})$$

The same yields for the distributed mass of the cantilever. Recall, this is expressed by the density per unit length ρ .

$$\rho_L(x) = \rho_m h b(x) \quad (\text{H.14a})$$

$$\rho_L(x) = \rho_m h (b_0 - \Delta b \frac{x}{L}) \quad (\text{H.14b})$$

Substituting this in equation H.11 yields:

$$f_n \approx \left\{ \frac{1}{2\pi} \right\} \left\{ \frac{3.664}{L_0^2} \right\} \sqrt{\frac{E \frac{h^3}{12} (b_0 - \Delta b \frac{x}{L})}{\rho_m h (b_0 - \Delta b \frac{x}{L})}} \quad (\text{H.15})$$

$$f_n \approx \left\{ \frac{1}{2\pi} \right\} \left\{ \frac{3.664}{L_0^2} \right\} \sqrt{\frac{E \frac{h^2}{12}}{\rho_m}} \quad (\text{H.16})$$

Notice that the width is eliminated against each other in equation ???. Therefore it can be concluded that the eigenfrequency is analytically independent of the degree of tapering.

Eigenfrequency tapered cantilevers

The eigenfrequency of tapered cantilevers is independent of the degree of tapering at free vibration without proof mass.

Stiffness of cantilever

The stiffness of cantilever beams is given by the parameterized equation H.17. Where the stiffness of the cantilever is a function of the length, since the inertia is not constant over the length.

$$k(x) = \frac{3EI(x)}{L^3} \quad (\text{H.17})$$

$$k(x) = \frac{3E}{L^3} \frac{h^3}{12} \left(b_0 - \Delta b \frac{x}{L} \right) \quad (\text{H.18a})$$

$$= \frac{Eh^3}{4L^3} \left(b_0 - \Delta b \frac{x}{L} \right) \quad (\text{H.18b})$$

Stiffness rectangular cantilever

$$k = \frac{Eh^3 b_0}{4L^3} \quad (\text{H.19})$$

Stiffness tapered cantilever

$$k = \frac{Eh^3 b_0}{8L^3} \quad (\text{H.20})$$

Effective mass

The effective mass can be calculated by the eigenfrequency formula, since the stiffness and eigenfrequency are known.

$$m_{eff} = \frac{k}{\omega^2} \quad (\text{H.21a})$$

$$= \frac{\frac{3E}{L^3} \frac{h^3}{12} \left(b_0 - \Delta b \frac{x}{L} \right)}{2} \quad (\text{H.21b})$$

$$\left(\frac{3.664}{L_0^2} \sqrt{\frac{E \frac{h^2}{12}}{\rho_m}} \right)$$

$$= \frac{\frac{3}{L^3} h \left(b_0 - \Delta b \frac{x}{L} \right)}{\left(\frac{3.664^2}{L_0^4} \frac{1}{\rho_m} \right)} \quad (\text{H.21c})$$

$$= 0.223Lh\rho_m \left(b_0 - \Delta b \frac{x}{L} \right) \quad (\text{H.21d})$$

$$= 0.223Lh\rho_m \frac{1}{L} \int_0^L \left(b_0 - \Delta b \frac{x}{L} \right) dx \quad (\text{H.21e})$$

$$= 0.223Lh\rho_m \frac{1}{L} \left[b_0 x - \Delta b \frac{x^2}{2L} \right]_0^L \quad (\text{H.21f})$$

$$= 0.223h\rho_m \left(b_0 L - \Delta b \frac{L}{2} \right) \quad (\text{H.21g})$$

$$(\text{H.21h})$$

Effective mass rectangular

For a rectangular cantilever without tip mass the equations would be

$$m_{eff} = 0.223\rho_m b_0 h L_0 = 0.223m \quad (\text{H.22})$$

Effective mass fully tapered cantilever

For the fully tapered cantilever $\Delta b = b_0$.

$$m_{eff} = 0.223h\rho_m \left(b_0 L_0 - b_0 \frac{L_0}{2} \right) \quad (\text{H.23a})$$

$$= 0.1115h\rho_m b_0 L_0 \quad (\text{H.23b})$$

For semi tapered cantilevers $\Delta b = 0.5b_0$.

$$m_{eff} = 0.223h\rho_m \left(b_0 L_0 - \frac{b_0}{2} \frac{L_0}{2} \right) \quad (\text{H.24a})$$

$$= 0.16725h\rho_m b_0 L_0 \quad (\text{H.24b})$$

Stress distribution

The maximum average strain over a cantilever beam is given by equation H.25, assumed an homogeneous bimorph cantilever with thickness t_c . It is defined as the strain along the length (x) and the thickness (z).

$$S_{average} = \frac{1}{t_c/2} \frac{1}{L} \int_0^{t_c/2} \int_0^L \frac{z}{\rho(x)} dx dz \quad (\text{H.25})$$

Where $\rho(x)$ is the radius of bending curvature along the length of the cantilever. For triangular cantilevers, the radius of curvature is constant over the length. Which implies that the strain over the length (x) is also constant.

Bibliography

- [1] Definition of reliability in English by Oxford Dictionaries. URL <https://en.oxforddictionaries.com/definition/reliability>.
- [2] Abdul Hafiz Alameh, Mathieu Gratuze, Mohannad Y. Elsayed, and Frederic Nabki. Effects of proof mass geometry on piezoelectric vibration energy harvesters. *Sensors (Switzerland)*, 18(5), 2018. ISSN 14248220. doi: 10.3390/s18051584.
- [3] Steven R Anton and Henry A Sodano. A review of power harvesting using piezoelectric materials (2003-2006). *Smart Materials and Structures*, 16, 2007. doi: 10.1088/0964-1726/16/3/R01. URL <http://iopscience.iop.org/article/10.1088/0964-1726/16/3/R01/pdf>.
- [4] Jessy Baker, Shad Roundy, and Prof Paul Wright. Alternative Geometries for Increasing Power Density in Vibration Energy Scavenging for Wireless Sensor Networks. *3rd International Energy Conversion Engineering Conference*, 2005. ISSN 2005-5617. doi: 10.2514/6.2005-5617. URL <http://arc.aiaa.org>.
- [5] S.P. Beeby, R.N. Torah, and M.J. Tudor. Kinetic energy harvesting. In Neil Beeby, Stephen; White, editor, *Energy Harvesting for Autonomous systems*, number January, chapter 4, pages 91–134. Artech House, 2010. ISBN 978-1-59693-718-5. URL <http://eprints.soton.ac.uk/340665/>.
- [6] A Bosotti, R Paparella, and F Puricelli. PI piezo Life Time Test Report. Technical report, 2005. URL https://www.pi-usa.us/fileadmin/user_upload/pi_us/files/technotes_whitepapers/PI_Piezoactuator_Cryogenic_Temperature_Superconducting_Cavity_10_Years_LifeTimeTestReportC.pdf.
- [7] E. Brusa, S. Zelenika, L. Moro, and D. Benasciutti. Analytical characterization and experimental validation of performances of piezoelectric vibration energy scavengers. volume 7362, page 736204. International Society for Optics and Photonics, 5 2009. doi: 10.1117/12.821425. URL <http://proceedings.spiedigitallibrary.org/proceeding.aspx?doi=10.1117/12.821425>.
- [8] Markys G Cain, Mark Stewart, Mark Gee, M G Cain, M Stewart, and M G Gee. Degradation of Piezoelectric Materials. Technical Report January, National Physical Laboratory Management Ltd, Teddington, Middlesex, TW11 0LW, UK, 1999.
- [9] Pierre Curie and Paul-Jacques Curie. Développement, par pression, de l'électricité polaire dans les cristaux hémihédres à faces inclinées. *Comptes rendus de l'Académie des Sciences*, (91): 294–383, 1880.
- [10] John M Dietl and Ephrahim Garcia. Beam Shape Optimization for Power Harvesting. *Journal of Intelligent Material Systems and Structures*, 21(6):633–646, 2010. doi: 10.1177/1045389X10365094. URL <http://jim.sagepub.com>.
- [11] Monika Gall and Barbel Thielicke. Life-span investigations of piezoceramic patch sensors and actuators. volume 6526, page 65260P. International Society for Optics and Photonics, 4 2007. doi: 10.1117/12.714756. URL <http://proceedings.spiedigitallibrary.org/proceeding.aspx?doi=10.1117/12.714756>.
- [12] Monika Gall, Barbel Thielicke, and Ingo Schmidt. Integrity of piezoceramic patch transducers under cyclic loading at different temperatures. *Smart Materials and Structures*, 18(10), 2009. doi: 10.1088/0964-1726/18/10/104009. URL <http://iopscience.iop.org/article/10.1088/0964-1726/18/10/104009/pdf>.

- [13] P Glynne-Jones, S P Beeby, and N M White. A method to determine the ageing rate of thick-film PZT layers. Technical report, 2001. URL www.iop.org/Journals/mt.
- [14] P. Glynne-Jones, S.P. Beeby, and N.M. White. Towards a piezoelectric vibration-powered micro-generator. *IEE Proceedings - Science, Measurement and Technology*, 148(2):68–72, 2001. ISSN 13502344. doi: 10.1049/ip-smt:20010323. URL http://digital-library.theiet.org/content/journals/10.1049/ip-smt_20010323.
- [15] Frank; Goldschmidtboeing and Peter Woias. Characterization of different beam shapes for piezoelectric energy harvesting. *Journal of Micromechanics and Microengineering*, 2008. doi: 10.1088/0960-1317/18/10/104013. URL <http://iopscience.iop.org/article/10.1088/0960-1317/18/10/104013/pdf>.
- [16] Richard F Hellbaum, Robert G Bryant, and Robert L Fox. Thin layer composite unimorph ferroelectric driver and sensor, 4 1995. URL <https://patents.google.com/patent/US5632841A/en>.
- [17] Jan Holterman and Pim Groen. *An Introduction to Piezoelectric Materials and Applications*. Stichting Applied Piezo, 2013. ISBN 978-90-819361-1-8.
- [18] Rouhollah Hosseini and Mohsen Hamed. An investigation into resonant frequency of trapezoidal V-shaped cantilever piezoelectric energy harvester. *Microsystem Technologies*, 22:1127–1134, 2016. doi: 10.1007/s00542-015-2583-7. URL <https://link.springer.com/content/pdf/10.1007%2Fs00542-015-2583-7.pdf>.
- [19] Jacopo Iannacci. Reliability of MEMS: A perspective on failure mechanisms, improvement solutions and best practices at development level. 2015. doi: 10.1016/j.displa.2014.08.003. URL <http://dx.doi.org/10.1016/j.displa.2014.08.003>.
- [20] Mir Imran. Energy harvesting mechanism for medical devices, 9 2009. URL <https://patents.google.com/patent/US9026212B2/en?q=artificial&q=cardiac+pacemakers&q=piezo&q=energy+harvesting&oq=artificial+cardiac+pacemakers+piezo+energy+harvesting>.
- [21] Lei Jin, Shiqiao Gao, · Xiaoya Zhou, and Guangyi Zhang. The effect of different shapes of cantilever beam in piezoelectric energy harvesters on their electrical output. *Microsystem Technologies*, 23:4805–4814, 2017. doi: 10.1007/s00542-016-3261-0. URL <https://link.springer.com/content/pdf/10.1007%2Fs00542-016-3261-0.pdf>.
- [22] T M Kamel, R Elfrink, M Renaud, and Al . Effect of length/width ratio of tapered beams on the performance of piezoelectric energy harvesters. 2013. doi: 10.1088/0964-1726/22/7/075015. URL <http://iopscience.iop.org/article/10.1088/0964-1726/22/7/075015/pdf>.
- [23] Seon-Bae Kim, Jung-Hyun Park, Hosang Ahn, Dan Liu, and Dong-Joo Kim. Temperature effects on output power of piezoelectric vibration energy harvesters. *Microelectronics Journal*, 42:988–991, 2011. doi: 10.1016/j.mejo.2011.05.005. URL www.elsevier.com/locate/mejo.
- [24] Eric J. Kjolsing and Michael D. Todd. The effects of damage accumulation in optimizing a piezoelectric energy harvester configuration. In Hoon Sohn, editor, *Sensors and Smart Structures Technologies for Civil, Mechanical, and Aerospace Systems 2018*, page 102. SPIE, 3 2018. ISBN 9781510616929. doi: 10.1117/12.2283053. URL <https://www.spiedigitallibrary.org/conference-proceedings-of-spie/10598/2283053/The-effects-of-damage-accumulation-in-optimizing-a-piezoelectric-energy/10.1117/12.2283053.full>.
- [25] K Komai, K Minoshima, and S Inoue. Fracture and fatigue behavior of single crystal silicon microelements and nanoscopic AFM damage evaluation. Technical report, 1998. URL <https://link-springer-com.tudelft.idm.oclc.org/content/pdf/10.1007%2Fs005420050137.pdf>.

- [26] Wen G. Li, Siyuan He, and Shudong Yu. Improving power density of a cantilever piezoelectric power harvester through a curved L-shaped proof mass. *IEEE Transactions on Industrial Electronics*, 57(3):868–876, 2010. ISSN 02780046. doi: 10.1109/TIE.2009.2030761.
- [27] Yabin Liao, Henry A Sodano, Simon Paquin, and Yves St-Amant. Improving the performance of a piezoelectric energy harvester using a variable thickness beam. *MATERIALS AND STRUCTURES Smart Mater. Struct.*, 19:105020–105034, 2010. doi: 10.1088/0964-1726/19/10/105020. URL <http://iopscience.iop.org/article/10.1088/0964-1726/19/10/105020/pdf>.
- [28] Zdeněk Majer, Oldřich Ševeček, Zdeněk Machů, Kateřina Štegnerová, and Michal Kotoul. Optimization of Design Parameters of Fracture Resistant Piezoelectric Vibration Energy Harvester. *Key Engineering Materials*, 774:416–422, 8 2018. doi: 10.4028/www.scientific.net/kem.774.416.
- [29] Kuok H. Mak, Stewart McWilliam, Atanas A. Popov, and Colin H.J. Fox. Performance of a cantilever piezoelectric energy harvester impacting a bump stop. *Journal of Sound and Vibration*, 330:6184–6202, 2011. ISSN 0022460X. doi: 10.1016/j.jsv.2011.07.008.
- [30] S Mall and J M Coleman. Monotonic and fatigue loading behavior of quasi-isotropic graphite/epoxy laminate embedded with piezoelectric sensor. Technical report, 1998. URL <http://iopscience.iop.org/article/10.1088/0964-1726/7/6/010/pdf>.
- [31] Loreto Mateu and Francesc Moll. Optimum Piezoelectric Bending Beam Structures for Energy Harvesting using Shoe Inserts. *Journal of Intelligent Material Systems and Structures*, 16(10): 835–845, 10 2005. ISSN 1045-389X. doi: 10.1177/1045389X05055280. URL <http://journals.sagepub.com/doi/10.1177/1045389X05055280>.
- [32] S. Mehraeen, S. Jagannathan, and K.A. Corzine. Energy Harvesting From Vibration With Alternate Scavenging Circuitry and Tapered Cantilever Beam. *IEEE Transactions on Industrial Electronics*, 57(3):820–830, 3 2010. ISSN 0278-0046. doi: 10.1109/TIE.2009.2037652. URL <http://ieeexplore.ieee.org/document/5345740/>.
- [33] Seyed Mohammad, Karim Tabatabaei, · Saeed Behbahani, and Pouya Rajaeipour. Multi-objective shape design optimization of piezoelectric energy harvester using artificial immune system. *Microssystem Technologies*, 22:2435–2446, 2016. doi: 10.1007/s00542-015-2605-5. URL <https://link.springer.com/content/pdf/10.1007%2Fs00542-015-2605-5.pdf>.
- [34] Morgan. *Piezoelectric Ceramics Data Book for Designers*. 1999.
- [35] Karla M. Mossi and Richard P. Bishop. Characterization of different types of high-performance THUNDER actuators. (July 1999):43–52, 1999. doi: 10.1117/12.352812. URL <http://proceedings.spiedigitallibrary.org/proceeding.aspx?articleid=983087>.
- [36] Karla M Mossi, Gregory V Selby, and Robert G Bryant. Thin-layer composite unimorph ferroelectric driver and sensor properties. *Materials Letters*, 35(1-2):39–49, 4 1998. ISSN 0167-577X. doi: 10.1016/S0167-577X(97)00214-0. URL <https://www.sciencedirect.com/science/article/pii/S0167577X97002140>.
- [37] Karla M. Mossi, Zoubeida Ounaies, Ralph C. Smith, and Brian Ball. Prestressed curved actuators: characterization and modeling of their piezoelectric behavior. (August):423, 2003. doi: 10.1117/12.484749. URL <http://proceedings.spiedigitallibrary.org/proceeding.aspx?doi=10.1117/12.484749>.
- [38] Asan G A Muthalif and N H Diyana Nordin. Optimal piezoelectric beam shape for single and broadband vibration energy harvesting: Modeling, simulation and experimental results. *Mechanical Systems and Signal Processing*, 54-55:417–426, 2014. doi: 10.1016/j.ymsp.2014.07.014. URL <http://dx.doi.org/10.1016/j.ymsp.2014.07.014>.

- [39] Mitsuhiro Okayasu, Go Ozeki, and Mamoru Mizuno. Fatigue failure characteristics of lead zirconate titanate piezoelectric ceramics. *Journal of the European Ceramic Society*, 30(3):713–725, 2 2010. ISSN 0955-2219. doi: 10.1016/J.JEURCERAMSOC.2009.09.014. URL <https://www.sciencedirect.com/science/article/pii/S095522190900466X>.
- [40] Jung Hyun Park, Junsuk Kang, Hosang Ahn, Seon Bae Kim, Dan Liu, and Dong Joo Kim. Analysis of stress distribution in piezoelectric MEMS energy harvester using shaped cantilever structure. *Ferroelectrics*, 409(1):55–61, 2010. ISSN 00150193. doi: 10.1080/00150193.2010.487125.
- [41] P Pertsch, S Richter, D Kopsch, N Krämer, J Pogodzick, and E Hennig. Reliability Of Piezoelectric Multilayer Actuators. Technical report. URL <http://www.piceramic.com>.
- [42] P. Pillatsch, N. Shashoua, A. S. Holmes, E. M. Yeatman, and P. K. Wright. Degradation of piezoelectric materials for energy harvesting applications. *Journal of Physics: Conference Series*, 557(1), 2014. ISSN 17426596. doi: 10.1088/1742-6596/557/1/012129.
- [43] P Pillatsch, B L Xiao, N Shashoua, H M Gramling, E M Yeatman, and P K Wright. Degradation of bimorph piezoelectric bending beams in energy harvesting applications. *Smart Materials and Structures*, 26, 2017. doi: 10.1088/1361-665X/aa5a5d. URL <https://doi.org/10.1088/1361-665X/aa5a5d>.
- [44] S Srinivasulu Raju, M Umapathy, and G Uma. Design and analysis of high output piezoelectric energy harvester using non uniform beam Design and analysis of high output piezoelectric energy harvester using non uniform beam. 2018. doi: 10.1080/15376494.2018.1472341. URL <http://www.tandfonline.com/action/journalInformation?journalCode=umcm20>.
- [45] Tamil Selvan Ramadoss, Hilaal Alam, and Prof Ramakrishna Seeram. Profile Geometric Effect of Cantilever Piezoelectric Device Using Flexural Mechanism. (September), 2018.
- [46] M. Renaud, Z. Wang, M. Jambunathan, S. Matova, R. Elfrink, M. Rovers, M. Goedbloed, C. de Nooijer, R. J. M. Vullers, and R. van Schaijk. Improved mechanical reliability of MEMS piezoelectric vibration energy harvesters for automotive applications. In *2014 IEEE 27th International Conference on Micro Electro Mechanical Systems (MEMS)*, pages 568–571. IEEE, 1 2014. ISBN 978-1-4799-3509-3. doi: 10.1109/MEMSYS.2014.6765704. URL <http://ieeexplore.ieee.org/document/6765704/>.
- [47] S. Roundy, E.S. Leland, J. Baker, E. Carleton, E. Reilly, E. Lai, B. Otis, J.M. Rabaey, V. Sundararajan, and P.K. Wright. Improving Power Output for Vibration-Based Energy Scavengers. *IEEE Pervasive Computing*, 4(1):28–36, 1 2005. ISSN 1536-1268. doi: 10.1109/MPRV.2005.14. URL <http://ieeexplore.ieee.org/document/1401840/>.
- [48] Shad Roundy, Janusz Bryzek, Curtis Ray, Micheal Malaga, and David L. Brown. Method for generating electric energy in a tyre, 10 2010. URL <https://patents.google.com/patent/US7260984B2/en?q=US+Patent+7%2C260%2C984>.
- [49] Shadrach Joseph Roundy. *Energy Scavenging for Wireless Sensor Nodes with a Focus on Vibration to Electricity Conversion*. PhD thesis, THE UNIVERSITY OF CALIFORNIA, BERKELEY, 1996. URL <http://users.cecs.anu.edu.au/~Shad.Roundy/paper/ShadThesis.pdf>.
- [50] Mohammed Salim, Hanim Salleh, Eric Wooi, Kee Loh, · Mhd Khir, and Dhia Salim. New simulation approach for tuneable trapezoidal and rectangular piezoelectric bimorph energy harvesters. *Microsystem Technologies*, 23:2097–2106, 2017. doi: 10.1007/s00542-016-2999-8. URL <https://link-springer-com.tudelft.idm.oclc.org/content/pdf/10.1007%2Fs00542-016-2999-8.pdf>.
- [51] Walter A Schulze and Kiyoshi Ogino. Review of literature on aging of dielectrics. *Ferroelectrics*, 87(1):361–377, 1988. doi: 10.1080/00150198808201399. URL <http://www.tandfonline.com/action/journalInformation?journalCode=gfer20>.

- [52] R.W. Schwartz and M. Narayanan. Development of high performance stress-biased actuators through the incorporation of mechanical pre-loads. *Sensors and Actuators A: Physical*, 101(3): 322–331, 10 2002. ISSN 0924-4247. doi: 10.1016/S0924-4247(02)00263-7. URL <https://www.sciencedirect.com/science/article/pii/S0924424702002637>.
- [53] M. S M Soliman, E. M. Abdel-Rahman, E. F. El-Saadany, and R. R. Mansour. A wideband vibration-based energy harvester. *Journal of Micromechanics and Microengineering*, 18(11), 2008. ISSN 09601317. doi: 10.1088/0960-1317/18/11/115021.
- [54] V T Srikar and Stephen D Senturia. The reliability of microelectromechanical systems (MEMS) in shock environments. 11(3):206–214, 2002.
- [55] W. T. Thomson and M. D Dahleh. Theory of Vibration With Applications. Technical report, Englewood Cliffs, New Jersey, 1998.
- [56] Jirawat Thongrueng, Toshio Tsuchiya, and Kunihiro Nagata. Lifetime and Degradation Mechanism of Multilayer Ceramic Actuator. *Japanese Journal of Applied Physics*, 37, 1998.
- [57] Learn Wang Tom J. Kazmierski. *Energy Harvesting Systems : Principles, Modelling and Applications*. 2011. ISBN 9781441975652. doi: 10.1007/978-1-4419-7566-9.
- [58] Y. Tsujiura, E. Suwa, F. Kurokawa, H. Hida, and I. Kanno. Reliability of vibration energy harvesters of metal-based PZT thin films. *Journal of Physics: Conference Series*, 557(1):3–8, 2014. ISSN 17426596. doi: 10.1088/1742-6596/557/1/012096.
- [59] R. van Schaijk, R. Elfrink, J. Oudenhoven, V. Pop, Z. Wang, and M. Renaud. A MEMS vibration energy harvester for automotive applications. volume 8763, page 876305. International Society for Optics and Photonics, 5 2013. doi: 10.1117/12.2016916. URL <http://proceedings.spiedigitallibrary.org/proceeding.aspx?doi=10.1117/12.2016916>.
- [60] Ziyang Wang, Rene Elfrink, Madelon Rovers, Svetla Matova, Rob van Schaijk, and Michael Renaud. Shock Reliability of Vacuum-Packaged Piezoelectric Vibration Harvester for Automotive Application. *Journal of Microelectromechanical Systems*, 23(3):539–548, 6 2014. ISSN 1057-7157. doi: 10.1109/JMEMS.2013.2291010. URL <http://ieeexplore.ieee.org/document/6674988/>.
- [61] R Wieman and Rc Smith. Displacement models for THUNDER actuators having general loads and boundary conditions. *Signal Processing and Control in Smart Structures*, (August 2001):252–263, 2001. ISSN 0277-786X. doi: 10.1117/12.436479.
- [62] C Wilson, A Ormeggi, and M Narbutovskih. Fracture testing of silicon microcantilever beams. *Journal of Applied Physics*, 79:5840, 1996. doi: 10.1063/1.361102. URL <http://aip.scitation.org/toc/jap/79/5>.
- [63] Y. H. Yang, Y. H. Fu, C. T. Chen, S. C. Lin, Jay Shieh, Martin Veidt, and W. J. Wu. The Reliability Testing and Fatigue Behavior Study of Micro Piezoelectric Energy Harvester. In *Volume 2: Mechanics and Behavior of Active Materials; Structural Health Monitoring; Bioinspired Smart Materials and Systems; Energy Harvesting; Emerging Technologies*, page V002T07A006. ASME, 9 2018. ISBN 978-0-7918-5195-1. doi: 10.1115/SMASIS2018-8022. URL <http://proceedings.asmedigitalcollection.asme.org/proceeding.aspx?doi=10.1115/SMASIS2018-8022>.
- [64] Zhengbao Yang, Shengxi Zhou, Jean Zu, and Daniel Inman. Review: High-Performance Piezoelectric Energy Harvesters and Their Applications, 2018. ISSN 25424351.
- [65] Guangyi Zhang, Shiqiao Gao, Haipeng Liu, and Shaohua Niu. A low frequency piezoelectric energy harvester with trapezoidal cantilever beam: theory and experiment. *Microsystem Technologies*, 23:3457–3466, 2017. doi: 10.1007/s00542-016-3224-5. URL <https://link.springer.com/content/pdf/10.1007%2Fs00542-016-3224-5.pdf>.